Halogen-free flame-retardant cable compounds based on highly filled EVA/LLDPE blend systems -

Influence of the coupling mechanisms

Von der Fakultät für Ingenieurwissenschaften

der Universität Bayreuth

zur Erlangung der Würde eines

Doktor-Ingenieur (Dr.-Ing.)

genehmigte Dissertation

von

Dipl.-Ing. Michael Heinz

aus

Hof

Erstgutachter: *Prof. Dr.-Ing. Volker Altstädt*
Zweitgutachter: *Prof. Dr.-Ing. Dietmar Drummer*
Tag der mündlichen Prüfung: *16.08.2022*

Lehrstuhl für Polymere Werkstoffe
Universität Bayreuth
2022

Acknowledgement

This work and my whole journey through the exciting world of polymer engineering would not have been possible without the support of many people whom I want to thank hereby.

I want to express my special appreciation to Prof. Dr.-Ing. Volker Altstädt for supervising my PhD studies, using his open management style which gave me the ability to grow and improve my fundamental understanding. Furthermore, I want to thank Prof. Dr.-Ing. Dietmar Drummer as a second assessor. Thank you to Dr. Marie-Luise Lang and Dr. Xiaole Cheng for reviewing this thesis.

I am also grateful to my company Corning for the opportunity of this collaboration. I want to thank Dr. Waldemar Stöcklein and Mike Ellwanger for their belief in me and the continuous support in my personal development. I also want to thank my colleagues who supported me and helped with my workload - I feel honored and proud working in this international team.

All the shown experiments, analysis and outcomes result from a big effort made by an amazing group of people working together in difficult and uncertain times. Everyone's dedication and motivation helped me through intense times and when faced with drawbacks. I want to emphasize the never-ending organizational support and technical input offered by Christoph Callsen who turned from a colleague into a friend. I also want to thank Alexander Kiel for his motivation and patience with my ideas resulting in more than 100 compounding and testing sets. I will never forget whole weeks that we spent in the lab, sitting between bags of raw materials. I owe the high-quality results to Ute Kuhn and Annika Pfaffenberger who set new records in thermo-analysis and electron microscopy while answering my questions in parallel. Another big thank you goes to Roger Peterson who performed hundreds of internal tests growing the understanding towards cable application. I also want to thank Andreas Mainz for introducing me to the world of polymers testing in 2007 and Dr. Mike Szameitat to the world of cables in 2011 - both have set a clear direction for my personal development.

In the end, I like to express my ultimate gratitude to my mother Silvana, my father Siegfried and my brother Carsten for their love, support and encouragement to follow my goals. Without them, I would not be the person that I am today and couldn't have achieved what I have now.

Last but not least, I want to thank my love, my best friend and dear wife Christina who shares already half of my life with me. She experienced my whole journey of studies, polymer engineering and cabling. She always supported my decisions, even working in Hong Kong or North Carolina.

Short summary

The objective of this work was to generate a fundamental scientific understanding of the influence of different coupling mechanisms on the structure-properties-relationships of highly filled, flame-retardant EVA/LLDPE based cable compounds. EVA/LLDPE blend systems, maleic-acid-anhydrite coupling agents and different magnesium-di-hydroxide (MDH) surface modifications were investigated.

The morphologies of the incompatible EVA/LLDPE blends were theoretically and analytically described. This was also performed on filled versions using the identified filler location and blend component viscosity ratios. The compound properties were mainly affected by three factors: the ratio of EVA/LLDPE, the filler content and the filler coupling agent. Key role of the flame-retardant filler was not only the improvement of the reaction to fire but in many cases also the compatibilization of both polymers. This was strongly related to the occurrence of polymer-filler interactions which were further controlled by polymeric coupling agents and filler surface coatings.

The filler dispersion affected the compound properties and was influenced by the type and strength of filler-polymer interactions. EVA interacted with uncoated and aminosilane coated MDH via hydrogen bonds which led to increased filler uptake. These observed interactions obsoleted the usage of MAA-g-EVA coupling agent. Vinylsilane has shown no polymer interaction with neither EVA nor LLDPE. By adding MAA-g-LLDPE coupling agent, a covalent bonding to the uncoated and aminosilane coated MDH was observed. This led to an incorporation of the filler in the EVA/LLDPE interphase. While this was observed completely for uncoated MDH, aminosilane coated MDH remained partially in EVA. The difference was caused by a stronger interaction between aminosilane and EVA. Vinylsilane coated fillers have shown to diminish the bonding efficacy but still show signs of interaction with the coupling agent. This is expected to be related to an incomplete coverage of the surface coating. The usage of polymeric coupling agents has shown stronger improvements in comparison to the usage of filler coatings. No significant differences in burning behavior were observed comparing the different versions of coatings and coupling agents.

This led to the conclusion, that the usage of uncoated MDH with MAA-g-LLDPE gives the best filler-polymer interaction throughout the investigated systems. Further tools to control the filler coupling and therefore balance the compound performance were identified and applied.

Kurzfassung

Ziel der vorliegenden Arbeit war es, den Einfluss verschiedener Kopplungsmechanismen auf die Struktur-Eigenschafts-Beziehungen von hochgefüllten flammgeschützten EVA/LLDPE Compounds zu untersuchen. EVA/LLDPE-Blendsysteme, der Einfluss von Maleinsäure-anhydrid basierten Kopplungsadditiven und von Oberflächenmodifizierungen des beigegebenen Magnesiumhydroxid-Flammschutzmittels (MDH) wurden untersucht.

Die Morphologien der inkompatiblen EVA/LLDPE Blends wurden qualitativ und quantitativ beschrieben. Durch Füllstofflokalisierung und Viskositätsmessungen konnten die Ergebnisse auch auf gefüllte Systeme übertragen werden. Die Compoundeigenschaften wurden hauptsächlich von drei Faktoren beeinflusst: dem EVA/LLDPE-Mischungsverhältnis, dem Füllgrad und der Füllstoffkopplung. Das mineralische Flammschutzmittel verbesserte die Brandeigenschaften und in einigen Fällen auch die Kompatibilisierung der Polymerphasen. Dies war abhängig von auftretenden Polymer-Füllstoff-Wechselwirkungen, die durch die Verwendung von Kopplungs-additiven und Oberflächenbeschichtungen gesteuert werden konnten.

Die Dispergierung des Füllstoffs bestimmt die Compoundeigenschaften und hängt von Art und Stärke der vorherrschenden Wechselwirkungen ab. Unbeschichtetes und Aminosilan-beschichtetes MDH interagierte mit EVA durch Wasserstoffbrückenbindungen. Daraus resultierte eine vollständige Füllstoffeinlagerung. Diese Interaktion machte die Verwendung eines MAA-g-EVA-Kopplungsadditivs überflüssig. Vinylsilan zeigte keine Interaktion mit EVA oder LLDPE. Bei Zugabe eines MAA-g-LLDPE-Kopplungsadditivs zu unbeschichtetem oder Aminosilan-beschichtetem MDH wurde eine kovalente Kopplung beobachtet. Diese führte zur Verlagerung des MDH aus dem EVA in die Grenzschicht bei unbeschichtetem MDH und zur Teileinlagerung in LLDPE bei aminosilan beschichtetem MDH. Der Unterschied war hierbei eine stärkere Wechselwirkung des Aminosilans mit der EVA-Phase. Vinylsilan-beschichteter Füllstoff zeigte keine merkliche Kopplung, bei Verwendung des Haftvermittlers jedoch eine leichte Verbesserung, was auf eine unvollständige Füllstoffbeschichtung hinweist. Der Einsatz von einem polymeren Kopplungsadditiv zeigte deutlichere Effekte als die untersuchten Füllstoffbeschichtungen. Die Brandeigenschaften der Compounds wurden durch die Modifikation der Polymer-Füllstoff-Interaktion nicht signifikant beeinflusst.

Abschließend zeigte sich, dass die Verwendung von unbeschichtetem MDH in Verbindung mit einem MAA-g-LLDPE-Kopplungsadditiv zu den besten Wechselwirkungen führt. Weitere Werkzeuge zur gezielten Steuerung der Polymer-Füllstoff-Interaktion wurden identifiziert und mit den Erkenntnissen ein bestimmtes Eigenschaftsprofil erzielt.

Table of contents

Abbreviations

AlPi	Aluminum diethylphosphinate
APP	Ammonium polyphosphate
AS	Aminosilane
ATH	Aluminum tri-hydroxide
BET	Specific surface area (by Brunauer, Emmett and Teller)
CA	Coupling agent
$CaCO_3$	Calcium carbonate
CE	Conformité Européenne
CPR	Construction product regulation
CTE	Coefficient of thermal expansion
DMA	Dynamic mechanical analysis
DSC	Differential scanning calorimetry
EDX	Energy dispersive X-Ray composition analysis
EVA	Ethylene-vinyl acetate
HALS	Hindered amine light stabilizers
HDPE	High density polyethylene
HFFR	Halogen free flame-retardant
L/D	Length/diameter ratio
LDPE	Low density polyethylene
LLDPE	Linear low-density polyethylene
LOI	Limited oxygen index
MAA-g-EVA	Maleic-acid anhydrite grafted ethylene-vinyl acetate
MAA-g-LLDPE	Maleic-acid anhydrite grafted linear low-density polyethylene
MAA-g-PP	Maleic-acid anhydrite grafted polypropylene
MDH	Magnesium-di-hydroxide
MFR	Melt flow rate
MPF	Maximum packing fraction
MVR	Melt volume rate
phr	Parts per hundred resin
PHRR	Peak heat release rate
PP	Polypropylene
PT	Percolation threshold
PVC	Polyvinylchloride
rpm	Potations per minute
SEM	Scanning electron microscopy
TEM	Transmission electron microscopy
TGA	Thermo-gravimetric analysis
THR	Total heat release rate
TMA	Thermo-mechanical analysis
UV	Ultraviolet radiation
VA	Vinyl acetate
vol%	Volumetric percent
VS	Vinylsilane
WAXS	Wide angle X-ray scattering
wt%	Weight percent
WP	Working package
X	Hydrolysable group
XLPE	Crosslinked Polyethylene
Y	Organic group

Symbols

$\emptyset$	Phase concentration
ΔH	Reaction enthalpy
D_{ro}	Rotary diffusivity
M_w	Molecular weight
P	Aspect ratio
T_g	Glass transition temperature
T_m	Melt temperature
η	Viscosity

1 Introduction and Motivation

Based on latest studies, telecommunication was the major contributor in the fastest growing business segments from 2017 to 2019, data center traffic is expected to triple reaching 2022. It is also expected, that 95 % of data center traffic will come from cloud applications. While being initially used mainly in outdoor distribution and backbone networks, this increasing demand for bandwidth drives optical fibers further deeper into the networks. As soon as optical cables are installed within buildings, fire retardancy is an additional crucial product requirement [1].

The usage of PVC and halogen containing cable materials in buildings was faced with negative publicity after the airport fire in Düsseldorf with many casualties in 1996 [2]. Current materials used in the European market are <u>h</u>alogen <u>f</u>ree <u>f</u>lame-<u>r</u>etardant (HFFR) compounds, mainly based on polyolefin blends. These compounds are used as cable insulation or sheathing and are applied through extrusion processing in a stepwise or continuous production process. In Figure 1 can be seen that in comparison to all other polymeric materials used in cables, these HFFR compounds only represent a relatively small portion. But with a grow from 6 % to 10 % in global consumption from 2016 to 2019 and up to 16 % expected for 2023, it is the fastest growing portion of cable materials [3], [4].
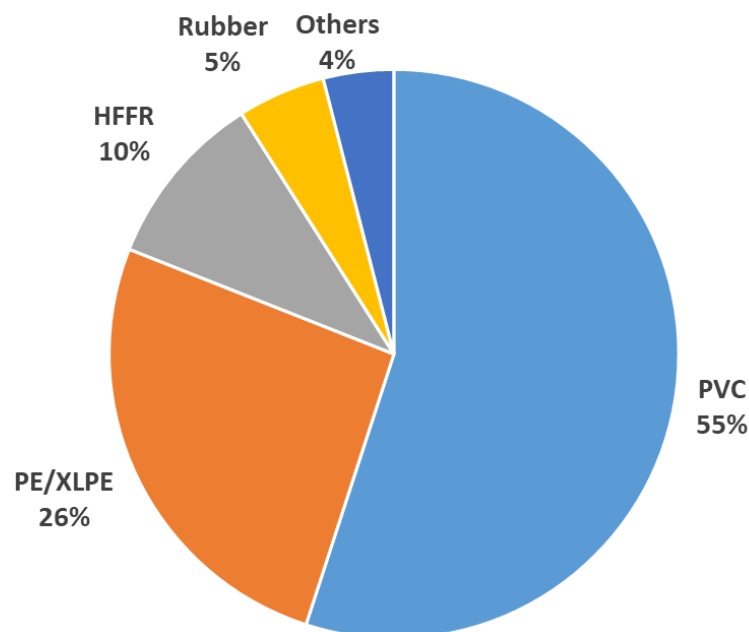

Figure 1   Usage of compounds in the global cable industry in 2019 [3]

Due to a wide variety of cable types, designs and properties in cable application, the compounds used in the cable industry are often mixtures with a high complexity. The flexibility of a cable product is directly affected by the stiffness of its sheathing material. Mechanical performance of a cable compound is a result of the used polymer types and ratio, but also the type, amount and functionality of incorporated additives. Due to a wide range of application environments, the mechanical performance (e.g. tensile, twist or bend load) not only at room temperature, but also at elevated or cold temperatures needs to be considered. While maintaining certain thermo-mechanical cable performance, further demands like fire retardancy, color stability, resistance against solvents or rodents, etc. need to be fulfilled. While some cable performance like mechanical strength can be directly controlled by the polymeric ingredients, other properties require the addition of further additives. Parameters like extrusion processing, production line speed, cable storage and handling, surface quality and stability like UV resistance must be considered. Another major driver for the compound composition is the balance between cost and material performance. Therefore, typical cable compounds contain up to 20 different additives which are added to the polymer mixture. Examples are particulate fillers, flame-retardants and synergists, processing aids, internal and external lubricants, slip agents, antistatics, antioxidants, UV stabilizers, acid scavengers, laser markers and pigments [5], [6], [7].

Examples for typical cable requirements and the resulting tests for the cable materials are shown in Table 1.

Table 1   Example of typical cable properties and resulting test methods [6]

Cable properties	Material tests	Test standard
Mechanical properties	Tensile test	IEC 60811-501
	Torsion test	IEC 60794-1
	Hardness	ISO 868
Thermo-mechanical resistance	Heat shock	IEC 60811-509
	Hot pressure test	IEC 60811-508
	Cold bend test	IEC 60811-504
	Cold impact	IEC 60811-506
	Hot / cold elongation	IEC 60811-505
	Heat ageing	IEC 60811-401
Fire resistance	UL 94	UL-94
	LOI	ISO 4589-2
	Cone calorimeter	ISO 5660-1
	Acidity of evolved gases	IEC 60754-2
Processability	MFR	ISO 1133

In 2011, the European Union released the construction product regulation (CPR) which resulted in mandatory testing and CE marking of all products which are permanently installed in buildings beginning in June 2016. This new regulation came up with more stringent burn test procedures which increases the requirements for flame-retardant materials to be used in cable sheathing application [8]. Due to the different cable designs, fiber optic cables contain a higher amount of combustible materials in comparison to copper-based cables. This leads to a demand of further improved material and cable product performance. An example of a fiber optic cable design is shown in Figure 2. Each optical fiber is surrounded by acrylate-based coatings and then insulated, bundled and organized in different manufacturing steps using halogen free flame-retardant polymeric materials. Often, aramid yarns (yellow) are incorporated to achieve the longitudinal mechanical strength that is required during installation and application.
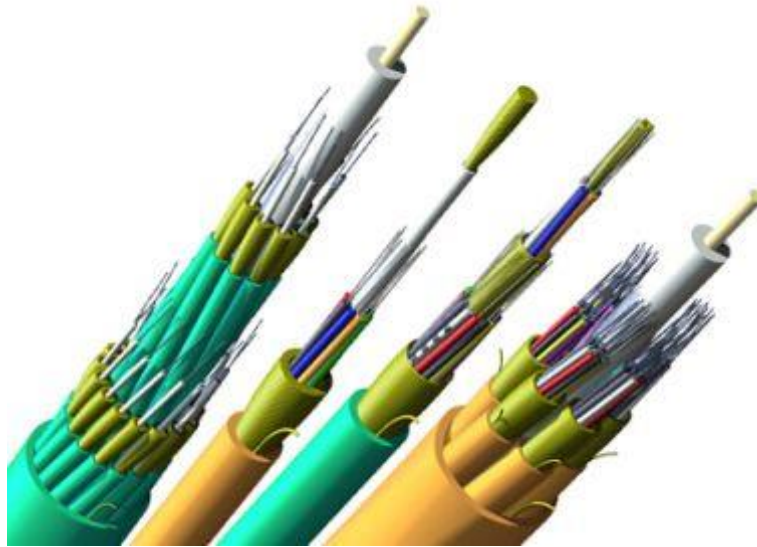
Figure 2   Examples of fiber optic cables using halogen free flame-retardant insulation and sheathing materials [9]

In comparison to other market segments like injection molding, halogen free flame-retardant cable compounds represent a relatively small portion in the compound market. "Cable production contributes 3 % to the European polymer consumption" [3]. Based on the latest numbers, this resulted in a portion of 0.48 % polymer market contribution of halogen free flame-retardant compounds in Europe in 2017. Due to this quantity, producers for cable compounds are mainly small and medium sized companies with less than 200 employees [3]. State of the art compounds are the result of developments throughout many years, that were driven by demands of single customers with focus on profitability in the development. This supplier environment leads to the observed situation, that deeper technical or scientific investigations were not carried out very

often. Although, halogen free flame-retardant compounds are in the market for quite a while, the influence of key ingredients on material characteristics, resulting compound properties and cable performance was not investigated in a structured way or results were not published [2], [4].

Especially critical properties for the cable application (e.g. thermal expansion/shrinkage, thermo-mechanical properties, rheology) are not yet covered extensively in literature.

To further improve the fire resistance of cable compounds without losing other attributes like mechanical properties, it is crucial to understand the structure properties relationship of the key ingredients. Therefore, this work is focused on creating a better understanding of the influence of the constituents and the formulation on the behavior of highly filled flame-retardant compounds for cable application.

2 State of the art

2.1 Halogen free flame-retardant cable compounds

2.1.1 Standards & requirements for indoor cables

An overview about typical mechanical and physical requirements of compounds used in cable applications was given in Table 1. Requirements can be mainly divided in different categories: mechanical performance, product stability and resistance to fire. These properties are often closely related. Based on application space and country, the standards require certain minimum mechanical properties before and after heat ageing. Typical measures of the material performance are tensile strength and elongation at break at different temperatures [6].

As already mentioned, a key property for the usage of cables in buildings is a certain resistance to fire which is covered by the recently released construction product regulation (CPR). The regulation leads to the CE marking of construction products after classification of the reaction to fire [10]. The reaction to small scale fire is tested in the single cable burn (EN 60332-1-2), the reaction under fire conditions in a larger scale is tested according to EN 50399. In this test, multiple cables are mounted on a defined ladder and exposed to a 20.5 kW burner for 20 minutes. Test results that lead to the CPR class are flame spread, heat release rate and their growth rates. More details about the test setup are given in Figure 3.
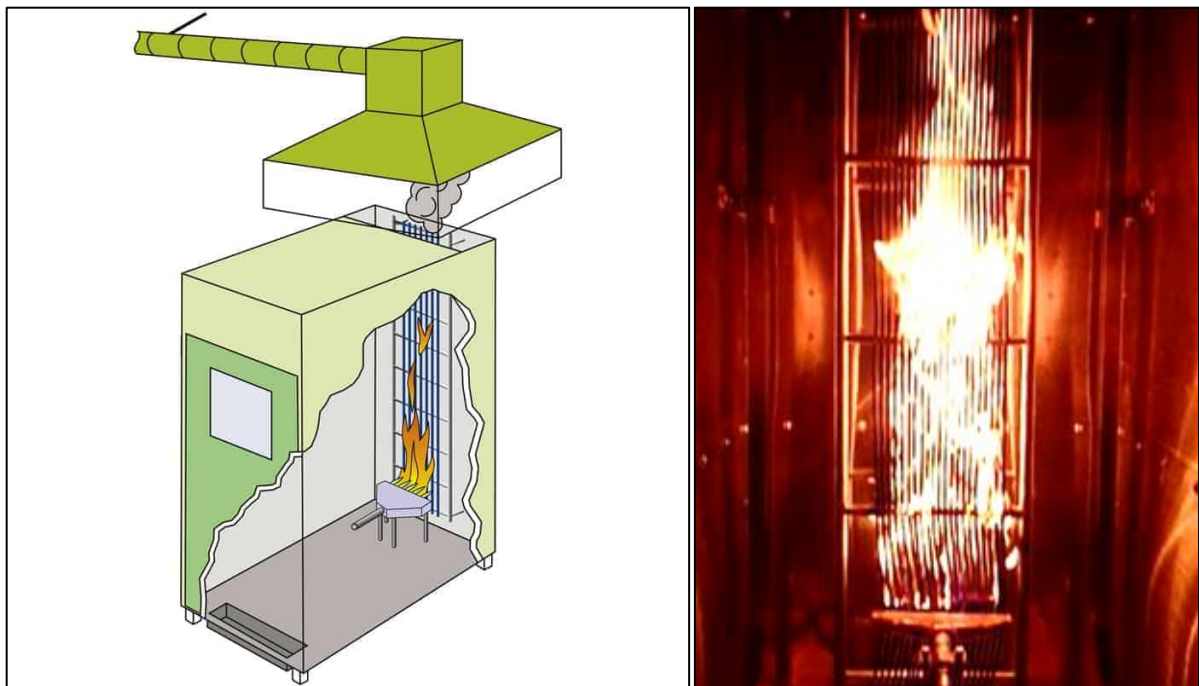

Figure 3   Schematic test setup according to EN 50399 (left) [11], test in progress (right)

The tests for CPR rating do not only cover the reaction to fire, but also additional rate the smoke density (EN 61034-2), acidity and corrosivity of the combustion gases (EN 60754-2). All results together translate into a product classification [10].

Based on the above-mentioned requirements, the applied materials must exhibit a certain strength, flexibility and stability [6]. In addition, the material must deliver enough flame-retardant performance to protect the cable core from external flames. The composition of the combustion products needs to stay within the limits of the mentioned standards [8]. This set of properties is currently realized by using a compound of different polymers and functional additives.

2.1.2   Flame-retardant mechanisms and additives

Polymers are materials with a high variety in mechanical performance and show good processability at a relative low cost. This fits well to cable application and the high demands in regard of mechanical performance and a continuous production process. Unfortunately, most polymers are highly flammable which results in increased fire risk. To overcome this disadvantage, it is possible to use flame-retardant additives which show different effects to protect the material during combustion. Lately, much research was carried out in regard of improving the fire resistance of polymeric materials. This is the result of more stringent requirements, environmental, health and safety aspects and increasing price pressure. As this work focusses on halogen free flame-retardant compounds, halogen containing flame-retardant additives will be disregarded in the following section [12].

Before designing material compositions, the fire behavior of the polymer needs to be understood (see Figure 4). Through ignition or thermal irradiation, polymeric decomposition products are formed which react with oxygen from the air and create a flame which results in further heat. This heat can be transferred back to the solid phase and continue the decomposition process which sustains the burn [13]. Depending on the chemical structure, some polymers have the tendency to form a char which reduces the emission of volatiles during combustion. This already represents the first approach of improving fire retardancy: the formation of a residue during combustion which acts as a thermal and gas transport barrier. Flame-retardant additives can act in solid, liquid or gas phase to delay ignition or reduce fire propagation. To cut off the chain reaction during burn, it is required to eliminate the production of combustible gases or to enhance the formation of a strong char [14], [15].
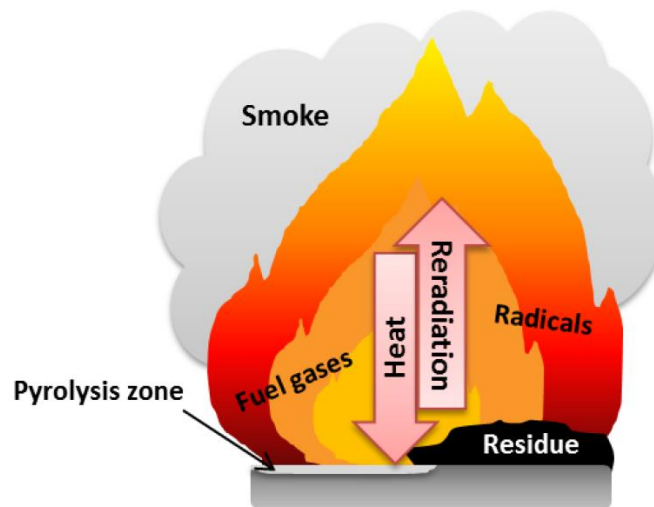
Figure 4   Phenomena occurring during burn of material [13]

The modes of action of flame-retardants can be divided into two classes: [16]

- Physical effects like cooling the substrate by an endothermic process, dilution of the combusted gases or creation of a protective, non-permeable layer
- Chemical effects like flame inhibition through radical reaction (scavenging effect)

As any change to a polymeric system will affect its properties, the type and dosage of flame-retardant additives need to be well balanced [13].
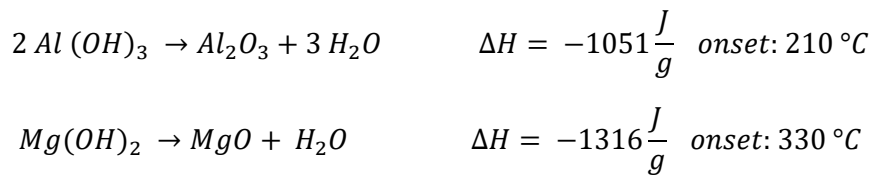
Three major groups of flame-retardant additives with different chemical composition are common in the market: phosphorous, nitrogen and mineral based flame-retardants [12].

Phosphorous based flame-retardants can both act in the gas phase as radical scavengers or in the solid phase to promote residue formation. Typical phosphorous based additives are aluminum diethylphosphinate (AlPi) and ammonium polyphosphate (APP). While AlPi reacts more in the gas phase with H- and OH- radicals, APP's mode of action is in the condensed phase to create intumescence. The reaction of an acid source, a blowing agent and a char former result in a swelling of the material to create an insulation layer. The application space of each additive differs with the polymer type but is also affected by the higher cost structure in comparison to mineral fillers. AlPi is mainly focused on technical thermoplastic materials like Polyesters, APP is additionally used in commodity niche applications like Polypropylene [13], [17].

Nitrogen based flame-retardants can be used in a synergistic combination to phosphorous based additives. They show physical effects by endothermic decomposition and the creation of a heat sink. In addition, inert gases dilute the oxygen and fuel in the gas phase. The most common

application in the cable industry is the combination of thermoplastic polyurethane with melamine-cyanurate [13].

Flame-retardants based on mineral fillers represent the largest portion of flame-retardant additives in the cable industry. This has a simple reason: a lower cost in comparison to the above-mentioned solutions makes it economical attractive to be combined with commodities like polyolefins. The metal hydroxides work predominantly in the condensed phase, decompose endothermically and release water. This leads to a heat sink in the substrate and a dilution effect of the combustion gases [14]. Aluminum tri-hydroxide (ATH) and magnesium di-hydroxide (MDH) represent the major market share of these additives. Both differ in decomposition reaction, temperature and reaction enthalpy ΔH [18]:

$$2\,Al\,(OH)_3 \rightarrow Al_2O_3 + 3\,H_2O \qquad \Delta H = -1051\frac{J}{g} \quad onset\!: 210\,°C$$

$$Mg(OH)_2 \rightarrow MgO + H_2O \qquad \Delta H = -1316\frac{J}{g} \quad onset\!: 330\,°C$$

The higher decomposition temperature of MDH allows a higher processing temperature of compounds containing this flame-retardant. The tradeoff is the price which is approx. double of the ATH (but still below organic additives). The decomposition behavior and the resulting amount of residue of ATH and MDH measured in TGA are shown in Figure 5.
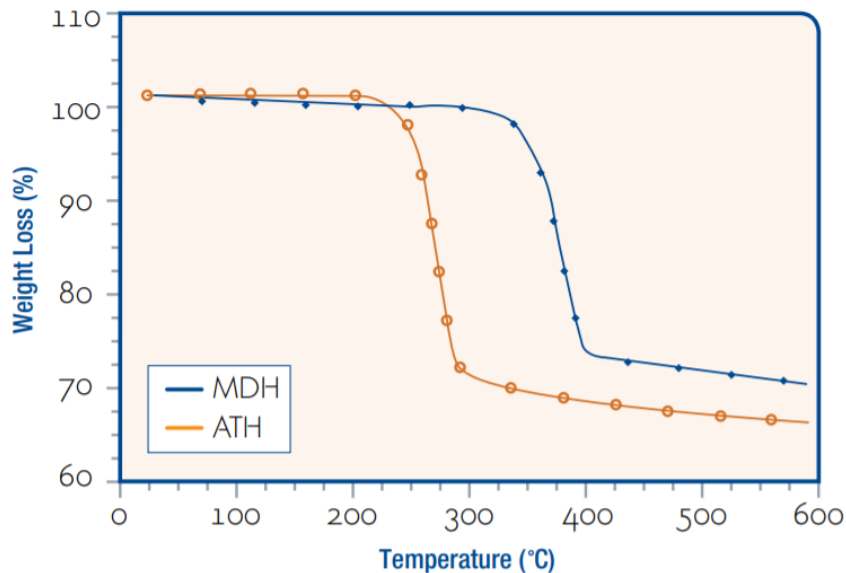

Figure 5   Thermogravimetric analysis of ATH and MDH [19]

Typical application spaces are spread throughout many different polymer types like thermosets, technical thermoplastics and ethylene-copolymer cable sheathing compounds. In comparison to other flame-retardants, ATH and MDH exhibit a cost effective and low health hazard performance with additional smoke suppressing effects [15], [20]. The global consumption of MDH is only one tenth of ATH, for cable application it is estimated to be 20 % [18]. Both additives' delivery form is powder, commercially available in natural (ground) and synthetical (precipitated) particles. Synthetical precipitation after dissolution allows to produce a significantly higher purity, smaller particle size and more narrow particle size distribution. After drying, it is possible to apply different coatings to further modify the particle-polymer interaction [18]. More information to this topic will be given in section 2.3.3.

2.1.3   Typical cable compound formulations

To give an overview about the composition of halogen free flame-retardant cable formulations and typical ingredients, an exemplary recipe from literature is given in Table 2. To underline the already described transfer from required properties into a compound formulation, the ingredients are additionally commented. Further details about the materials will be given in the following sections.

Table 2   Exemplary compound formulation for flame-retardant cables [19], [21], [22]

Ingredient	Ratio / wt%	Comment
EVA	20 - 40	Soft copolymer to achieve flexibility
LLDPE	10 - 30	Stiff polymer to achieve thermal stability
MAA-g-LLDPE	2 – 5	Filler-polymer coupling agent
MDH	50 – 65	Flame-retardant
Stearate	1 – 2	Processing additive
Primary Antioxidant	0.1 – 2	Phenolic thermal stabilizer
Secondary Antioxidant	0.1 – 0.5	Phosphate stabilizer for processing
HALS	0.1 – 0.5	Hindered amine UV light stabilizer

As the shown compound consists of several ingredients and to further understand the related properties, the next sections will be split into the fields of polymer blends and highly filled polymers.

2.2 Polyolefins and polyolefin-copolymer blends

"Polyethylene is the largest volume of polymer produced globally with about 84 million metric tons produced. The success of polyethylene is due to a combination of its relatively low cost to produce, the large scale of the production plants […] and the variability of the physical properties possible." [23]

2.2.1 Linear low-density polyethylene (LLDPE)

Polyethylene is thermoplastic, semi-crystalline and consists of a polymer backbone composed of carbon and hydrogen. During the polymerization step of the monomers, not only unidirectional molecules, but also branching is created by statistically driven reaction kinetics. Based on the production process (high- or low-pressure polymerization), the degree and length of branching can be controlled. This results in either high-density polyethylene (HDPE) with nearly no branching or low-density polyethylene (LDPE) with a high degree of long chain branching. From a historical point of view, linear-low-density polyethylene (LLDPE) is the youngest version of Polyethylene as a production process established in 1970 using metallocene catalysis leads to a low-density polyethylene with short branching [24]. A change from ethene-monomers to α-olefinic monomers further improved the mechanical performance [25]. An overview about the basic structure and properties is given in Table 3.

Table 3   Comparison of PE types and their properties [26]

Material	HDPE	LLDPE	LDPE
Structure			
Density (g/cm^3)	0.93 – 0.96	0.91 – 0.93	0.91 – 0.93
Crystallinity (%)	70 – 80	55 – 60	50 – 55
Melting point (°C)	128 – 136	120 – 130	106 – 120
T_g (°C)	- 110	- 110	- 110

The reason for the application of LLDPE in halogen free flame-retardant cable compounds is driven by many factors: The price pressure, thermal stability and processability leads to the usage of polyethylene-based materials. HDPE exhibits a high mechanical and media resistance which leads to its application in non-flame-retardant outdoor cables [2]. By adding flame-retardant additives, the mechanical performance is affected and the brittleness of the material becomes an

issue that causes cracking at low temperature. The long-branched LDPE gives beneficial performance in this case, due to a higher degree of entanglements. But this material also shows disadvantages in cable application: lower degree of crystallinity leads to reduced toughness and steric hindering limits the ability to take up mineral filler. Furthermore, the long branching causes difficulties with increased post-extrusion shrinkage [26]. Therefore, LLDPE delivers the best balance between both material performances which also led to great success in the packaging industry [24].

The thermo-mechanical performance of the LLDPE material used in this work can be seen in Figure 6.
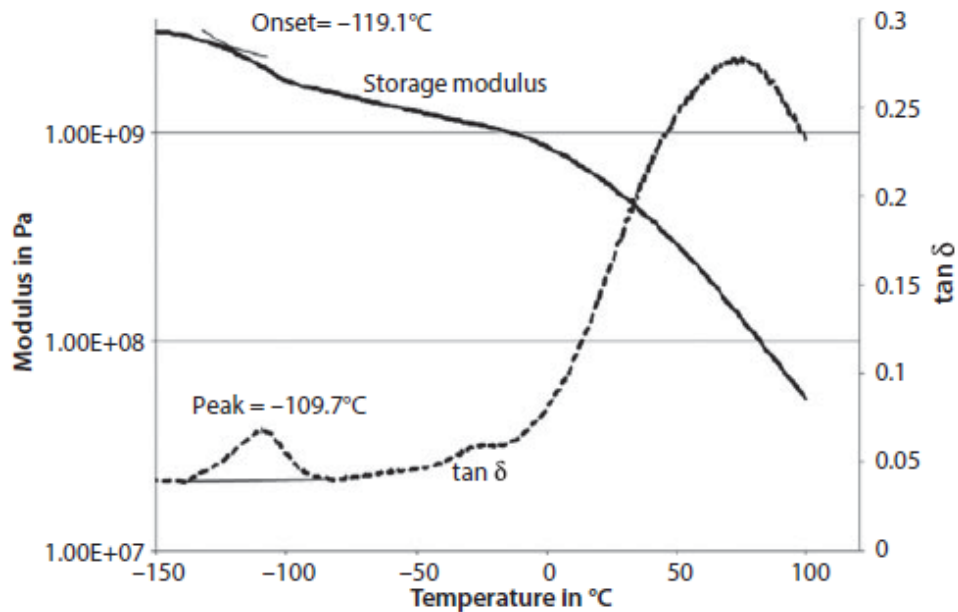
Figure 6   DMA run of a LLDPE sample with Tg identified at -109.7 °C [27]

To further reduce negative mechanical response to high filler addition in cable compounds, LLDPE is combined with a more flexible co-polymer based on polyethylene: ethylene vinyl acetate.

2.2.2   Ethylene vinyl acetate (EVA)

Ethylene vinyl acetate is a random copolymer of ethylene grafted with vinyl acetate monomers. The chemical structure is drawn in Figure 7 left. The vinyl acetate (VA) side group has two effects on the properties of EVA copolymers. The steric hindering disrupts crystallinity that is formed by long ethylene sequences (see Figure 7 right). The second effect is the addition of a polar nature from the acetoxy side chains to the unpolar polyethylene backbone [24], [26].

Figure 7   Chemical structure of EVA monomer (left) and observable influence of VA-content on crystallinity (right) [26, p. 113]

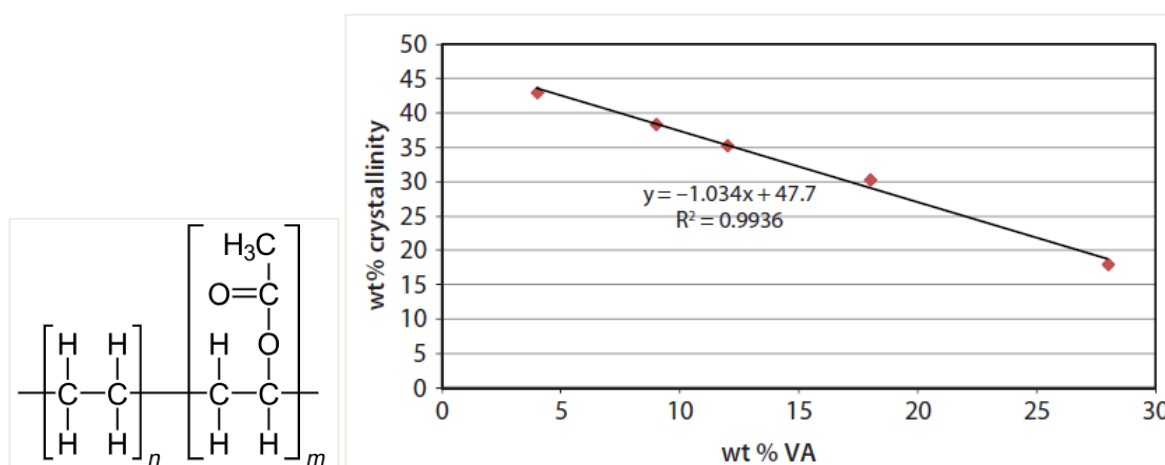The melting temperature and the stiffness drops with decreasing crystallinity until reaching fully amorphous structure above approx. 45 wt% VA content. Softening temperatures around room temperature result in pellet handling issues and blocking in feeders due to sticking. To overcome this issue during compounding and processing, special treatments with small amounts of silica powder are applied. The density is increasing with VA content although crystallinity is decreasing. EVAs have a high degree of long side chain branching which is beneficial for the melt strength in extrusion processing but can cause post-extrusion shrinkage. Due to the presence of weaker carbon-oxygen bonds in the molecule, the thermal stability is lower in comparison to PE. This can lead to the generation of acetic acid and the formation of cross-linked gels during high temperature melt processing above 230 °C [24], [26].

EVA is the largest volume of polar ethylene copolymers used today which results in a very attractive price situation. Typical application spaces are packaging films and flexible gaskets, textiles or foams. EVA exhibits a decreasing melting temperature from 92 – 50 °C with increasing VA content from 20 to 30 %. These higher strength versions are used for hot melt adhesives and wire and cable applications [26].

2.2.3   LLDPE/EVA blend systems

The trend in material development goes clearly towards the modification and combination of existing polymers to overcome their disadvantages and combine their positive properties. Polymer blends can be categorized into miscible and immiscible systems. While miscible blends obey linear mixing rules or show positive deviation, the response in immiscible systems is more

complex. The material performance is strongly related to the multiphase morphology and interphase effects. These are affected by the polymer properties, like rheological behavior, polarity or elasticity ratio. Another important factor influencing the blend morphology is processing (shear rate, temperature profile and cooling rate) [28-32].

The properties of the materials presented in sections 2.2.1 and 2.2.2 show several advantages but also drawbacks. While LLDPE shows good thermal stability and mechanical strength, the flexibility and ability to take up high amount of mineral filler is limited. In this field, EVA shows very positive performance but comes with weaker thermo-mechanical properties. PE/EVA blends are widely used in applications like shrink-films and the cable industry. They are reported to show improved toughness, environmental stress cracking resistance and good filler uptake [28], [29].

A major driving force in studies investigating PE/EVA blends was an unclear picture about the degree of miscibility [30]. This is an important factor as it strongly affects the blend properties. First studies concluded that using only DMA does not lead to fully understand the miscibility of these blend systems [31]. By correlating additional morphological and rheological studies, it was possible to prove a higher compatibility of LDPE/EVA over HDPE/EVA blends [32]. This effect was later described by partial miscibility in amorphous regions and the presence of individual crystalline areas in the blend systems. As LDPE shows less crystallinity in comparison to HDPE (see 2.2.1), this results in increased compatibility [33].

As differences in blend behavior between HDPE and LDPE were observed, further investigations focusing on LLDPE were carried out by Faker et. al [29]. Reviewing the influence of the LLDPE/EVA mixing ratio in rheological studies (see Figure 8), it was observed that the blends show a clear deviation from the mixing rule. This was described with higher interfacial interactions in PE-rich blend compositions due to the higher melt elasticity of LLDPE. According to the Van Oene equation, this leads to smaller phase diameters of EVA in the LLDPE [29], [34].
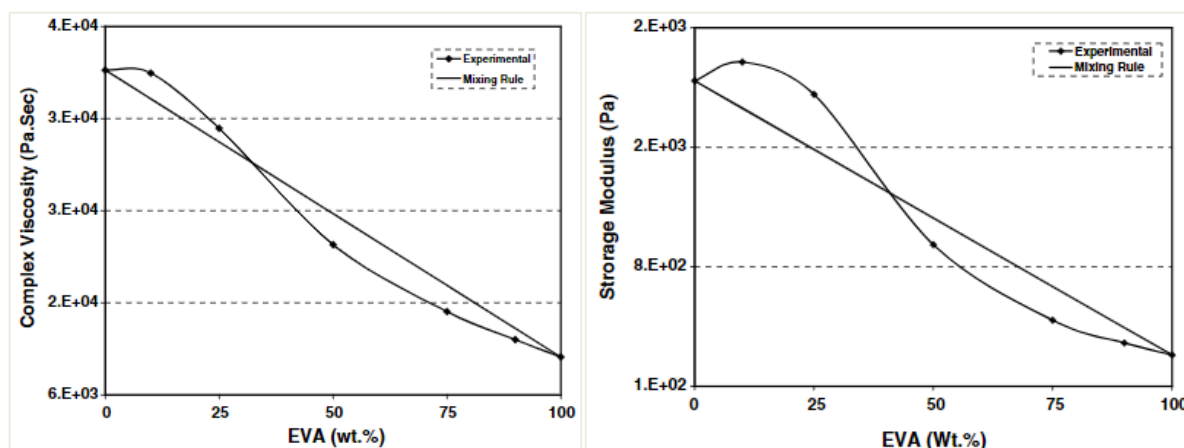
Figure 8   Complex viscosity and storage modulus versus blend composition at angular frequency 0.1 s^{-1} in correlation with mixing rule calculation [29]

The miscibility of the blend system was subsequently rated by SEM micrographs of blends after extraction of the EVA phase using xylene etching. Two examples of the observed morphology are given in Figure 9. Based on these investigations, the blends were rated immiscible with a two-phase morphology in the whole composition range. Matrix dispersed droplet morphology was also observed for the EVA rich blends. In alignment with the rheological studies, the dispersed phase sizes of the LLDPE rich blends are smaller than the ones observed in EVA rich [29].
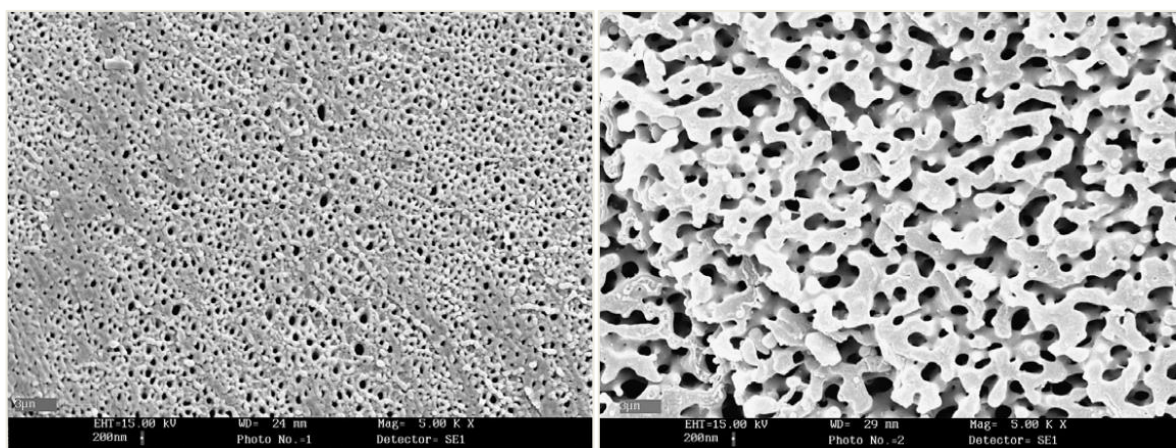
Figure 9   SEM micrograph of PE/EVA blends: 75/25 (left), 50/50 (right) after etching with xylene at 50 °C for 6 hours [29]

These observations lead to the clear picture that PE-rich blends show stronger interfacial interaction which leads to better interfacial adhesion and stress transmittance. The observations fit well to Palierne's emulsion model to predict resulting complex moduli as a function of dispersed particle size, interfacial tension and complex modulus [35]. To predict the phase inversion composition, this model was later combined with Krieger and Dougherty's model by

Ultracki [36] (see equation 1) and further developed by Steinman et al. [37] (see equation 2). These models allow to predict the phase inversion of immiscible blends considering the melt viscosity η, without taking the already mentioned melt elasticity into account.

$$\emptyset_2 = \frac{(1-\frac{log\left(\frac{\eta_1}{\eta_2}\right)}{[\eta]})}{2}, \quad [\eta] = 1.9 \tag{1}$$

$$\emptyset_2 = -0.12 \ log \ \left(\frac{\eta_1}{\eta_2}\right) + 0.48 \tag{2}$$

Thermal analysis of various blend compositions and the presence of two peaks for all blends further verified immiscibility (see Figure 10). A slight depression of the LLDPE melting temperature is the result of dilution effects by the EVA phase and possible co-crystallization. Nucleating effects of LLDPE crystallites affect the EVA crystallization temperature. This can be a sign for partial miscibility in melt state which would lead to the assumption of a possible partial miscibility in the solid amorphous phase (analog to observations in LDPE/EVA blends). On the other hand, relatively close melting temperatures and structural backbone similarity can also be a reason for co-crystallization effects [29], [32].
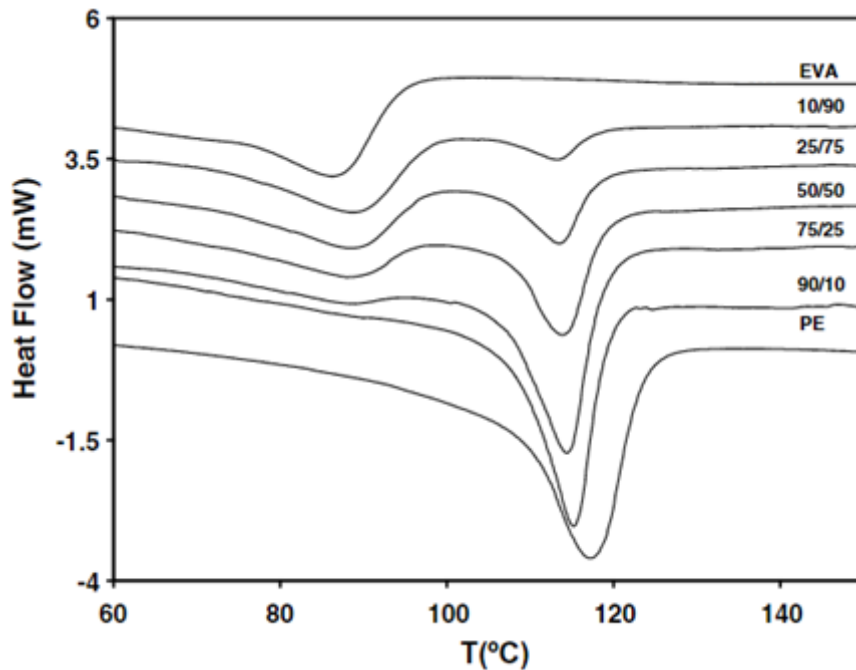

Figure 10   DSC measurements for LLDPE/EVA blends (endothermal) [29]

Investigations of the mechanical performance of PE/EVA blends were carried out in several publications and have shown a huge difference, caused by the different polymer types and grades (e.g. VA content of the EVA). A clear influence can be seen by materials and their mixing ratio. Comparative to the rheological properties, latest studies have revealed a clear deviation from rule of mixture with major influence from morphology on the mechanical properties (see Figure 11) [29], [38].
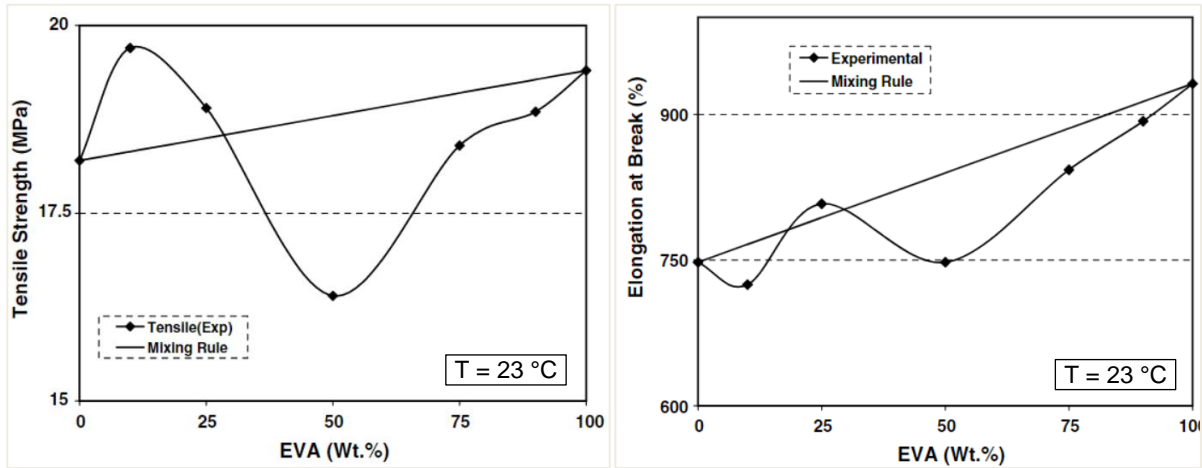
Figure 11   Tensile strength and elongation at break for different LLDPE/EVA blends at room temperature [29]

A positive deviation from rule of mixture regarding rheology and mechanical performance for the PE-rich compositions was reported [29]. Unfortunately, this advantage cannot be transferred into cable compound application. By adding over 50 wt% of flame-retardant filler into a PE majority matrix, the compound stiffness and mechanical performance will not be suitable for the usage in cables. Further information about polymer material response to filler addition will be given in the next section.

2.3 Highly filled polymer compounds

"For decades, the incorporation of inorganic and organic fillers into a polymer matrix has been of significant industrial importance, as this is one of the most effective ways to develop new materials with desirable properties adapted to specific applications." [39, p. 24]

2.3.1 Structural description of fillers

Concerning the nature of particles, two types of suspensions can be classified: Brownian and non-Brownian suspensions. Brownian suspensions are composed of small particles (<<1 µm) which can be affected by thermal fluctuations (Brownian motion). With increasing particle size, diffusion time becomes larger and Brownian thermal forces can be neglected. While a micro-composite (filler size 1 – 100 µm) is considered as a non-Brownian system, nanocomposites with particles smaller 100 nm are often affected by Brownian motion. An overview about typical filler types and their size range is given in Table 4 [39], [40].

Table 4   Filler description and examples for fillers applied in polymer compounds [39]

Particle Type	Size	Filler examples
Brownian particles	Nanostructured	• Wollastonite ($CaSiO_3$) • Fumed silica (SiO_2) • Carbon nanotubes
	Micro-sized to nanometric particles	• Organoclays
Non-Brownian particles	Micro sized (>> 0.1 µm)	• Fibers (e.g. glass, carbon) • Calcium carbonate • Talc • ATH / MDH

Fillers exhibit different shape which plays an important role on final composite properties and processing. The major effect of geometry is a change in diffusivity for Brownian particles and a change of viscosity for non-Brownian particles [41]. Both effects are described in Figure 12 and Figure 13. The addition of spherical fillers affects compound viscosity less severe than the addition of platelets or fibrous structured fillers. This is caused by the aspect ratio and the specific surface [43].
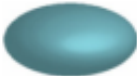
Aspect ratio (p)		Rotary diffusivity (D_{ro})
	Particles nearly spherical shape $p \approx 1$	$D_{ro} = \frac{k_b T}{\pi \eta_s d^3}$
	Circular disk-like particle $p < 1$	$D_{ro} = \frac{3 k_b T}{4 \eta_s d^3}$
	Prolate spheroids $p > 1$	$D_{ro} = \frac{3 k_b T(\ln 2p - 0.5)}{\pi \eta_s L^3}$
	Fibers, rods $p \gg 1$	$D_{ro} = \frac{3 k_b T(\ln(p - 0.8)}{\pi \eta_s L^3}$

Figure 12   Influence of geometry on the diffusivity of nanostructured particles [39]
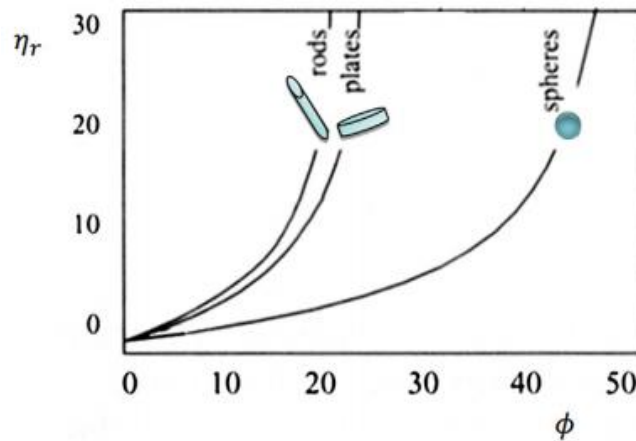
Figure 13   Schematic representation of the effect of particle shape and concentration (∅) on the relative viscosity of composites (η_r) [39]

The compounds covered in this work use micro sized fillers above 50 % dosage. Therefore, it is obvious from Figure 13, that rheology is a key property to investigate and the aspect ratio needs to be considered when judging observed effects. In addition to the shape and the dosage of the filler, also particle size distribution has an influence on the way the fillers interact with each other and with the system. To determine resulting properties in the investigated highly filled systems, the maximum packing fraction (MPF) and the rheological percolation threshold (PT) are of interest. Physically, MPF defines the maximum packing arrangement of particles while remaining a continuous (polymer) matrix material [44]. This parameter is strongly related to the geometry,

not to the particle size. As an example, for unimodal spherical particles, the MPF is 64 vol% [45]. This value can be increased by a multimodal combination of filler particle sizes as it is shown in Figure 14, where smaller particles can fill the interstices which allows a higher packing density [46].
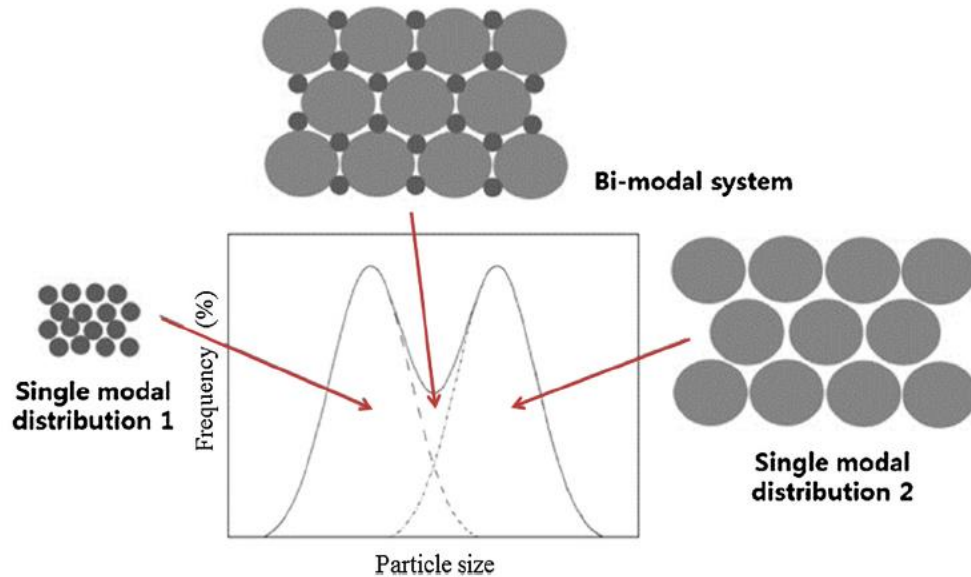
Figure 14   Schematic representation of a bimodal particle distribution [39]

The percolation threshold (PT) is often of interest for conductive fillers in polymers. The PT is defined as the concentration where filler particles start to be in contact with their closest neighbors. In this work, the rheological PT is of most interest. Above a certain concentration, the formed particle network creates bridges and paths throughout the material which increases viscosity significantly and hinders rheological and relaxation effects [47]. While the MPF does not react to changing unimodal particle size, PT decreases with particle size. This is caused by increased specific surface of the filler and the resulting capacity increase to form a network structure [48]. In general, it was found, that fillers smaller than 1 µm are propitious to form agglomerates which require a high-quality dispersion process. This is very close to the filler particle size used in this work which further highlights the need for a sufficient sample compounding methodology [44].

2.3.2   Compounding process

"Mixing of highly-filled polymeric systems is of paramount importance and determines the final properties of the mixture." [39, p. 32]

The compounding process is defined by incorporation of the filler into the polymer system, followed by dispersion and distribution through the matrix. Dispersive mixing describes the breakdown of a cohesive component (e.g. an agglomerate) which then needs to be distributed and spread through the matrix by convective transport. A schematic drawing of both effects is given in Figure 15. Distribution happens by stretching and reorientation of the matrix material. Due to the high viscosity of polymer melts, diffusion effects occur relatively slowly and do not contribute significantly during compounding [49], [50].
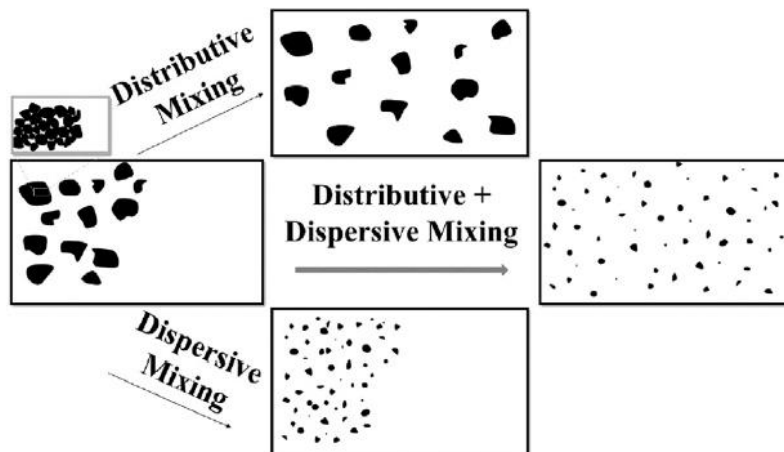
Figure 15   Schematic representation of distributive and dispersive mixing [49, p. 961]

During the mixing process, two types of forces act on the filler: cohesive forces (e.g. Van der Waals, electrostatic or capillary) which favor the formation of agglomerates and hydrodynamic viscous forces to disperse the agglomerates. As soon as the second category overcomes the first, dispersion caused by collision, rupture and erosion occurs [51].

Several mixing methods are commercially available and applied to incorporate enough hydrodynamic force into compounds. Due to the relatively high viscosity of the polymer melt and further increase by filler addition, highly filled compounds are processed on shear intense equipment like twin screw extruders, co-kneaders, two-roll-mills and internal mixing chambers. The processing equipment and parameters need to be chosen based on the raw materials and their processing limitations. Shear forces must be high enough to incorporate a certain amount of dispersive energy without initiating degradation effects or reactions caused by shear or temperature. Therefore, most of the mixing equipment show several opportunities to tune the process parameters and design mixing elements. This allows to influence shear force, residence time and temperature to control the materials viscosity in the processing steps [52], [53].

2.3.3 Polymer-Filler coupling mechanisms

It was observed that particle interactions dominate in low viscosity matrix materials below 100 Pas. Molten polymers are generally above this threshold, where these interactions are hindered. Nevertheless, as soon as particles come close enough, these interactions still occur. This led to the latest understanding, that from a certain value of filler level, the surface chemistry and filler shape play an important role. Studies showed starting interparticle interactions above a level of 20 vol%. The observed colloidal forces are either attraction or repulsion between particles which lead to agglomeration or dispersion. It was also proven, that with increasing filler content, the contribution of particle interactions versus hydrodynamic forces is growing [54], [55].

In most cases, the objective of filler incorporation is the modification of compound properties by particle-matrix interaction and not particle-particle interaction. These interactions depend on particle geometry, matrix material and surface chemistry of the filler. The usage of coupling agents allows to gain influence at the interface and increase polymer-particle interaction. This increased interaction often leads to increased dispersion quality. Another possibility to further improve particle dispersion is to increase interparticle-repulsive forces [5], [54].

Both approaches are commercially used for all fillers shown in Table 4 and find their application in polymeric compounds and suspensions. Often, both effects contribute together to a successful filler-polymer coupling system. Although a focus on mechanical strengthening effects leads the research trend towards increased polymer-particle interactions, dispersion quality and the resulting specific particle surface can also be influenced by surfactant effects. A large application space for surfactants is the stabilization of suspensions for ceramics production. By decreasing the elastic contribution to the viscoelasticity, the suspension character changes from being predominantly elastic to a viscous liquid [55], [56].

Most of the filler coupling agents in highly filled compounds target the improvement of mechanical properties by increased degree of dispersion and interaction. A relatively new application is the modification of nanoparticles to generate exfoliation effects of nanoclays in flame-retardant compounds [13].

According to literature, four key properties must be met to allow an effective coupling: [39]
- The adsorbed polymer layer needs to be thick and covering enough for building up interaction forces. [57]
- The polymer needs to be strongly anchored to the filler surface.
- The polymer should be soluble in the matrix material.

The conformation of the adsorbed layer of coupling agent is strongly related to its chemical nature, from a molecular point of view four configurations exist (see Figure 16). Different mechanisms of adsorption can be found: ligand exchange, ionic interaction by acid-base reaction, hydrogen bonding and chemisorption [41].
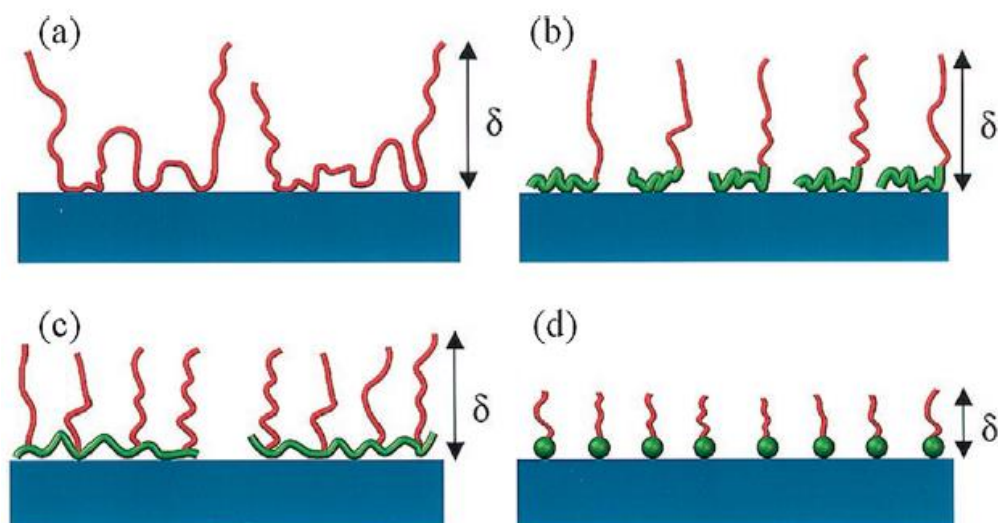
Figure 16   Schematic representation of coupling agents' structures: (a) homopolymer, (b) diblock copolymer, (c) comb like block-copolymer, (d) functional short chain polymer [39]

Mechanical reinforcement is achieved by a force transmission to the particles or fibers through the filler surface. This force transmission can be improved by enhancing the filler coupling using the already described methods. It is crucial, that the polymeric chain of the coupling agent is above a critical molecular weight to ensure proper matrix entaglement. The combination of different chain lengths was reported as beneficial due to a reduced steric hindering of the surface modification. This was also proven in preliminary trials where too high amounts of coupling agent have shown performance limitations [58], [59].

To further highlight the effect of coupling, some examples of commercial coupling agents and their reaction are given in the following paragraph. Two major classes of materials are used to connect polymers with inorganic fillers: silanes and grafted copolymers [55]. The typical structure of a silane is $X_3Si-R-Y$, where Y is an organofunctional group (to bond with the polymer) and X is a hydrolysable group. X either reacts in water to Si-OH or with mineral hydroxide groups (M-OH) to form an oxane bond M-O-Si. R represents an organic structure with various chain length and functionality. Typical organic groups (Y) used in thermoplastic polymer systems are vinyl, allyl, amino, methacryloxy and epoxy. Due to its chemical nature, silane is very famous in the modification of the interface between polymer and glass [58]. The reaction of a silane in the

interface between polymer and magnesium-di-hydroxide filler is shown in Figure 17. The silane creates a functional structure on the inorganic filler by hydrolysis which allows the polymer to interact with. Based on the type of organofunctional group, the silane can be coupled by hydrogen bonds or Van der Waals forces. Additional coupling can be achieved by combination with functional peroxides to create covalent bonding to the polymer phase. This step of reactive extrusion can be performed during compounding but requires a very controlled processing and dosing ability. The amount and type of peroxide, as well as processing temperature and shear force show an effect on the resulting coupling functionality. Suppliers of flame-retardant fillers have developed grades which are pre-coated with different silane types. This enables a more even dispersion of the coupling agent throughout the filler and reduces the number of processing steps before compounding. This also solved a common issue with limited shelf life of compounds due to hydrolysis of the silane caused by humidity during storage [54], [55], [58], [59].
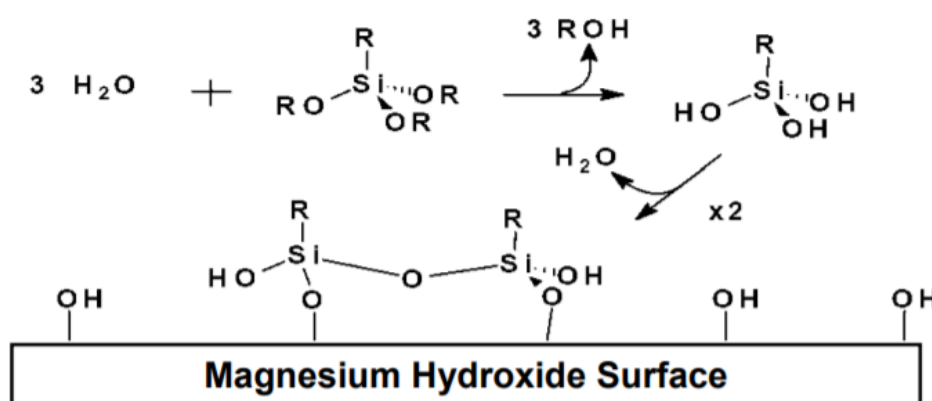
Figure 17   Schematic view of interfacial bonding by a silane coupling agent [60]

While silanes are reported to be used since 1951, a newer approach is the usage of grafted copolymers. This was developed to overcome the complexity of reactive extrusion generating sufficient interaction with the polymer matrix [61]. While the silane reacts with the OH-groups of the filler relatively reproducible, a stable interaction with the polymer matrix (that often is a blend system) can be challenging. Therefore, the approach was to separate the step of peroxide grafting to better control the amount and type of polymer that is grafted. Common coupling agents for the coupling of inorganic filler in polyolefins are maleic-acid-anhydrite grafted. They are simply mixed into the polymer matrix in a certain ratio to provide the coupling effect [62]. A typical coupling reaction is shown in Figure 18 where maleic acid anhydrite (MAA) grafted Polypropylene (PP) reacts with the surface of a cellulose fiber. The MAA opening reaction is triggered by temperature (above 180 °C) or change in pH value, which allows a controlled coupling point in the compounding process. The reaction products can be either a mixture of

covalent and hydrogen bonds (bottom left) or pure covalent bonding (bottom right). The ratio of MAA-g-PP affects the coupling strength if the polymer backbone is long enough to generate entanglements or crystalline areas. The reactivity of the coupling agent is controlled by the amount of MAA groups and the accessibility for the filler surface [63]. The successful application of such coupling additives has led to the development of terpolymers which have the MAA group built into the polymeric chain. This resulted in reports of reduced reactivity but more stable bonds with reduced water migration and permittivity for gases [55], [59].

This mentioned method of filler coupling is growing, due to the relatively easy handling in the compounding process. The functional copolymer is added by dry-blending with the polymeric matrix and does not show as severe shelf-life issues as silane does [63].
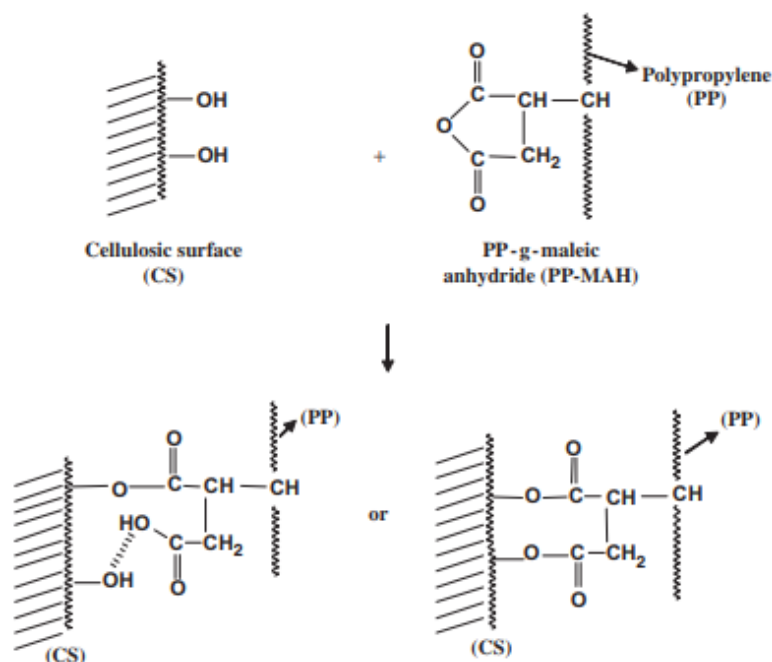
Figure 18   Esterification reaction at the interface of a cellulosic fiber and MAA-g-PP used as coupling agent [63]

2.3.4   Properties of highly filled polymer compounds

A brief overview about filler types was given in section 2.3.1. This highlights the resulting difference in properties of compounds made with different filler types and the need for the right filler in the right spot. To stay focused on the performed investigations, the following overview will focus on particulate fillers in a dosage above 30 vol%.

Investigations of highly filled polymer compounds give one clear statement regarding their properties: a fully dispersed and stable state leads to optimal properties. Every particle

agglomerate leads to a defect and reduced material performance. While a certain aspect ratio of fillers (e.g. in short glass fibers) is used to improve mechanical strength or stiffness, some fillers like calcium carbonate are added to reduce cost of the material. Nevertheless, all highly filled compounds undergo a certain behavior with increasing filler content which differs from their unfilled version [64].

The composition of the matrix strongly influences the response to filler addition – the reinforcing effect increases with decreasing matrix stiffness. This was shown in a comparison in Figure 19 between a filled LDPE and rigid PVC composite. The stiff PVC responded with a drop in mechanical performance while the more flexible LDPE showed increased yield stress [43]. Another important factor is the already mentioned aspect ratio which results in different mechanical response (highlighted in Figure 19 the right side). The stiffening effect of inorganic filler addition is often limited by the effect of filler aggregation which results in agglomerates and defects. This can be improved by the addition of coupling agents, but never can be avoided [43], [41]. Aggregation happens more likely, the smaller the filler particles are (see Figure 20). Another important effect that creates morphological differences between filled and unfilled polymer systems is a change in crystallinity in semi-crystalline resin systems. Small amounts of fine dispersed particulate fillers act as nucleating agents. Different strength in nucleating effects is mainly dominated by topological factors. A change of the crystallization structure of polymers by affecting the crystallization temperature in highly filled PP systems was reported (see Figure 20 right) [43].
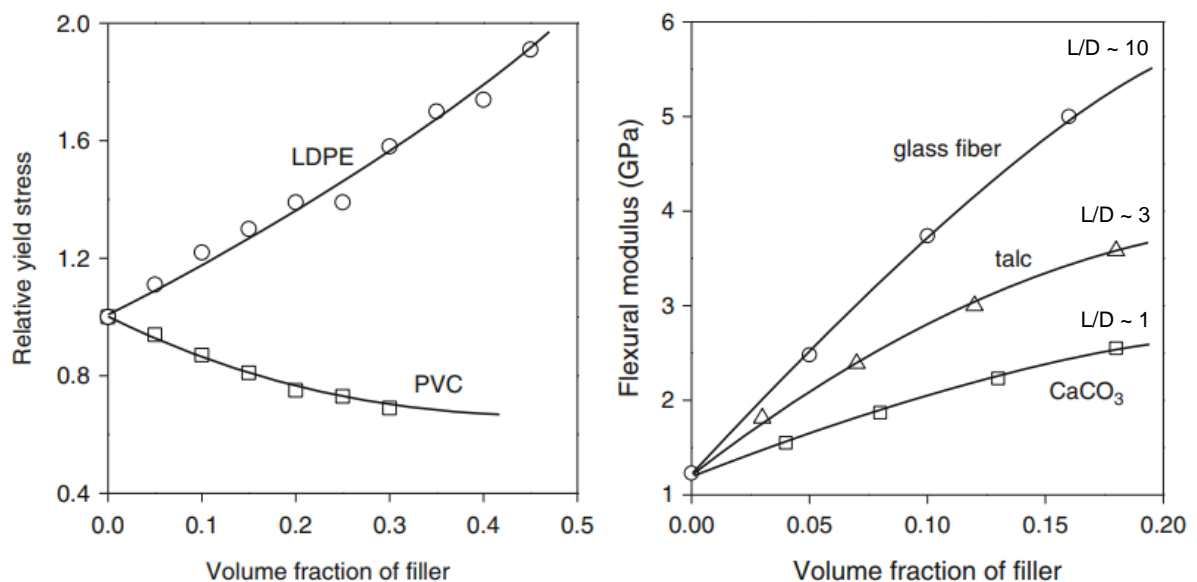
Figure 19   Effect of matrix compositions in CaCo3 filled composites (left) and different filler types in a PP based compound (right) [43, p. 55 & 58]
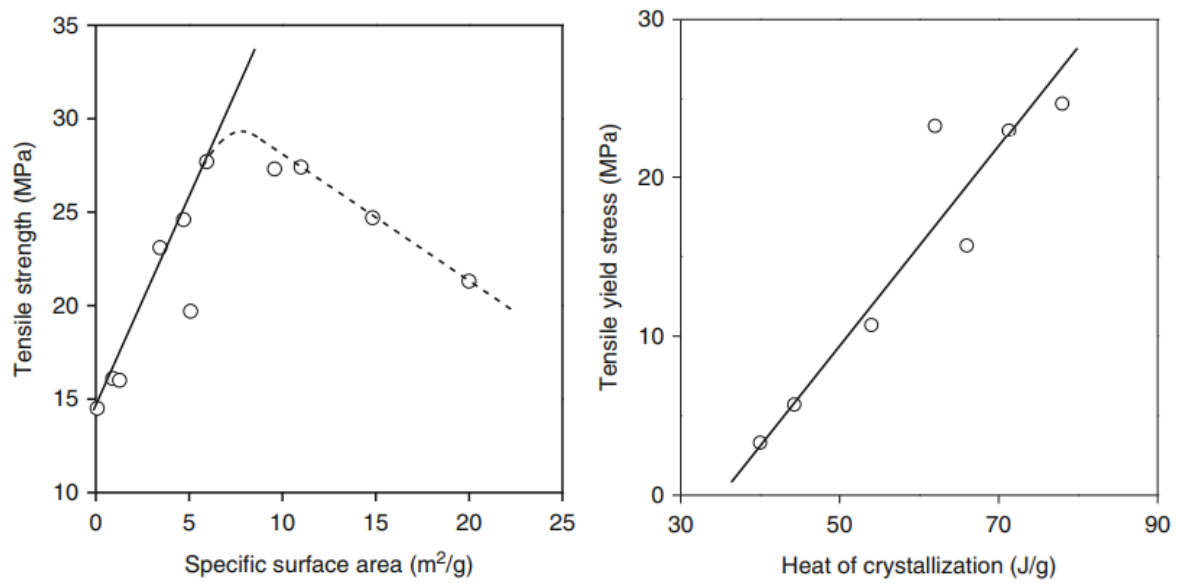
Figure 20   Strength of PP/CaCO3 plotted as a function of specific surface (left) and correlation of heat of crystallization with yield stress of PP/CaCO3 composites (right) [43, p. 63 & 60]

Reviewing literature regarding this topic, it becomes clear that a good mechanical performance is dependent on sufficient interaction of the filler with the polymer which is mainly realized by surface treatment [63]. An example of the mechanical response in highly filled systems to successful and insufficient coupling is given in Figure 21, where good and poor adhesion results in completely different material performance.
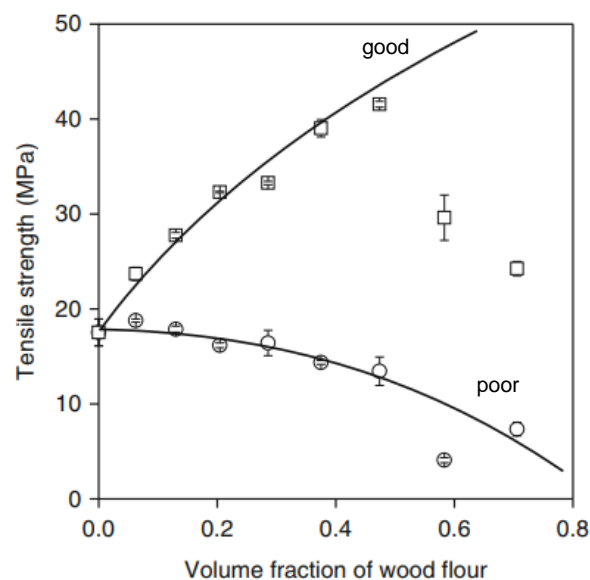
Figure 21   Dependence of tensile strength in PP/wood flour composites with poor adhesion (o) and good adhesion (□) [63]

A response to the addition of filler can not only be seen in the mechanical performance, but also in the rheology of the material. Processing of filled compounds implies structural reorganization of filler particles in addition to polymer chains which can result in the formation of filler networks or particle interlocking [39]. Most highly filled polymer systems show shear thinning behavior. Three different types of regimes were observed for highly filled suspensions which are described in Figure 22 [65]. No rheological behavior changes were observed for low particle concentrations (< 0.18). Up to a concentration of 0.43, the suspensions show a Newtonian plateau for low shear rates. This is a sign for a contact-percolation threshold where a three-dimensional filler network is maintained in low shear rates in rheological measurements. The continuous increase to infinity for higher filler levels at low shear rates is called "yield stress effect". Suspensions in low viscous phase and high filler quantities have been reported to require a certain stress to bring the suspension to flow [66]. Beyond a filler rate of 0.28, the suspensions show a shear thinning behavior with increasing shear rate. The stress transmitted through the matrix is high enough to disrupt the 3D structure and the distances between particles. This leads to increased distance in normal direction and decreases in flow direction. This forms a layered structure with less resistance to flow. The higher the network formation effect is, the higher is the tendency to shear thinning behavior [67]. With increased shear rates and high degree of filling (< 0.43), the viscosity increases which is caused by physical interlocking of the particles. The observed effect of shear thickening behavior was differentiated from dilatancy in some publications. It is important to note that not all matrix-filler combinations exhibit all the mentioned regimes and an interface modification has strong influence on the general behavior [68], [40]. Moving closer to investigated systems of polyolefins, the influence of increased filler content in a thermoplastic polymer is shown in Figure 23. The Newtonian plateau becomes shorter with increased filler level, shear thinning behavior is observed for all concentrations. Within the tested range, no yield stress or shear thickening effects are observable [69].
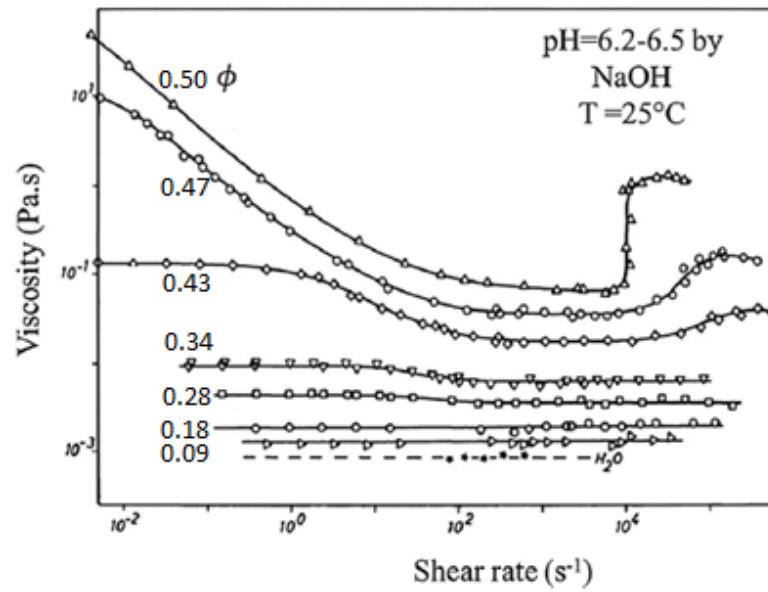
Figure 22   Viscosity versus shear rate of SEBS latex particles at different particle concentrations in an aqueous polymer dispersion [65]
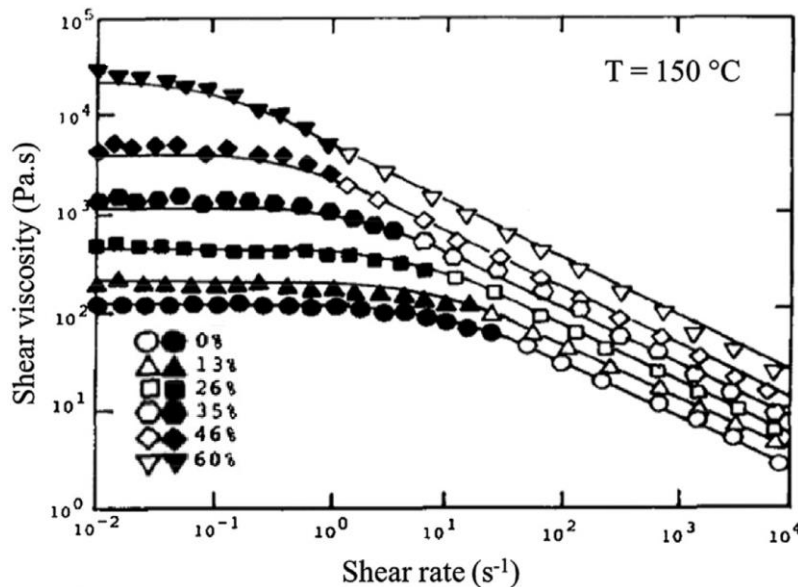
Figure 23   Shear viscosity of glass spheres suspended in molten thermoplastic polymer [69]

2.3.5   Filler surface modification in highly filled polymer systems of interest

The concept of surface treatment of filler using silanes was introduced in section 2.3.3. The type of silane for modification needs to be chosen to fit the type of matrix polymer. Typical coatings to be used in combination with polyolefins are vinylsilane for reactive extrusion (grafting of polyethylene) and aminosilane for more polar components (like EVA). Silane coatings of flame-retardant fillers in LDPE were reported to increase dispersion quality as it can be seen in Figure

24. Furthermore, the usage of Amino- (b), Dodecyl- (c) and Vinylsilane (d) have shown improvements in electrical insulation in comparison to untreated filler (a). The vinylsilane coating showed the best performance among all samples. Stronger polymer-filler interaction was proven, but the effect not yet understood [70].
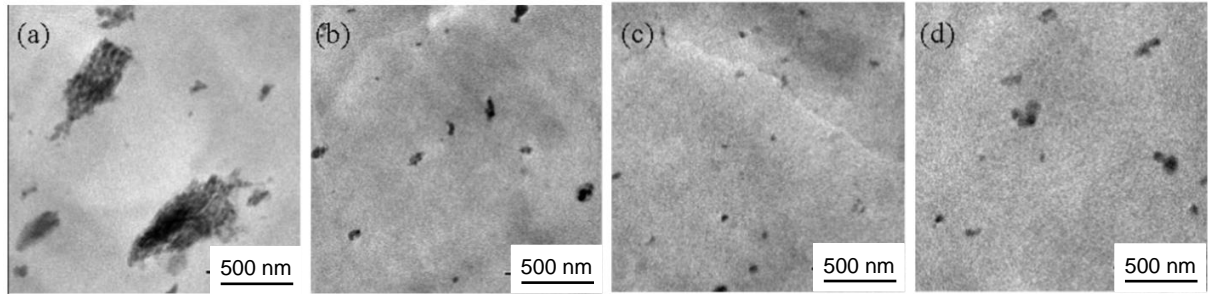
Figure 24   TEM micrographs of LDPE nanocomposites filled with 3 phr nanoparticles:
(a) R-MgO, (b) A-MgO, (c) D-MgO, and (d) V-MgO [70]

Investigations by Chen et al. [60] focusing on surface treated flame-retardant fillers in EVA have shown differences in filler-polymer interaction. This was identified by tensile testing and different levels of torque during compounding (see Figure 25). Uncoated (MDH-1) and aminosilane-coated (MDH-2) MDH showed the highest compounding torque which represents high interaction. Vinysilane coating (MDH-3) shows significantly reduced values, slightly above the control sample with fatty-acid (MDH-5) which is designed to avoid any polymer interaction. The resulting mechanical properties fit very well to this observation with the samples having a higher torque also showing the best combination of elongation at break and tensile strength. Aminosilane shows the highest coupling effect to EVA.
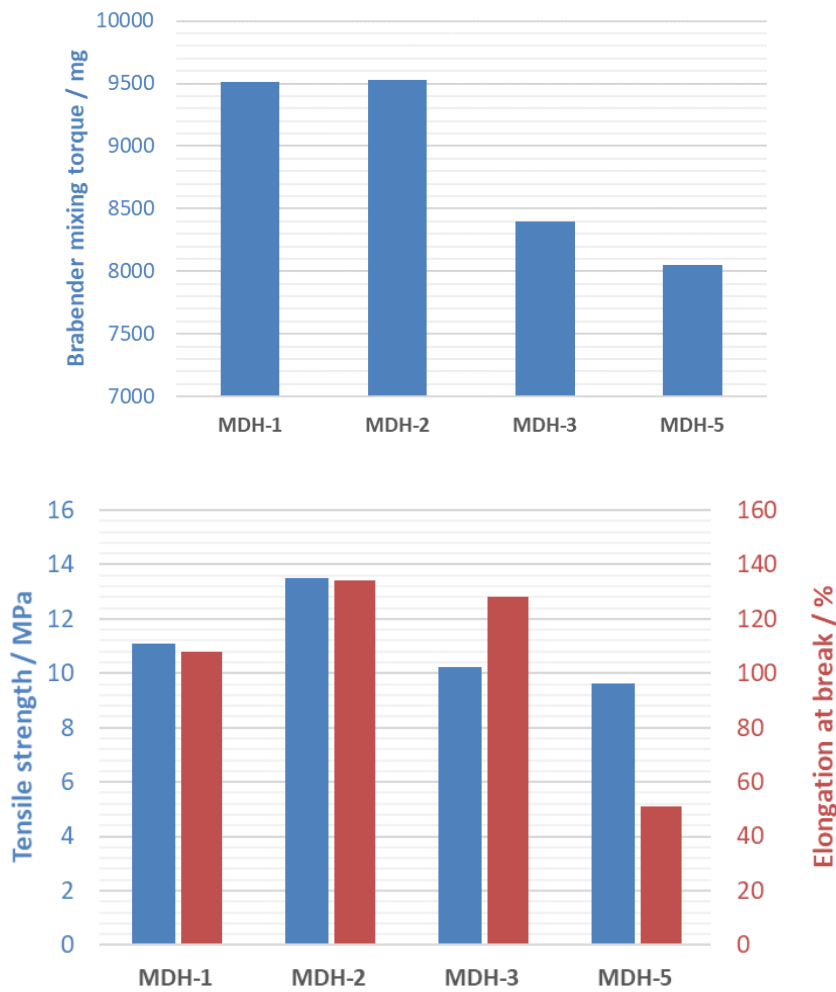
Figure 25   Compounding torque and mechanical properties of EVA filled with coated
               Magnesiumhydroxide: uncoated (1), Aminosilane (2), Vinylsilane (3), Fatty-acid (5) [60]

The aminosilane coating was designed to enable interaction with EVA through hydrogen bonds. Furthermore, Tham et al. [71] recently observed interaction of silica nanoparticles in EVA even in absence of aminosilane. This led to the theory of interaction that is shown in Figure 26. As the surface of magnesium-di-hydroxide (MDH) is also covered in OH groups, an interaction of uncoated filler with EVA can be possible.
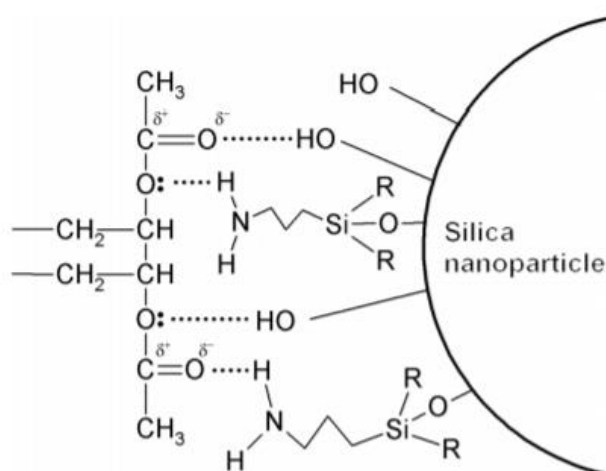
Figure 26   Proposal scheme of hydrogen bonds between ethylene vinyl acetate copolymer (EVA) and silica modified by aminosilane [71]

The shown investigations of filler coupling and surface modification effects are mainly covering either pure LLDPE or pure EVA as a polymer matrix. Blends of both were not investigated within this focus. Furthermore, the reported effects are neither comparable, nor fully understood.

3   Objective and Structure

As shown in the recent section, there is still a need for deeper investigation and understanding of highly filled halogen free flame-retardant compounds used in the cable industry.

Therefore, the objective of this work is to generate a fundamental scientific understanding of the influence of various coupling mechanisms on the structure-properties-relationships of highly filled, flame-retardant EVA/LLDPE based cable compounds.

Based on the complexity of the EVA/LLDPE compounds, it must be considered, that several ingredients are interacting with each other in a complex way. Therefore, the investigations are split into different systematical working steps. The graphical abstract in Figure 27 is describing the major working packages (WP). From these working packages, the following sub-objectives are derived:

- **Understanding the influence of the mixing ratio of EVA and LLDPE and the applied coupling agent on the blend morphology and structure-property-relationships.**

  To ensure a stable quality of samples and results throughout the whole work, standardized processing and test procedures were developed prior to further investigations (WP0). These are applied in WP1 (chapter 6.1), where unfilled polymer blends of EVA and LLDPE are investigated. The mixing ratios are varied from 0 to 100 % EVA in 25 % steps. A recipe with 45 % EVA is added to investigate the expected phase inversion point between 45 % and 50 % EVA according to literature. Furthermore 67 % of EVA is chosen as this represents a typical cable compound recipe. Commercially available maleic-acid-anhydrite grafted EVA and LLDPE are added as coupling agents in different dosages (0-10 %) based on supplier recommendations. This shall answer the question, how coupling agents themselves affect the polymer blend. The goal is to generate a broad picture of the target polymer systems and the response to different mixing ratios without flame-retardant filler.

- **Determination of the influence of Magnesium-di-hydroxide filler concentration as a flame-retardant on the compound morphology and structure-property-relationships.**

  Based on the results and observed effects from WP1, key formulations were defined and applied in WP2 (chapter 6.2). They are chosen as 0 %, 45 %, 50 %, 67 % and 100 % of EVA to cover the pure polymers, the regions before and after phase inversion and a typical cable recipe. The formulations are filled with different ratios (10, 30, 60 %) of a flame-retardant additive (Magnesium-di-hydroxide). Objective is to investigate the response of the polymeric

system's morphology to the filler addition. All samples are compounded with and without the coupling agent to further understand the effects of the maleic-acid-anhydrite grafted copolymers.

- **Understanding the influence of maleic-acid-anhydrite copolymer and silane filler coatings as coupling systems on compound morphology and structure-property-relationships.**

  In WP3 (chapter 6.3), the influence of the flame-retardant filler with different silane coatings are investigated. The used fillers are commercially available, and pre-coated with vinylsilane (recommended for reactive extrusion) or aminosilane (recommended for EVA based systems). The two coatings are chosen to represent different types of filler-polymer interaction: the ability to form covalent bonds in the presence of radicals (vinylsilane) and the ability to form hydrogen bridges (aminosilane). The resulting properties are compared with recipes from WP2 using uncoated filler. The polymer formulations stay the chosen from WP2, the filler concentrations were set as 30 % and 60 % as they have shown distinct effects in WP2.

- **Optimization of the compound formulation regarding concurrent mechanical properties and flame retardancy based on the derived structure-property-relationships.**

  By summarizing the key learnings and understandings, the best properties and synergistic effects are chosen to optimize the performance of the investigated halogen free flame-retardant cable compound.

To generate a broad understanding of the structure-properties-relationships, the following properties are investigated in each working package:

- Polymer, blend and filler morphology
- Thermal properties
- Thermo-mechanical performance
- Material relaxation and rheological behavior
- Filler location
- Fire retardancy
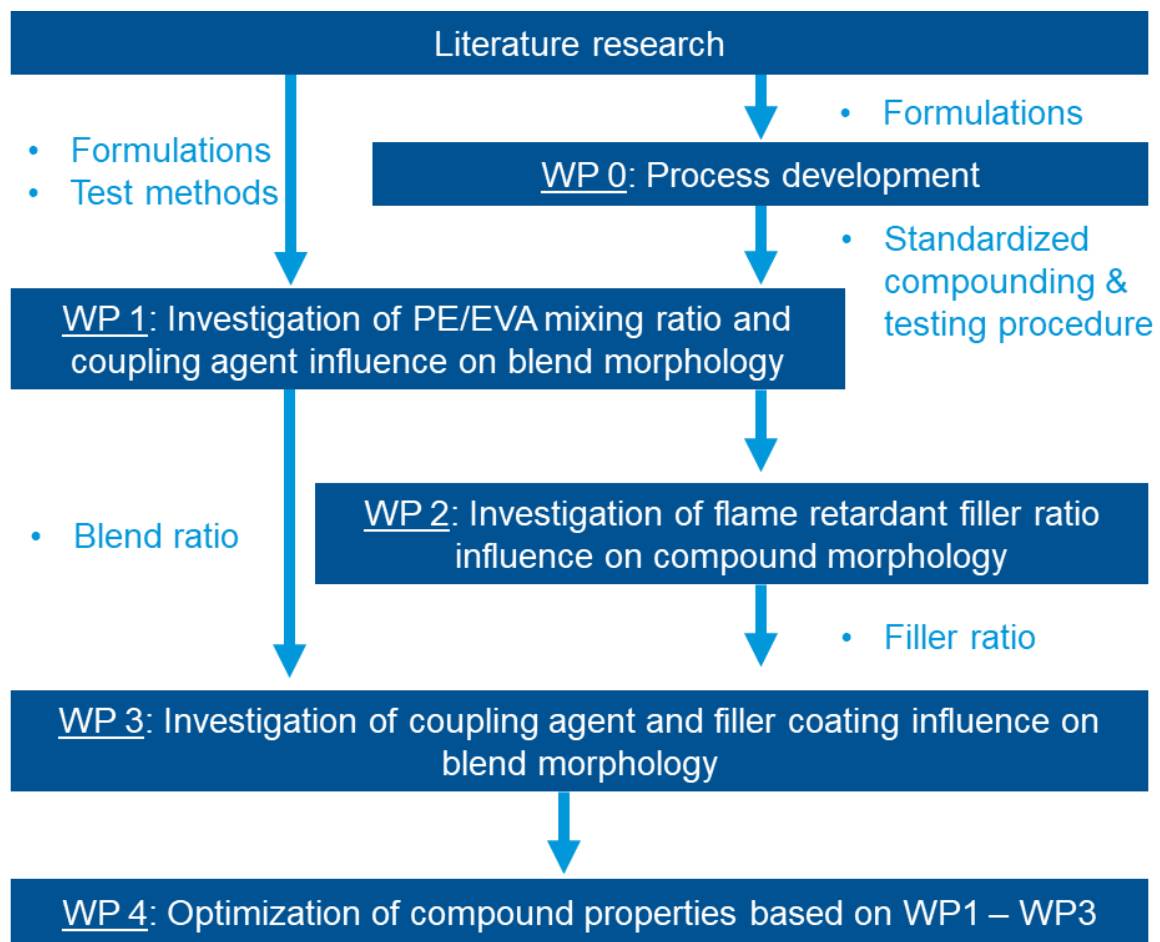
Figure 27   Graphical overview about the structural approach defining different working packages (WP)

4 Materials

4.1 Linear low-density polyethylene (LLDPE)

LLDPE is a commonly used material in halogen free flame-retardant cable compounds [2]. Due to the high mechanical requirements and thin layer extrusion, in this work Dowlex 2045G from DOW was chosen. It is a Ziegler-Natta catalyzed 1-octene co-monomer LLDPE for blown film applications with high toughness and high tear strength [72]. The technical properties are given in Table 5.

Table 5   Properties of the used LLDPE from technical datasheet [73] (*), performed measurements (**), literature [72] (***)

Property	Value		Standard
Grade name	Dowlex 2045G		
Density*	0.92	g/cm^3	ASTM D792
Tensile strength**	32.9	MPa	EN ISO 527-2
Yield strength**	10.4	Mpa	EN ISO 527-2
Elongation at break**	1060	%	EN ISO 527-2
Vicat Softening Temperature*	106	°C	ASTM D1525
Melting Point*	119	°C	ISO 11357-3
MFR (150 °C/21.6 kg) **	12.8	g/10min	ISO 1133-1
Molecular weight M_w***	108700	g/mol	GPC

4.2 Ethylene-vinyl-acetate (EVA)

To overcome increasing stiffness and improve the flexibility of LLDPE in combination with mineral filler, LLDPE is blended with EVA [2]. The Ethylene-vinyl-acetate used in this work was Evatane 24-03 from Arkema with a vinyl-acetate content of 24 wt%. This type gives a balance between flexibility and filler uptake while maintaining a certain mechanical strength and processability. The technical properties are given in Table 6.

Table 6   Properties of the used EVA from technical datasheet [74] (*) and performed measurements (**)

Property	Value		Standard
Grade name	Evatane 24-03		
Vinyl-acetate content*	24	wt%	FTIR (internal method)
Density*	0.94	g/cm^3	ISO 1193
Tensile strength**	25.1	Mpa	EN ISO 527-2
Yield strength**	3.3	Mpa	EN ISO 527-2
Elongation at break**	1400	%	EN ISO 527-2
Vicat Softening Temperature*	46	°C	ASTM D1525
Melting Point*	80	°C	ISO 11357-3
MFR (150 °C/21.6 kg) **	43.9	g/10min	ISO 1133-1

4.3 Filler: Magnesium-di-hydroxide (MDH) flame retardant

To create halogen free flame-retardant cable compounds, the mentioned LLDPE/EVA blends are combined with metal-hydroxide based fillers [22]. The functionality of these mineral fillers is as described in chapter 2.1.2. In this work, it was decided to use Magnesium-di-hydroxide (MDH) due to the commercial availability and high reproducibility in particle sizes and surface modifications. The decomposition temperature of 330 °C allows a broader processing window than ATH (210 °C). The specific surface area (BET) is kept stable for all filler types to avoid any influence of different particle sizes. A comparison of the properties is given in Table 7. As different couplings mechanisms shall be investigated, Magnifin from Huber with different surface modifications was used. The chemical structures of the surface coatings are described in section 4.4.2. To give a picture of the particle morphology, a SEM micrography of Magnifin H-5 is shown in Figure 28. The particles exhibit a hexagonal platelet structure close to the plates described in section 2.3.1.

Table 7   Properties of the used MDH types [75]

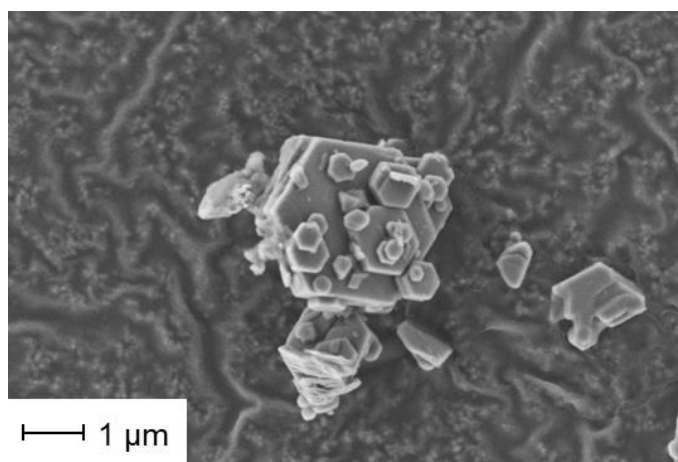| Property	Magnifin H-5	Magnifin H-5A	Magnifin H5-IV
Formula	$Mg(OH)_2$		
Spec. surface area (BET)	4.0 – 6.0		
Particle Size D50	1.6 – 2.0 µm		
Density	2.4 g/cm^3		
Physical form	Powder		
Particle morphology	Hexagonal platelet		
Surface coating	none	vinylsilane	aminosilane
Sample name	MDH	MDH VS	MDH AS

Figure 28   SEM micrograph of Magnesium-di-hydroxide particles

4.4 Filler coupling agents

4.4.1 Functional co-polymers

The polymers described in section 4.1 and 4.2 were combined with the flame-retardant additives from section 4.3. To further modify and improve the polymer-filler interaction, coupling agents based on functionalized co-polymers were used. Maleic-acid-anhydrite grafted versions of LLDPE and EVA were chosen to ensure the miscibility with each of the base polymers. The functionality of the grafted maleic-acid-anhydrite group is described in section 2.3.3. The used MAA-g-LLDPE is Tabond 3044 from Silon, the MAA-g-EVA is Orevac 9304 from Arkema. Properties of the used coupling agents are listed in Table 8.

Table 8   Properties of the used coupling agents from technical datasheets [76], [77] (*) and performed measurements (**)

Property	Tabond 3044	Orevac 9304	Standard
Graft type	random	random	
Base polymer type	LLDPE	EVA	
Vinyl-acetate content*	-	25 %	FTIR (internal method)
Density*	0.94 g/cm^3	0.94 g/cm^3	ISO 1193
Tensile strength**	28.9 MPa	24.1 MPa	EN ISO 527-2
Yield strength**	9.1 MPa	2.9 MPa	EN ISO 527-2
Elongation at break**	840 %	720 %	EN ISO 527-2
Melting Point*	122 °C	80 °C	ISO 11357-3
MFR (150 °C/21.6 kg) **	6.1 g/10min	75 g/10min	ISO 1133-1

4.4.2 Filler coatings

The usage of silane surface modified fillers as it was described in section 2.3.3 gives the ability to control the polymer-particle interaction. It was decided to investigate fillers coated with two silane types shown in Figure 29 due to their commercial relevance and the state of the art shown in section 2.3.5. The filler is commercially available and is based on the uncoated grade of MDH shown in section 4.3. This gives a high degree of reproducibility and stability throughout the work.
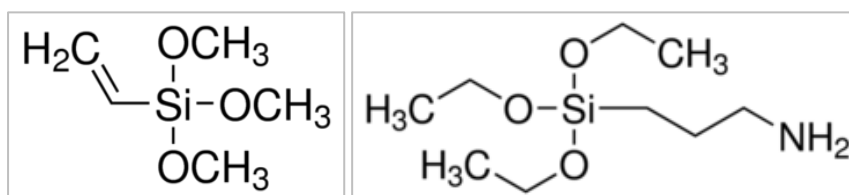
Figure 29   Chemical structure of filler coating types: vinyltrimethoxysilane (left) and (3-aminopropyl)triethoxysilane (right) [55]

The reaction mechanisms of both silane coatings are described by the supplier and drafted in Table 9. Vinylsilane is able to form covalent bonds in reactive extrusion in the presence of radicals (e.g. by adding peroxides). Early-stage trials have shown signs of interaction with maleic-acid-anhydrite copolymers. To investigate possible coupling effects with these copolymers, vinylsilane is part of this work. Peroxide grafting reactions were excluded from this work because of the complexity and reported crosslinking reactions with the EVA polymer [55] [62] [59].

Aminosilane has the ability to form hydrogen bridges with EVA. Furthermore, the formation of covalent bonds with the just described MAA-grafted coupling agents was reported [59].

Table 9   Schematic overview of the silane surface coating coupling functionality with the investigated EVA & LLDPE polymers and MAA-grafted coupling agents [78]

Vinylsilane	Aminosilane	
Coupling with Polyethylene	Coupling with EVA	Coupling with MAA-g-Copolymer
Covalent bonding in the presence of radicals	Hydrogen bridges	Covalent bonding

5   Experimental methodology

5.1   Sample production and preparation

To ensure sufficient compounding and sample processing quality throughout the filler concentration range of the planned formulations, initial trials were carried out. Compounding process parameters were varied, using a basic set of formulations known from cable production and based on internal development. In the following, the material was further processed into sample specimen. The chosen settings of sample production and preparation were then used in this work to ensure a contin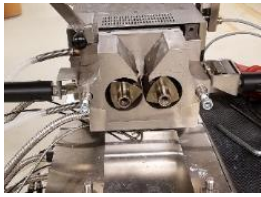uous and stable process. An overview about the processing methods and resulting specimens is given in Table 10, all steps are described more detailed in the following sections.

Table 10   Overview of used equipment for sample preparation and resulting specimen

Equipment			
Kneader	Rotary Mill	Extruder	Heat press
Resulting specimen			
Melt pieces	Pellets	Strands	Plates

5.1.1   Compounding process

The investigated materials were compounded on a discontinuous counter-rotating kneader (Brabender 350E). The process order was adapted from larger scale continuous compounding units where the ingredients are added in different ports along the processing length. The raw materials are filled stepwise into the 150 °C heated processing chamber with turning blades at 30 rpm. Starting with the polymers, the powder shaped additives are added in the second step after a 3-minute time window for melting. The additives are added continuously within 4 minutes to ensure a stable and proper uptake by the polymer. After adding all powder content, the processing chamber is closed until the mixing and dispersion process in step 3 is finished. The

time and screw speed of the third step were varied in preliminary trials. The outcome and final defined settings are described in section 5.1.2.

After finishing the mixing process, the chamber is opened and disassembled, the melt is removed in pieces and cooled down in ambient temperature. For further processing steps, the pieces are pelletized in a rotary mill.

5.1.2   Preliminary mixing trials

The first practical step of this work was the evaluation of the sample processing methodology. As already described in section 2.3.4, filler dispersion is a key property affecting the performance of the targeted systems. To ensure a proper and stable quality, trials to investigate the influence of the mixing time and screw speed of compounding step 3 were carried out (see Table 11).

Table 11   Overview of investigated mixing parameters during compounding step 3

Setting	Screw speed	time
1	30 rpm	5 min
2	30 rpm	10 min
3	50 rpm	5 min
4	50 rpm	10 min

The compound formulations were chosen from literature [22] and Corning's own flame-retardant cable compounds. The compounds contained from 0 to 60 wt% filler with different LLDPE/EVA ratio. The mechanical performance of extruded strands was rated as this is a critical property to rate dispersion quality [56]. In addition, MFI and SEM micrographs were analyzed to check for agglomerates. Potential polymer degradation effects were excluded using rheological analysis (time sweep at the mixing temperature).

Based on the investigations, setting 3 (50 rpm for 5 minutes) showed the best results and was defined as a standard procedure for all further trials.

5.1.3   Strand extrusion

To perform mechanical and thermo-mechanical testing, the pelletized materials were extruded into 1 mm x 20 mm strands. The extrusion was performed on a 19 mm single screw extruder (Brabender) with an L/D of 25 using a 3-zone screw with a compression ratio of 2:1. The screw

speed was set to 30 rpm at the temperature profile given in Table 12. The strand is extruded onto a conveyor and cools down at ambient temperature.

Table 12   Temperature profile used for strand extrusion

Zone	Feed zone	Zone 2	Zone 3	Die
Temperature	150 °C	155 °C	160 °C	165 °C

5.1.4 Heat pressing

Sample sizes with a thickness higher than 1 mm (e.g. for Cone Calorimeter) were prepared by compression molding in a 2-level heat press (Servitec Polystat P200 T/2). The material is aligned in a steel frame between steel plates and heat-pressed at 170 °C with a two-step pressing program. The program allows the release of air inclusions during a 3 minute melting phase at 15 bar. This is followed by a pressure increase to 100 bar and held for 7 minutes, interrupted by a degassing step after 3 minutes. The press-package is then removed and put into the lower press level where it is actively cooled to 20 °C under pressure to avoid warping.

5.2 Characterization

5.2.1 Rheological characterization

5.2.1.1 Parallel plate rheology

The rheological studies were performed using a parallel plate rheometer (TA Instruments ARES-RDA III) in strain control mode. The frequency sweeps were carried out from 100 to 0.1 rad/s at a temperature of 150 °C and a shear deformation of 1 %. Investigations of polymer stability were additionally carried out in a time sweep at 150 °C, 1 rad/s and 10 % deformation for 1 hour.

5.2.1.2 Melt volume rate (MVR)

The compound melt viscosity was also measured using melt volume rate testing (Zwick MFlow). Although the parallel plate rheometry gives much broader information about the samples, the tests were carried out as they are of interest in the industrial application regarding incoming inspection and quality control. The tests were carried out according to ISO 1133 using a flat die with a diameter of 2.095 mm. The testing temperature was 150 °C and a load of 21.6 kg was used. Pre-heating time was set to 5 minutes before the piston was released.

5.2.2   Thermal characterization

5.2.2.1   Differential scanning calorimetry (DSC)

The melting and crystallization behaviors were determined by differential scanning calorimetry (TA Instruments DSC Q2000). The sample size varied from 3 – 10 mg in a temperature range from -60 °C to 200 °C under nitrogen atmosphere (50 mL/min). The heating rate was 10 °C/min, the cooling rate was set to 5 °C/min to ensure a stable cooldown. Some samples contained mineral filler which does not participate in enthalpy changes during the test. To compare the response throughout different filler loadings, the signals were normalized to the polymer content. The DSC curves showed a growing displacement with increased filler loading due to the heat capacity of the mineral based filler. To overcome this effect and allow the calculation of the crystallinity by integration, all measurements of filled samples were additionally corrected by pure MDH baseline subtraction. The results were obtained from the second heating cycle and analyzed using the universal analysis software from TA Instruments.

5.2.2.2   Thermo-gravimetric analysis (TGA)

The thermal decomposition behavior was determined using thermo-gravimetric analysis (Netzsch TG209 Libra). The measured temperature range was from 25 °C – 800 °C with a heating rate of 10 K/min in air atmosphere (50 ml/min). The amount of flame-retardant filler in the original sample was calculated based on the measured magnesium-oxide residue using the molar decomposition behavior shown in section 2.1.2.

5.2.3   Thermo-mechanical characterization

5.2.3.1   Tensile test

The characterization of the tensile performance was done according to EN ISO 527-2 on specimen type 2A which were die-cut from 1 mm thick extruded strands in extrusion direction. The tests were performed on a universal testing machine (Zwick) in ambient temperature of 23 °C and a relative humidity of 50 % (+/- 10 %). The elastic modulus determination was done at 1 mm/min testing speed, which was afterwards increased to 50 mm/min. Due to the high elongation values, the displacement was recorded through traverse channel. At least 5 specimens of each sample were tested.

5.2.3.2   Hysteresis measurement

To characterize the elasticity of the compounds, hysteresis measurements were carried out on the same setup used for tensile tests. The samples were cut in tensile bars in extrusion direction and

tested at 1 mm/min speed until 50 % strain, followed by a load relief phase until 0 MPa stress was reached in the same speed.

5.2.3.3 Dynamic mechanical analysis (DMA)

The thermo-mechanical properties were tested using dynamic mechanical analysis (Netzsch-Gabo Eplexor 500N). The samples were cut from extruded strands into 40 x 10 mm samples resulting in a parallel sample length of 25 mm and tested in tensile mode in extrusion direction. The tested temperature range was set from -100 °C to +100 °C with a heating rate of 2 K/min. The applied frequency was 1 Hz, strain controlled with 0.5 % static strain (maximum force 80 N) and 0.1 % dynamic strain (maximum force of 50 N).

5.2.3.4 Coefficient of thermal expansion (CTE)

The coefficient of thermal expansion was tested using a thermo mechanical analyzer (TA Instruments TMA Q400) in the temperature range of -45 °C to 70 °C (5 °K/min). The CTE was defined in the second heating step through linear regression of the displacement curve from -20 °C to 20 °C. The maximum temperature was limited by the melting point of the EVA. As the shrinkage of the cable sheath during temperature cycling is of interest, the expansion was measured in extrusion direction of a strand. Therefore, a 20x1x1 mm thick specimen was cut from a strand using parallel razorblades.

5.2.3.5 Contraction stress

To judge the thermal contraction in the cable application, a laboratory scale test was developed prior to this work. The samples are cut from of extruded strands in extrusion direction and tested using a Dynamic mechanical analyzer (DMA). While the sample movement is fixed, the stress built up by thermal expansion within a temperature range is measured. A high value in contraction stress can be correlated to a higher shrinkage in the cable application. The detailed test setup and further parameters are proprietary.

5.2.4 Morphological investigations & microscopy

5.2.4.1 Transmission electron microscopy (TEM)

The blend components and phase sizes were investigated using transmission electron microscopy (Zeiss EM 922 Omega). The samples were prepared using an ultra-microtome (Leica EM UC7). After cooling down to -170 °C in a cryo-unit (Leica EM FC7), the samples were cut on a -40 °C cold diamond blade (Diatome, angle 35°). The 50 nm thick cuts were transferred to copper-grids using

carbon film. The samples where then stained using ruthenium tetroxide vapor for 15 minutes to enhance the contrast of the EVA phase. The microscope images were taken using an acceleration voltage of 200 kV.

5.2.4.2   Scanning electron microscopy (SEM)

The morphology was investigated using scanning electron microscopy (Zeiss Ultra Plus) with an acceleration voltage of 3 kV. Cryo-fractured samples of the strands perpendicular to the extrusion direction were prepared using liquid nitrogen.

Parts of the samples were only stained, other parts only etched. Staining was performed with ruthenium tetroxide vapor for 30 minutes. The etching procedure was chosen referring to Faker et.al. [14] and Wattananawinrat et.al. [33] to dissolve the EVA phase in xylene at 50 °C for 6 hours. Due to incomplete results in the small phase sizes of the higher filled samples, the method was adjusted. The extraction time was increased to 48 hours and temperature to 60 °C for all samples, while the solvent was constantly flowing. The samples were then platinum sputtered (1.5 nm), followed by a vaporized carbon layer (20 nm).

5.2.5   **Fire retardancy**

5.2.5.1   Cone Calorimetry

The reaction to fire of the compounds was rated using a cone calorimeter (FTT iCone) in air according to ISO 5660. The samples of size 100 x 100 x 3 mm were heat pressed out of pelletized melt pieces. The distance to the radiation heater was set to 35 mm with a heat flux of 50 kW/m^2. The ignition time was marked manually, the samples were fully combusted to measure the residual weight.

6 Results and Discussion

6.1 Unfilled EVA/LLDPE blends

The purpose of this chapter is to describe the properties of the blend systems based on the ratio of EVA and LLDPE. Furthermore, the influence of the addition of a maleic acid anhydrite grafted coupling agent based on either EVA or LLDPE shall be understood. This is done to clearly differentiate observed effects in the following work between polymer-polymer and polymer-filler interaction.

Therefore, unfilled polymer blends of EVA and LLDPE are investigated. The mixing ratios are varied from 0 to 100 % EVA in 25 % steps. A recipe with 45 % EVA is added to investigate the expected phase inversion point between 45 % and 50 % EVA according to literature. Furthermore 67 % of EVA is chosen as this represents a typical cable compound recipe.

6.1.1 Rheological characterization

The morphology of immiscible polymer blends depends strongly on the rheology of the blend components [79]. Therefore, measurements using parallel plate rheology were carried out (see Figure 30). The viscosity curves show shear thinning behavior without a distinct Newtonian plateau within the measurement range for all EVA/LLDPE ratios. The observed trends fit to the results reported by Faker et al. [29] and show decreasing viscosity with increasing EVA content.
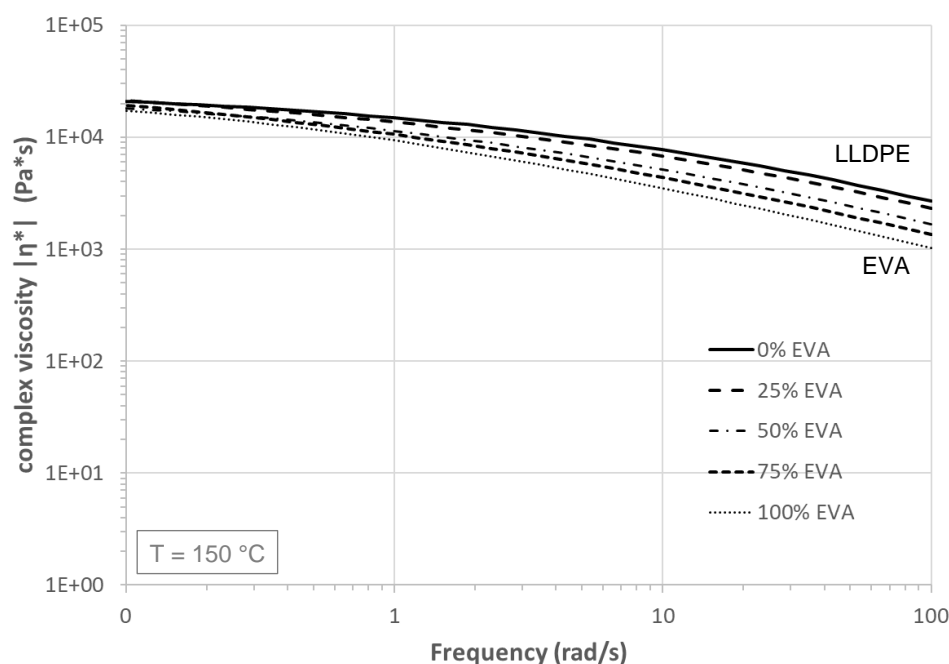
Figure 30   Frequency sweep of EVA/LLDPE blends at 150 °C in parallel plate rheology – influence
             of blend ratio

Faker et al. observed a phase inversion point between 45 % and 50 % EVA. The theoretical phase inversion of the incompatible blends can be calculated based on the shown equation (2) in section 2.2.3 used by Faker et al. [29] which was derived from Steinman et al. [37]. The viscosity values during mixing can be derived from viscosity measurements shown in Figure 30. The calculated phase inversion of the investigated EVA/LLDPE system according to this equation lies at 47.6 % EVA. This result will be further investigated and doublechecked in the following sections.

As the influence of the planned addition of co-polymeric coupling agents is of interest, rheological measurements with samples containing these were carried out. Therefore, 50/50 % - EVA/LLDPE blends with different amounts of maleic-acid-anhydrite (MAA) grafted coupling agents were compounded as described in section 5.1.1. Parts (5 and 10 %) of EVA or LLDPE were substituted with the MAA-grafted version of these, also a mixture of both coupling agents was used. The viscosity measurement results are shown in Figure 31. The tested samples do not show significant differences throughout the dosage and variation of the coupling agents. The observations lead to the assumption, that the grafted co-polymers mix well in the respective phase of the blend system as the concentration is relatively low and interaction is expected to start during filler coupling. Based on the rheological measurements, a change in phase inversion point is not expected but will be further investigated.
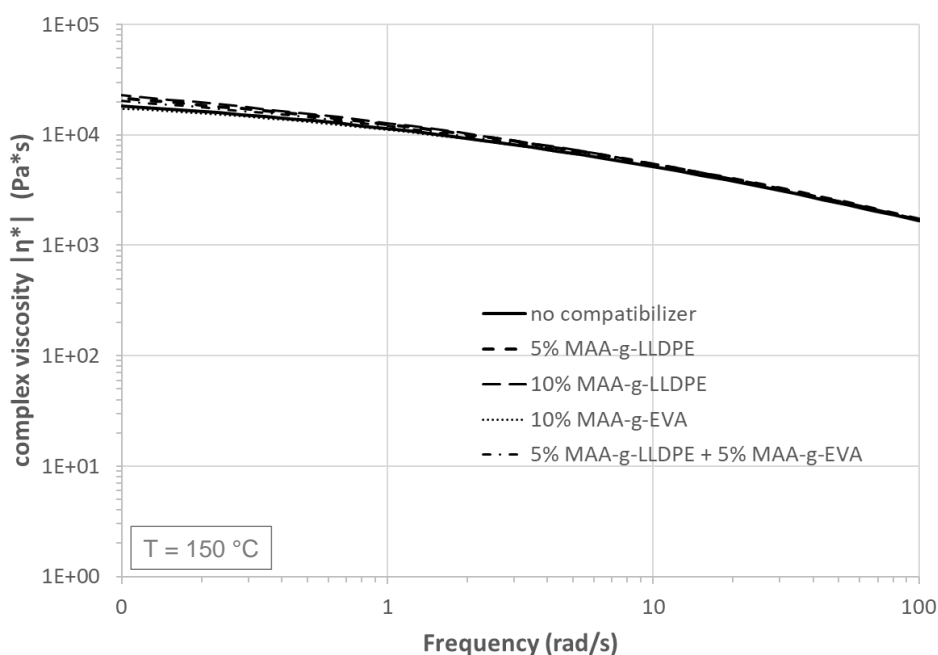
Figure 31   Frequency sweep of 50/50 % - EVA/LLDPE blends with different dosages of coupling agents – influence of coupling agent

6.1.2   Thermal characterization

To further understand the blend behavior during compounding and processing, the thermal properties are investigated using differential scanning calorimetry. Measurements with pure EVA, pure LLDPE and a 50/50 blend were carried out as reference data points for all future investigations (see Figure 32). The melting points of EVA (80 °C) and LLDPE (119 °C) can clearly be identified. EVA shows a slight peak around 120°C resulting from the Polyethylene backbone. According to the supplier, the used LLDPE is a Ziegler-Natta catalyzed grade with randomly distributed comonomer content. This results in a broad melting curve below 120 °C, followed by the polymer chains containing no co-monomer melting at 121 °C creating a shoulder. The 50/50 % - EVA/LLDPE blend system shows typical immiscible behavior by two distinct melting peaks.
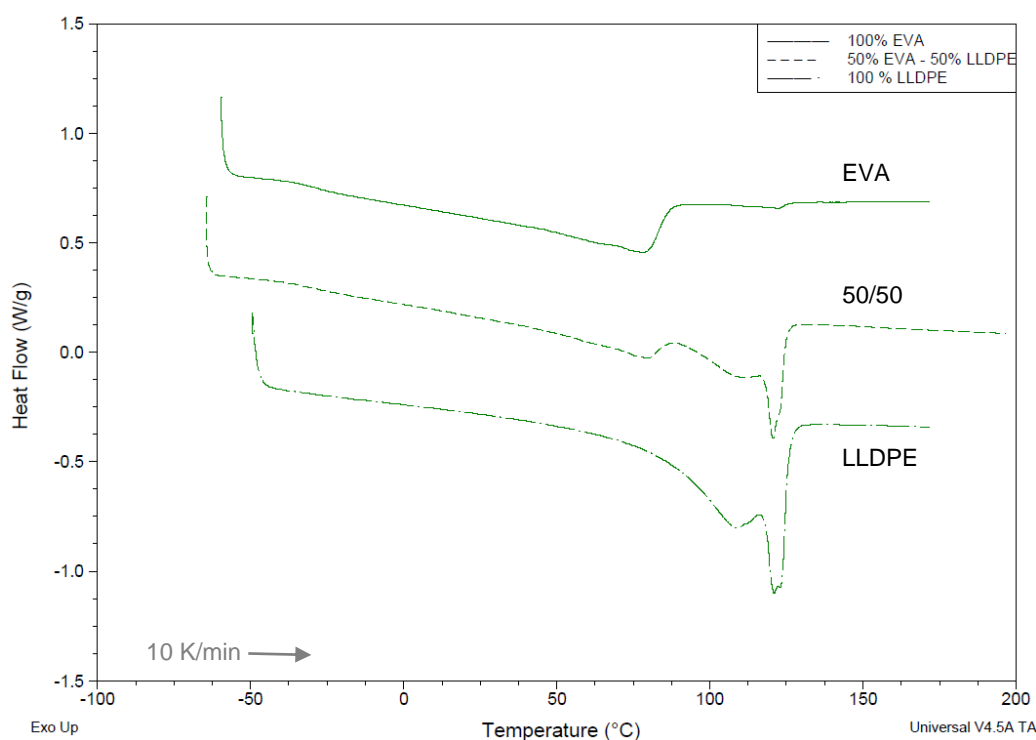
Figure 32   DSC measurements of EVA, 50/50 % - EVA/LLDPE blend and LLDPE
              (from top to bottom)

Substituting parts of the polymer by a grafted coupling agent did not show changes in rheology. To further understand the response of the thermal properties, the samples are investigated by DSC measurement shown in Figure 33. Therefore, 0 to 10 % of LLDPE in an EVA/LLDPE blend are replaced by MAA-g-LLDPE. The glass transition of the EVA fraction is marked and can be considered as stable throughout all samples. The same is seen for the melting points of both blend components. For all samples containing MAA-g-LLDPE coupling agent, the characteristic LLDPE shoulder around 121 °C is replaced by a single peak. Deeper investigations of this effect have shown that this is related to a superposition by a more intensive and narrower melting peak of the MAA-g-LLDPE at 122 °C. Differences in crystallinity could be ruled out by DSC and WAXS measurements. As a doublecheck for miscibility, 50/50 blends of EVA/MAA-g-EVA or LLDPE/MAA-g-LLDPE were investigated. Even in this high dosage of coupling agent, no changes in crystallinity or signs of incompatibility were observed.
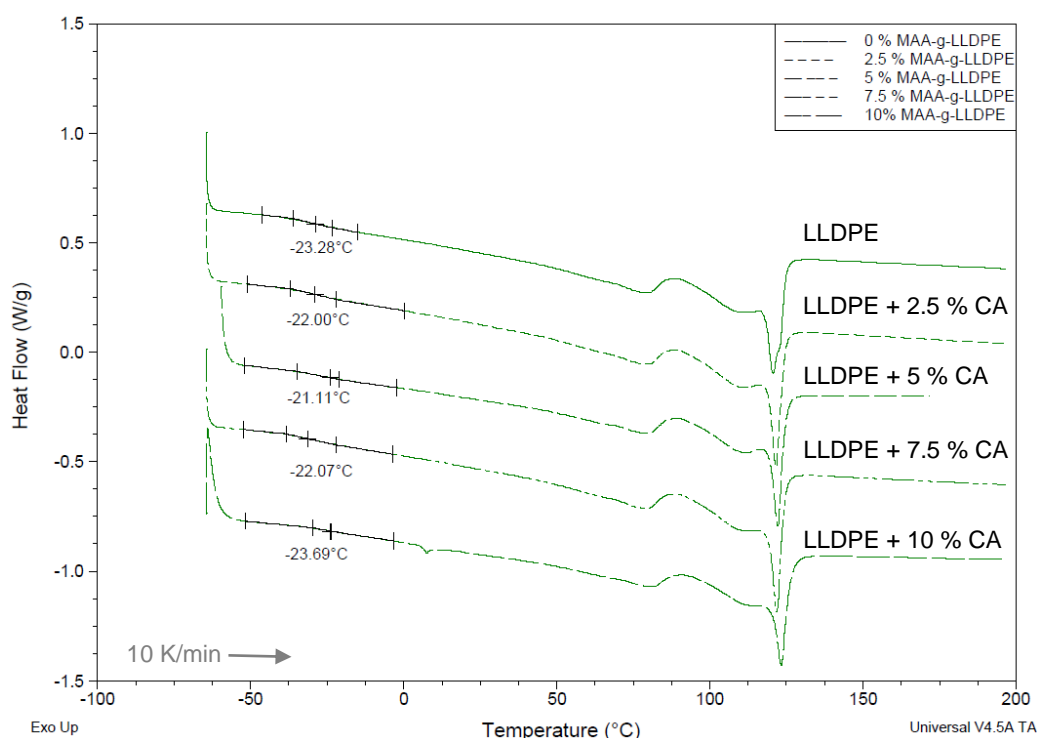
Figure 33   DSC measurements of 50/50 % - EVA/LLDPE blends with increasing amount of MAA-g-LLDPE coupling agent (CA)

6.1.3   Thermo-mechanical characterization

Important parts in the application as a cable sheathing material are the mechanical properties, especially a high resistance against external stresses. Therefore, tensile tests, hysteresis measurements and DMA analysis were carried out. To investigate the influence of the coupling agent (as described in section 6.1), samples containing 5 % MAA-g-LLDPE coupling agent were compared. The exception is the sample using pure EVA where 5 % MAA-g-EVA was used to ensure polymer compatibility.

Tensile tests of both series with and without coupling agent (CA) were performed. To give information about the basic material behavior, first tests of the samples without coupling agent are shown in figure Figure 34. Increasing LLDPE content leads to a more distinct yield point and increased strength. An increasing EVA content leads to a softer and more flexible material response. During testing, a high scatter of the tensile strength and elongation at break were observed. This resulted from strong strain hardening effects of all samples and the high elongation at break values. Slight instabilities in dispersion, sample thickness or sample cut lead to reduced elongation which affects the tensile strength significantly. Therefore, it was decided to focus on the yield strength as this region is more of interest for the cable application. In addition, elongation

at break will be further investigated as this is an important value in cable standards used during cable materials testing and qualification.
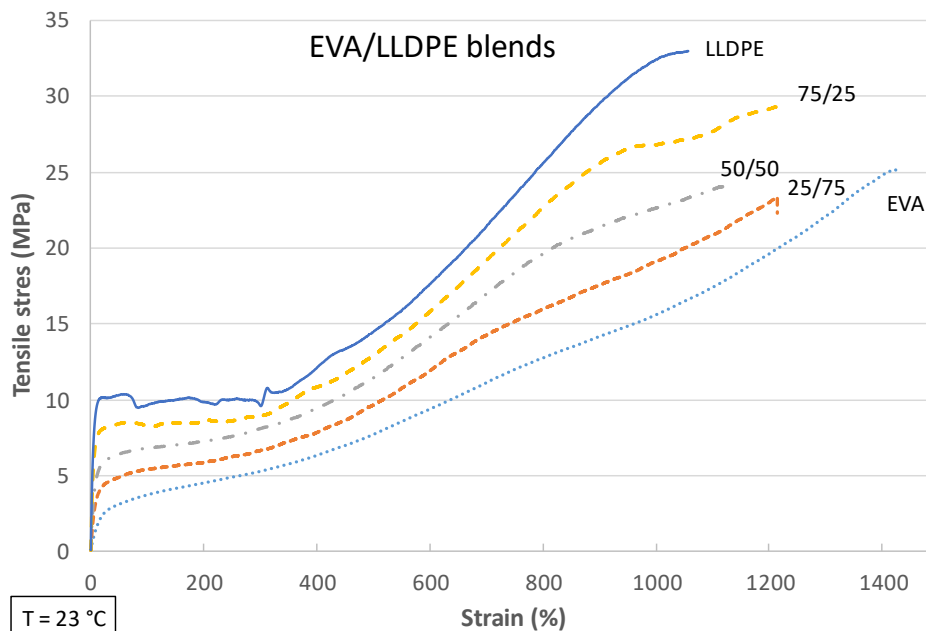
Figure 34   Stress/strain curves of EVA/LLDPE blends - influence of polymer ratio

A comparison of the mechanical properties of both sample sets (with and without coupling agent) are shown in Figure 35. The yield strength shows a clear function of the EVA content in the blend system. The results are as expected: the higher the EVA content, the lower the yield strength. The addition of 5 % coupling agent does not have a significant influence. Looking at the elongation at break values (b), no clear trend is observable. Positive and negative deviations from mixing rule in LLDPE and EVA rich regions were reported by Faker et al. [29], resulting in a description with potential partial miscibility of the backbones in the melt state. To check this, the sample number was increased and the tests extended. The fact that two polymers with relatively high elongation properties are mixed, does not lead to clear results to be correlated with the blend morphology. Observed effects are rather related to sample production or preparation. Nevertheless, the elongation of the blends stays in a range around 1000 % with pure LLDPE on the lower and EVA on the higher end.
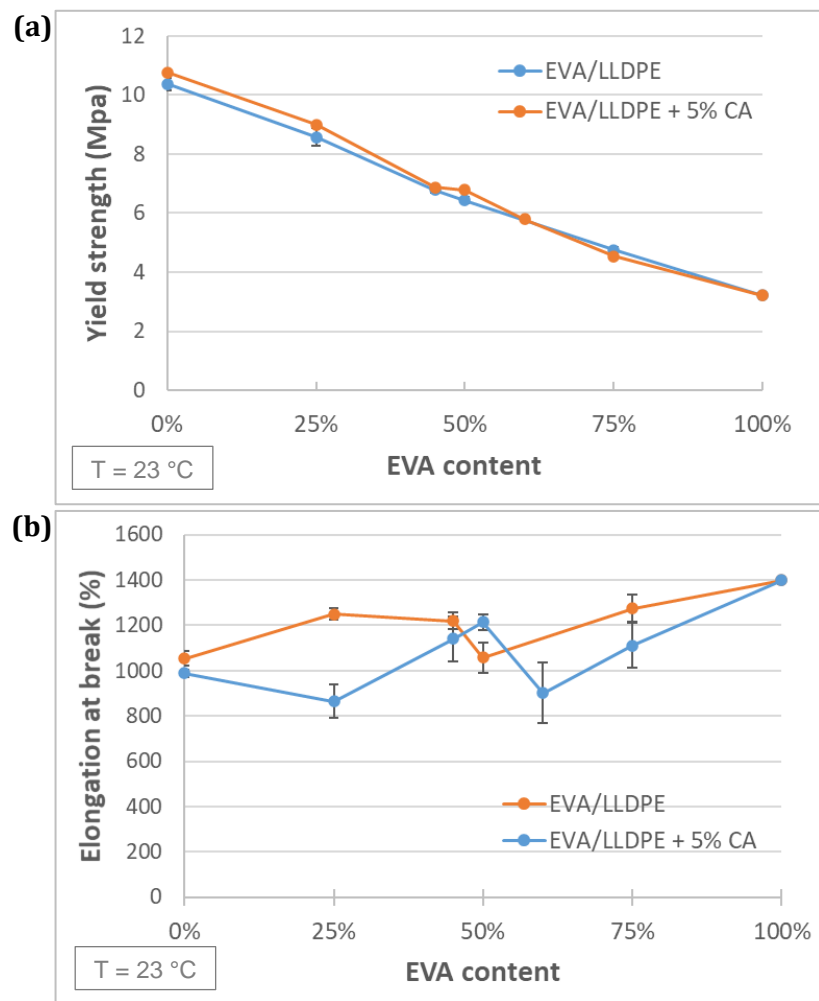
Figure 35   Yield strength (a) and elongation at break (b) of EVA/LLDPE blend systems with and without addition of coupling agent (CA)

As material flexibility and elasticity during bending is a key parameter for the cable application, additional hysteresis measurements were carried out. The curves of neat LLDPE, EVA and the 50/50 blend can be seen in Figure 36. LLDPE as the stiff component shows the highest stress levels and the highest tension set (21.3 %). EVA in comparison shows significant lower tensile stress response to the deformation and higher flexibility resulting in a tension set of 6.4 %. The curve of the 50/50 blend lies close in the middle. The curve is located slightly closer to the pure EVA in regard of tensile stress but closer to LLDPE in the tensile set (16 %). These results highlight that the required mechanical performance in regard of strength and flexibility is a balance to be achieved by the proper EVA/LLDPE ratio.
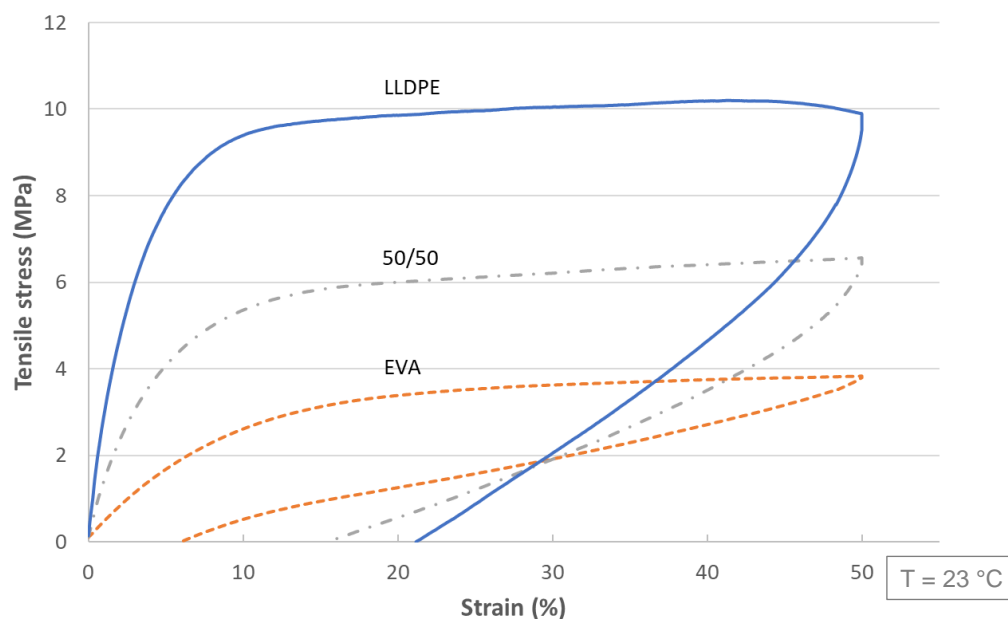
Figure 36   Hysteresis measurements of EVA, LLDPE and 50/50 % - EVA/LLDPE blend

The just shown limitations in tensile testing and the interest in temperature dependency led to the decision to investigate the blends in dynamic mechanical analysis (DMA). To cover all potential effects, the tests were performed from -100 °C to +100 °C. The detected storage modulus for the blend samples between 0 phr to 100 phr EVA is shown in Figure 37. The behavior of pure LLDPE (0 phr EVA) fits very well to the reported data from literature in section 2.2.1. All blends show similar performance in the range below -28 °C which is the glass transition temperature of EVA. Above the T_g, the blends containing EVA show a drop in storage modulus. This reduction becomes stronger with increasing EVA content. While the LLDPE richer blends (0, 45, 50 % EVA) maintain a certain integrity throughout the test, all EVA rich blends (67, 100 %) collapse above the melting temperature of EVA (80 °C). The 67 % EVA sample still shows better performance than the pure EVA. This is a sign that even above phase inversion, an existing LLDPE structure supports the thermo-mechanical stability.
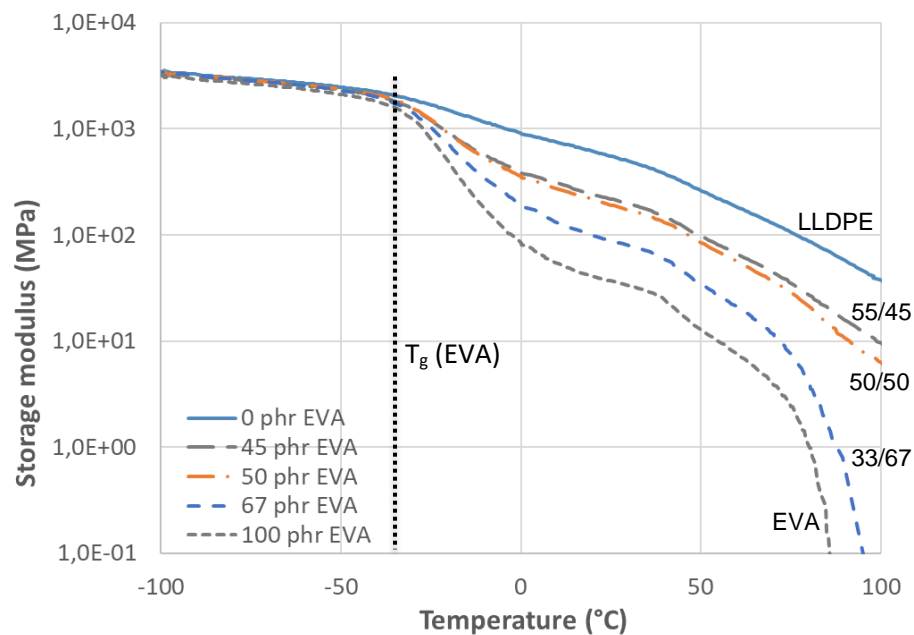
Figure 37   DMA storage modulus measurement of different EVA/LLDPE blends

To investigate the influence of the coupling agent, DMA tests of the 50/50 % blends of EVA/LLDPE combined with 5 or 10 % of MAA-grafted coupling agents were carried out. The results were comparable for all samples throughout the whole temperature range. As no influence of the coupling agent on the storage modulus was detectable, the graph will not be shown in this work.

As already mentioned in section 1, the shrinkage of a cable jacket material is of crucial interest. Source of the shrinkage in the later application is thermal contraction and the reduction of incorporated stresses and orientation from the extrusion step. Both result in a built-up shrinkage force along the cable sheath.

To quantify these effects, coefficient of thermal expansion (CTE) and contraction stress measurements were performed (see Figure 38). The CTE (a) shows strong influence by the polymer majority phase reacting in a step. While LLDPE and the 25 % EVA sample show values around 150 ppm/K, a higher EVA content causes values of approx. 200 ppm/K just like pure EVA. The addition of coupling agent does not change this effect remarkably. Looking at the contraction stress (b), the dependency is more linear. The contraction stress for the samples with and without coupling agent decreased with increasing EVA ratio, both curves can be considered as comparable.
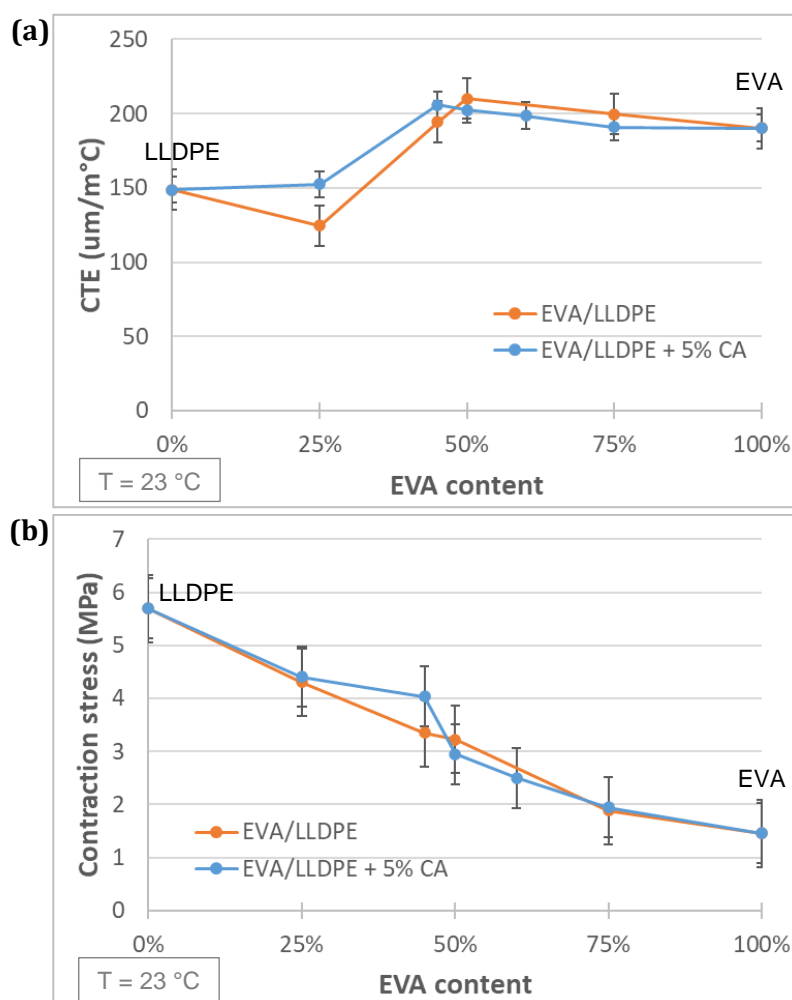
Figure 38   Coefficient of thermal expansion (a) and contraction stress (b) of different EVA/LLDPE
             blend systems with and without coupling agent (CA)

6.1.4 Morphological characterization

The similar polyethylene backbone of both materials makes it hard to distinguish the morphology in optical measurements. The blend phases were initially identified using transmission electron microscopy on stained samples (see Figure 39). Both phases were identifiable due to the enhanced contrast by staining. The black cracks on the 50 % sample are caused by sample preparation. The phase inversion point between 45 % and 50 % in a co-continuous morphology is clearly visible. This proves the calculated value from the rheological measurements around 48 %. But based on these images, it was not clear whether a co-continuous or droplet morphology occurs for the 25 % and 75 % EVA samples. The phase sizes vary between 1 to 3 µm.

25% EVA   45% EVA   50% EVA   75% EVA
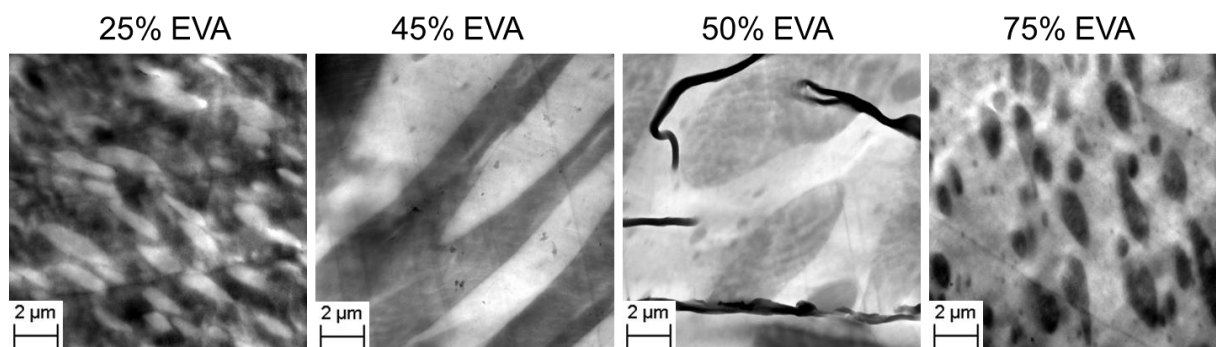
Figure 39   Transmission electron microscopy images of polymer blends made of EVA (bright) and LLDPE (dark)

To further investigate the morphology outside the phase inversion area, scanning electron microscopy was used. A procedure to selectively extract the EVA was developed and applied. The images obtained can be seen in Figure 40. The observed morphology for both samples is co-continuous which fits well to the results obtained in DMA measurement. This result is contrary to the droplet morphology reported by Faker et. al for 75/25 and 25/75 - EVA/LLDPE blends. [29]. The reason for this difference is that Faker did not manage to extract the EVA from the EVA rich blends. He only used 2 dimensional cryo fractured samples for analysis. The sample with 67 % EVA (left) shows smaller phase sizes of the residual LLDPE than the 50 % sample (right). This extraction method also allows to finally judge the compatibility of both polymers: the LLDPE surface is smooth and the polymers are clearly separated.
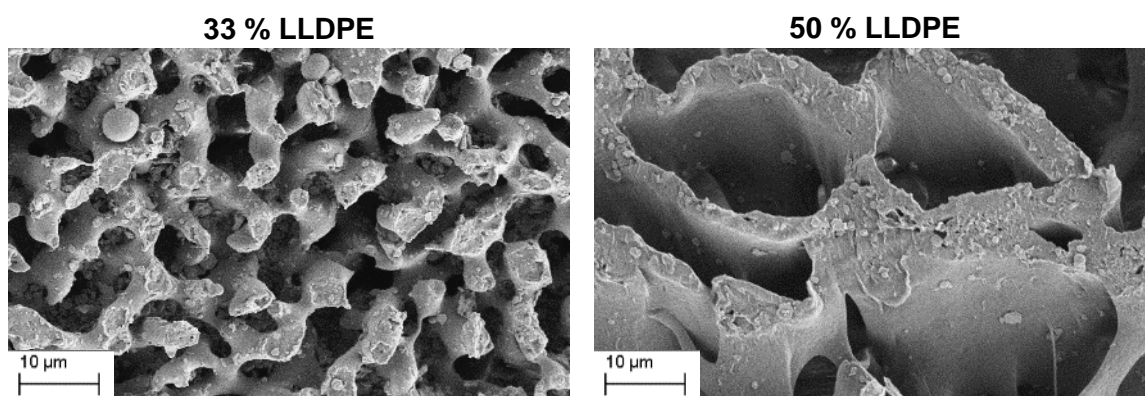
33 % LLDPE   **50 % LLDPE**

Figure 40   SEM micrographs of selective etched EVA/LLDPE polymer blends with residual 33 % LLDPE (left) and 50 % LLDPE (right)

SEM was also used to identify the influence of the coupling agent on the blend morphology. Blends with 50/50 % of EVA/LLDPE and 50/45/5 % of EVA/LLDPE/MAA-g-LLDPE were produced. The extruded strands were cryo-fractured and either only stained or exposed to EVA solvent extraction. The images captured in both sample preparation methods are shown in Figure 41. The

polymer phases can be distinguished in the cryo-fractured samples. The LLDPE shows slightly more ductile fracture behavior due to the lower glass transition temperature. While the sample without coupling agent shows co-continuous structures with comparable phase sizes, the LLDPE phase size in the sample using MAA-g-LLDPE decreases. This was further investigated by etching and removing the EVA portion. Here it becomes more obvious, that the phase structure changes by adding the coupling agent. The addition of 5 % MAA-g-LLDPE reduces the phase size of the LLDPE while maintaining a co-continuous morphology. This is a sign for increased compatibility of the immiscible blend. It is believed to be caused by an increase in polarity of the LLDPE phase due to functional maleic-acid-anhydrite groups in the coupling agent. The low amount of coupling agent in the system is the reason, that this effect is limited and obviously cannot overcome the immiscibility in the blend system.
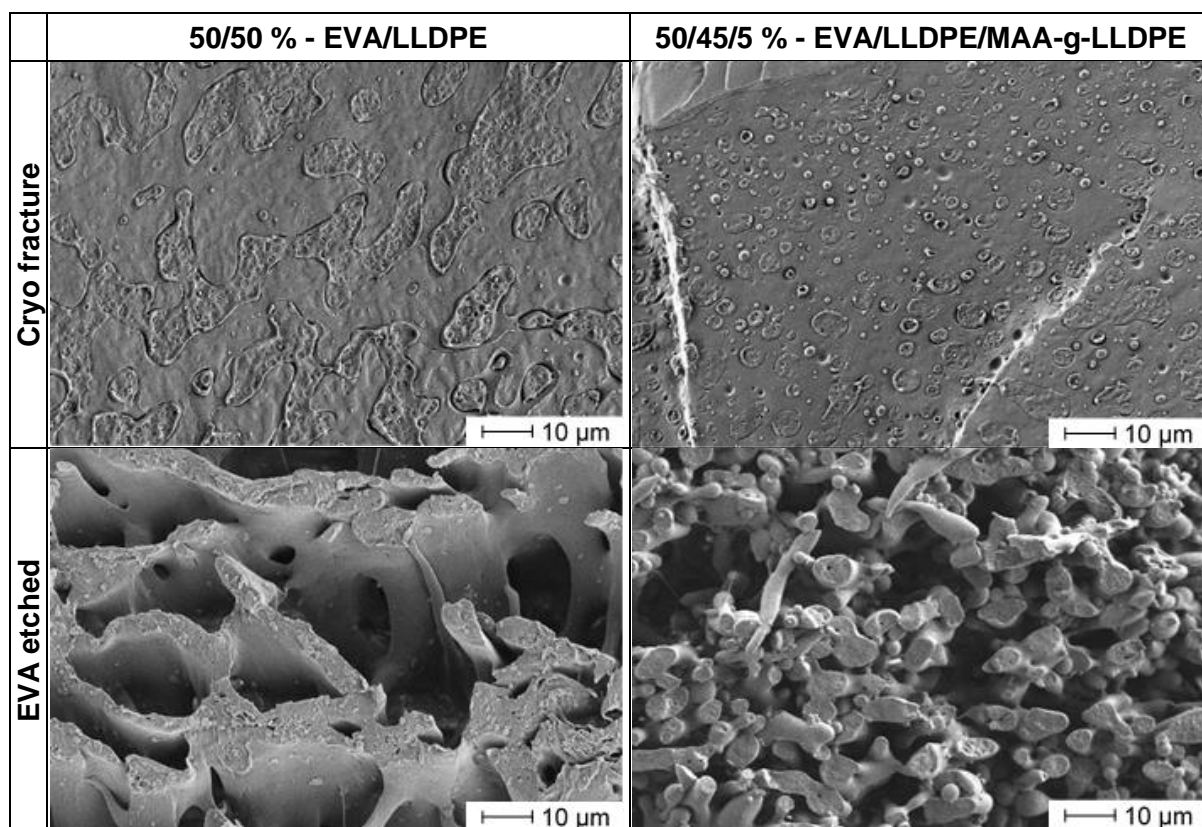
Figure 41   SEM micrographs of 50/50 % - EVA/LLDPE blends with (right) and without (left) coupling agent after cryo fracture (upper) and followed etching (lower)

6.1.5   Conclusion

The incompatibility of the investigated EVA/LLDPE blend systems was clearly visible in thermal analysis (DSC), mechanical analysis (DMA) and microscopy (TEM and SEM). It was possible to calculate the phase inversion point based on the viscosities of the blend partners by rheological

measurements (parallel plate). The morphology of both phases is co-continuous throughout the investigated range. The general properties of the EVA/LLDPE blends are mainly defined by the blend ratio. Increasing EVA content leads to a reduction in mechanical strength, increasing flexibility and reduced melt viscosity. The thermo-mechanical stability is affected by the glass transition and melting point of EVA which is improved by a co-continuous LLDPE structure throughout all investigated blends. The coefficient of thermal expansion is defined by the majority phase and reacts stepwise after phase inversion point.

The addition of up to 10 % of MAA-g-EVA or MAA-g-LLDPE coupling agents was investigated using rheological (parallel plate), thermal (DSC), mechanical (tensile testing, CTE) or thermo-mechanical (DMA) analysis. Although no significant differences were observable in these tests, an influence of the coupling agent on the morphology was detectable by SEM microscopy. The phase size of the LLDPE/MAA-g-LLDPE fraction decreased which is a sign for increased compatibility to EVA. This can be caused by the polarity of the functional MAA-groups. The phase size reduction is limited due to the low amount of MAA in the blend system. Therefore, differences are detectable but do not yet result in significant changes in blend properties.

This leads to the conclusion that any detectable influence from coupling agents in the next section are clearly relatable to polymer-filler interactions.

6.2 Filled EVA/LLDPE blends

This chapter aims to describe the properties resulting from the addition of a mineral based flame-retardant additive into the investigated systems from section 6.1. Furthermore, the interaction of the mineral filler with the maleic acid anhydrite-based coupling agents, the resulting blend properties and morphology shall be understood. Therefore, EVA/LLDPE blends consisting of 0 %, 45 %, 50 %, 67 % and 100 % of EVA were compounded to cover the pure polymers, the regions before and after phase inversion and a typical cable recipe. The formulations are filled with different ratios (10, 30, 60 %) of Magnesium-di-hydroxide (MDH). All samples were compounded with and without MAA-g-LLDPE coupling agent (CA), except for the 100 % EVA sample which was mixed with MAA-g-EVA (comparable to section 6.1). The dosage of CA was chosen based on supplier recommendations and then adjusted for the different filler amounts to achieve a constant ratio of 2 phr coupling agent per 10 wt% of mineral filler. The unfilled reference samples with coupling agent contain 5 % of the MAA-g-LLDPE.

6.2.1 Rheological characterization

To further understand the influence of filler addition on the blend morphology and to calculate a potential new phase inversion point, filled EVA, LLDPE and their blends were characterized in parallel plate rheometry. It is expected that the viscosity of the blends is affected by the filler dispersion: This can be an even distribution in both phases, only in one of each component or in the interphase.

A comparative overview of the rheological analysis in a frequency sweep for EVA (a), LLDPE (b) and 50/50 % – EVA/LLDPE (c) is shown in Figure 42. As already shown in section 6.1.1, the coupling agent does not have a measurable influence on the polymer blends. Therefore, only one measurement for the 0 % MDH sample is shown as reference. The samples without coupling agent are drawn in dotted lines, the samples containing coupling agent in solid lines.

As expected, the viscosity levels for all samples are increased by the addition of mineral filler. All samples show shear thinning behavior. None of the samples show a clear Newtonian plateau at low frequency within the measurement range. The unfilled samples (0 % MDH) show a plateau-like tendency which is less visible with increasing filler content. All samples containing 60 % MDH show a steeper progression throughout the measurement range. Such increase in viscosity in combination with a reduced Newtonian-plateau for increased filler content in thermoplastic

polymer was described by Poslinsky et.al. [69]. For all materials, the 10 % filled sample lies very close to the unfilled one.

The EVA (a) based samples show no effect caused by the addition of coupling agent, although an improved coupling to the filler was expected.

An influence of the coupling agent becomes visible at the highest filled LLDPE (b) sample. While the "60 % MDH" sample shows a significant increase in viscosity at low frequencies, this cannot be observed for the sample using coupling agent (60% MDH + CA). This "yield stress effect" was reported by Laun et. al. [65] after observing a viscosity increase to infinite values towards lower shear rates of dispersed latex particles in emulsion. This is caused by filler particle-interlocking and is a sign of insufficient polymer coverage or lack of coupling.

The tested 50/50 % - EVA/LLDPE blends with different filler ratio and coupling agent addition are shown in (c). No significant influence of the coupling agent can be observed for all amounts of filler loading. Both curves within the respective filler level are lying close to each other. Even for the 60 % filled samples, no signs of increased filler-filler interaction, like the mentioned "yield stress effect" can be observed.
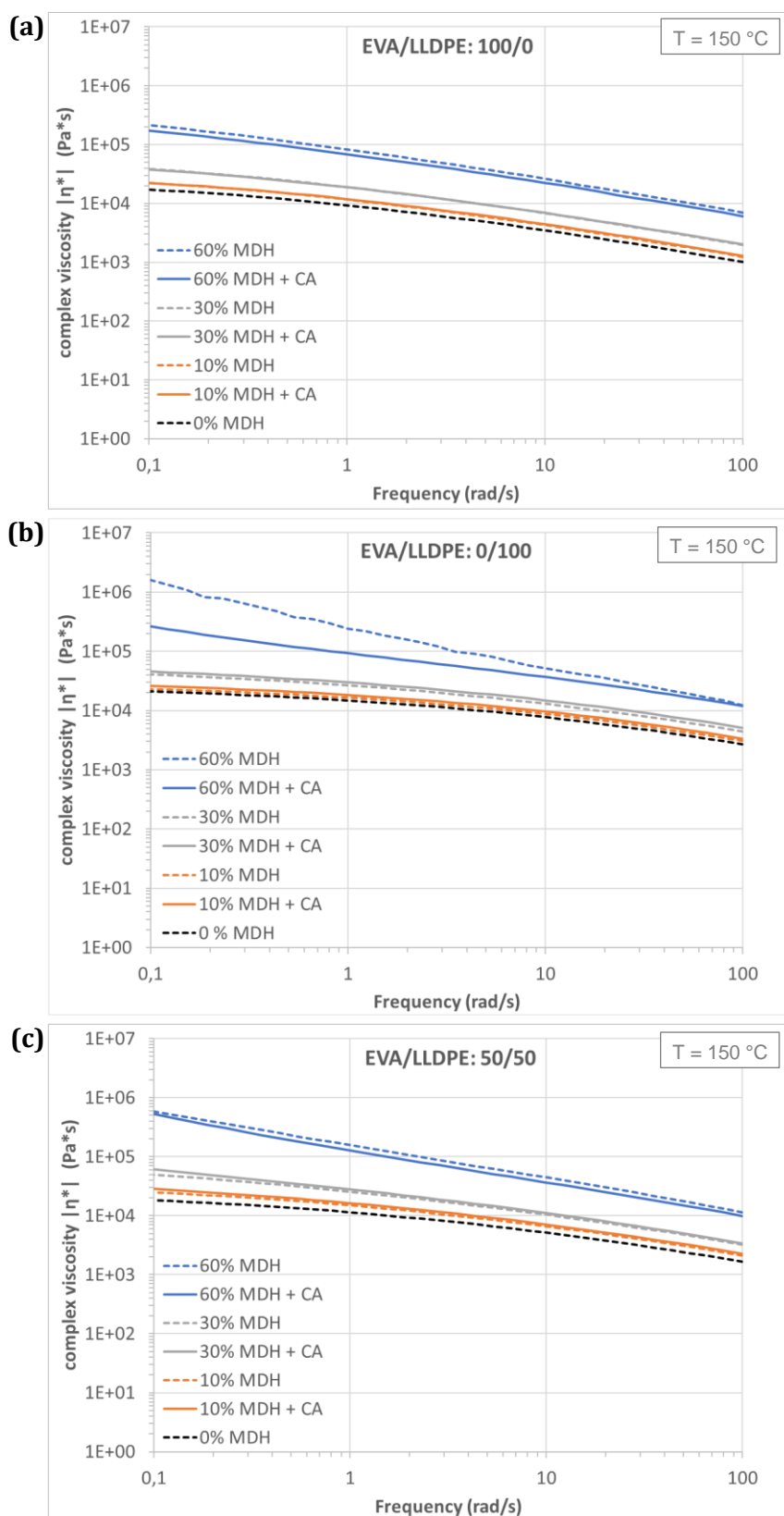
Figure 42   Frequency sweep of EVA (a) and LLDPE (b) and 50/50 % - EVA/LLDPE (c) with different
             dosages of magnesium-di-hydroxide (MDH), with and without MAA-grafted coupling
             agent (CA)

To understand whether the reported change in viscosity affects the morphology, the expected phase inversion point was recalculated, based on the new data using equation (2) used by Faker et.al. [29] shown in section 2.2.3. As it was not yet clear where the filler will be located, different scenarios needed to be considered. In the following Table 13, the equation was applied to different combinations of rheological curves. This allows to estimate the expected phase inversion points of the EVA/LLDPE morphology based on the filler location. The results for the unfilled samples (0 % MDH) are given as a reference. The phase inversion is mainly affected by the filler location. For the 60 % filled sample, the coupling agent in LLDPE causes an additional effect which results from the observed differences in the viscosity curves caused by the "yield stress effect". When the filler is located in both polymers, the phase inversion and so the expected phase size stays relatively stable. For the other two scenarios, the phase inversion ratio moves towards the polymer fraction that does not contain the filler. This result will be compared with the morphological studies using SEM.

Table 13   Calculated values of phase inversion ratio of EVA/LLDPE blends and compounds

		Calculated ratio of EVA/LLDPE phase inversion		
Scenario	**Coupling**	**0 % MDH**	**30 % MDH**	**60 % MDH**
Filler evenly distributed	-	48 / 52	49 / 51	49 / 51
	+ CA	48 / 52	48 / 52	49 / 51
Filler only in EVA	-	48 / 52	51 / 49	58 / 42
	+ CA	48 / 52	51 / 49	59 / 41
Filler only in LLDPE	-	48 / 52	45 / 55	38 / 62
	+ CA	48 / 52	44 / 56	40 / 60

In industrial applications, the melt flow rate (MFR) is of high interest as this test is performed much easier than the parallel plate experiments. To give a complete picture, the melt volume rate (MVR) of all tested samples is shown in Figure 43. Due to the variation in density caused by filler addition, MVR was chosen over MFR. The material was tested at 150 °C with relatively high load of 21.6 kg to increase the shear stress which is closer to the target process. The results are shown in Figure 43. The melt flow volume increases with increasing EVA content and decreases with increasing filler content. This fits well to the expectations based on literature [48], [65]. Furthermore, with 60 % filler loading, the influence of the polymer composition is relatively small. No significant influence of the coupling agent was visible throughout all sample compositions. This leads to the assumption that the quality of filler dispersion is high for all samples.

Figure 43   Melt volume rate (MVR) of filled EVA/LLDPE blends with different dosages of
             Magnesium-di-hydroxide (MDH) with and without MAA-grafted coupling agent (CA)

6.2.2   Thermal characterization

To investigate how filler addition changes the thermal properties of the investigated systems, DSC measurements were performed. Due to the contained mineral filler, weight correction was used. As the thermal capacity of the filler at such high loadings cannot be neglected, a baseline correction using a pure MDH curve was performed.

The resultsof 50/50 % - EVA/LLDPE are shown in Figure 44. The unfilled blends investigated in section 6.1.2 are shown for comparative reasons. As already discussed, the sample shows two separate melting peaks of EVA at 80 °C and LLDPE around 120 °C. For the unfilled sample containing coupling agent (0 % MDH + CA), this characteristic shoulder around 121 °C is replaced by a single peak caused by melting peak superposition by the coupling agent.

By the addition of a flame-retardant filler (MDH), the peak positions and shapes are not affected. The 60 % MDH sample shows a slight difference in the intensity of the LLDPE melting peak. Therefore, the melting peaks of the samples without coupling agent were compared as a doublecheck. The difference of -0.6 °C between the unfilled and the 60 % MDH sample can be neglected. Except for a slightly increased shoulder, no changes in peak position or crystallinity were observed.
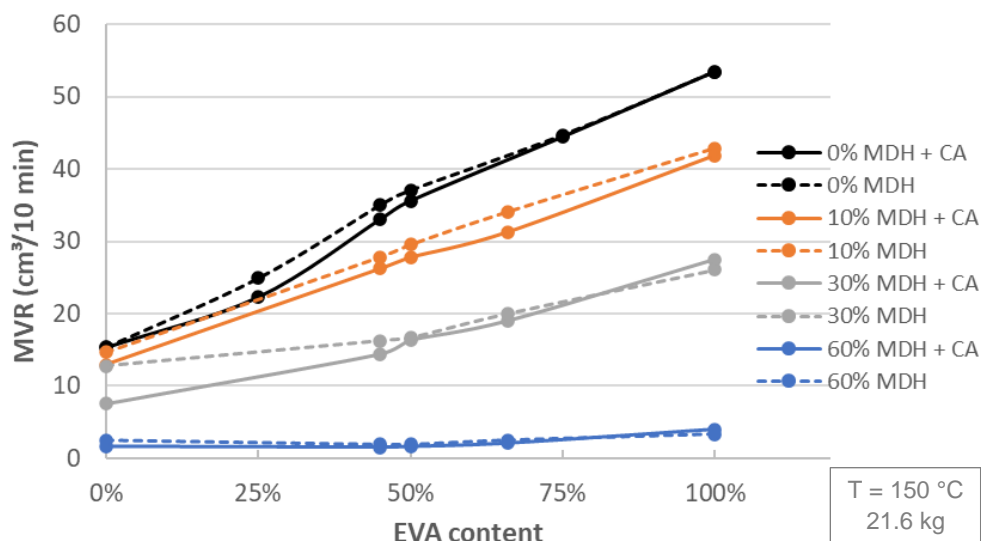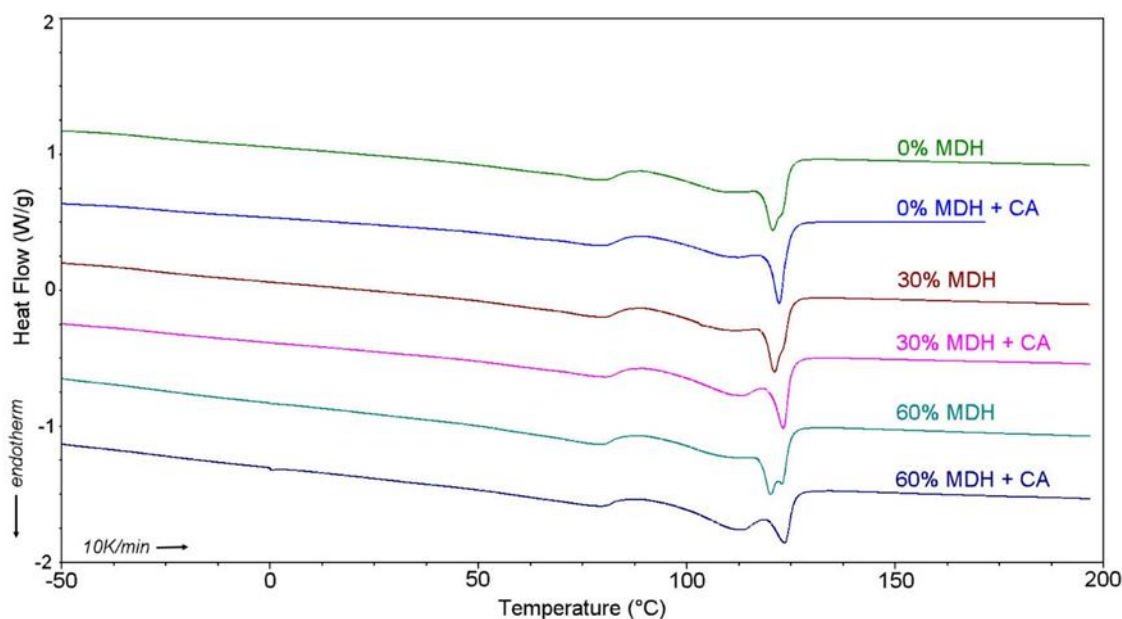
Figure 44   Differential scanning calorimetry of filled 50/50 % - EVA/LLDPE blends with different dosages of Magnesium-di-hydroxide (MDH) with and without MAA-grafted coupling agent (CA)

6.2.3 Thermo-mechanical characterization of filled EVA/LLDPE blends

The mechanical performance at room temperature was rated in tensile tests on extruded strands. The stress/strain curves for 10 %, 30 % and 60 % filled EVA, LLDPE and the 50/50 % blend is shown in Figure 45. As reported in literature [63], [43], the stiffness of the compounds increases with increasing filler content, resulting in a higher yield stress and reduced elongation at break. The samples of pure EVA with and without coupling agent lie relatively close to each other. Only marginal influence of the used MAA-g-EVA coupling agent can be seen. This is different for pure LLDPE, where the coupling agent causes significant increase in elongation at break and tensile stress. While the modulus is not so much impacted, a deviation in tensile stress is visible even at low elongation values. The effect of the used coupling agent grows with increasing filler amount. This effect can be also seen in the 50/50 % blend results. It seems that the presence of EVA reduces the difference between the samples with and without coupling agent, especially in the lower elongation values.
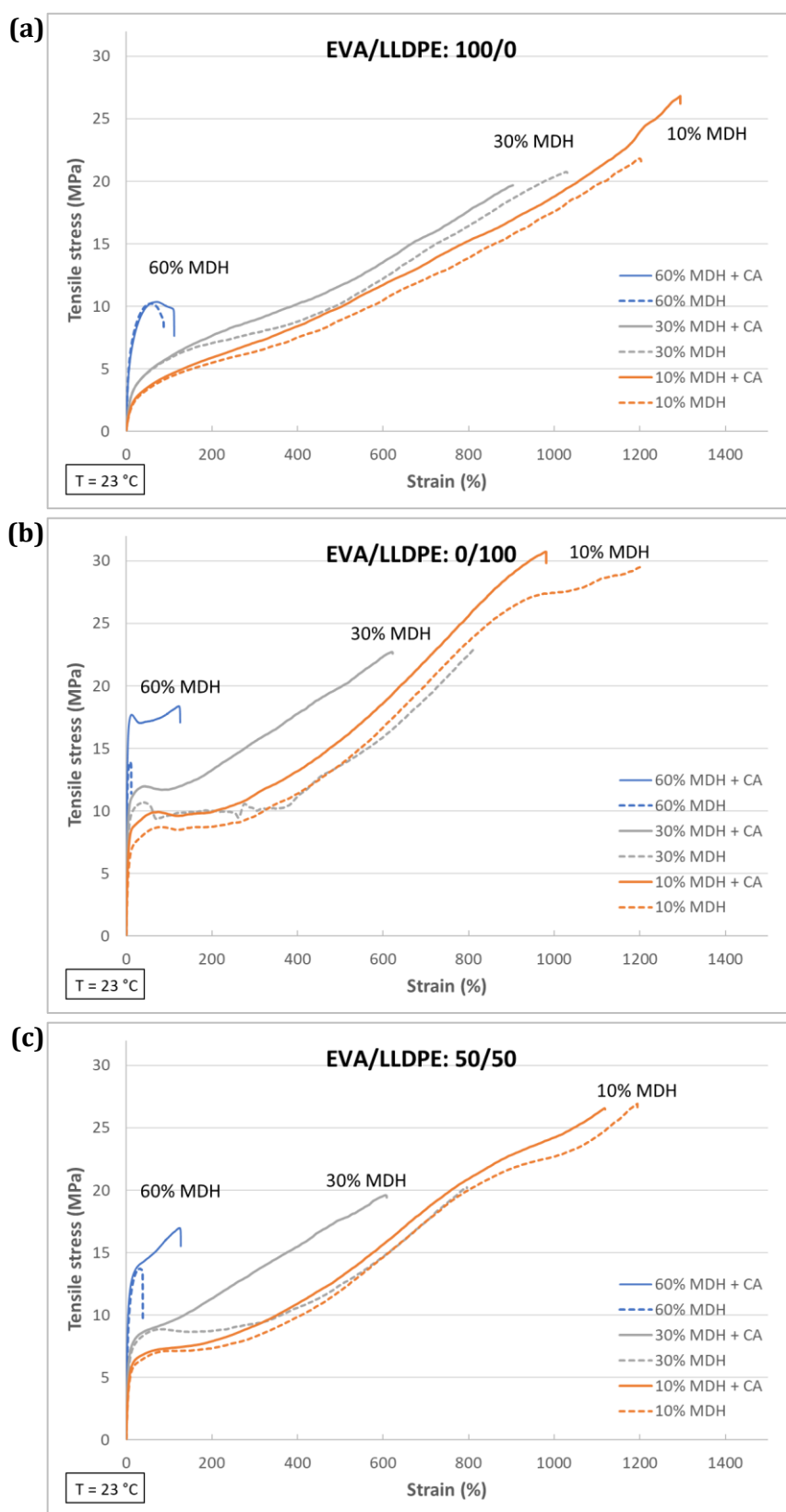
Figure 45   Stress/strain curves of EVA (a), LLDPE (b) and 50/50 % - EVA/LLDPE (c) with different dosages of magnesium-di-hydroxide (MDH), with and without MAA-grafted coupling agent (CA)

An overview of the yield strength (a) and elongation at break (b) for all EVA/LLDPE blend ratios is given in Figure 46. The yield strength (a) decreases with increasing EVA content, as already observed for the unfilled blend systems in section 6.1.3. As already shown in the stress/strain curves, strong differences in yield strength for the pure LLDPE are visible, which decrease with increasing EVA content until none is visible for pure EVA. Looking at the elongation at break values (b), the increasing stiffness caused by the mineral filler leads to a reduction in performance. It is observed that the elongation at break values of the 10 % and 30 % filled samples without coupling agent are higher than the ones using coupling agent. This is caused by a less hindered movement of the polymer chains around the filler particles. The behavior changes above a certain level of filler content which can be seen for the 60 % filled samples. The higher concentrated fillers act as obstacles which create stress concentrations within the polymer chains. An added coupling agent allows force transmission through the particles and therefore increases the overall elongation at break. It is also obvious, that the datapoints of pure EVA are lying very close to each other, which will become more important in a later stage of this work.
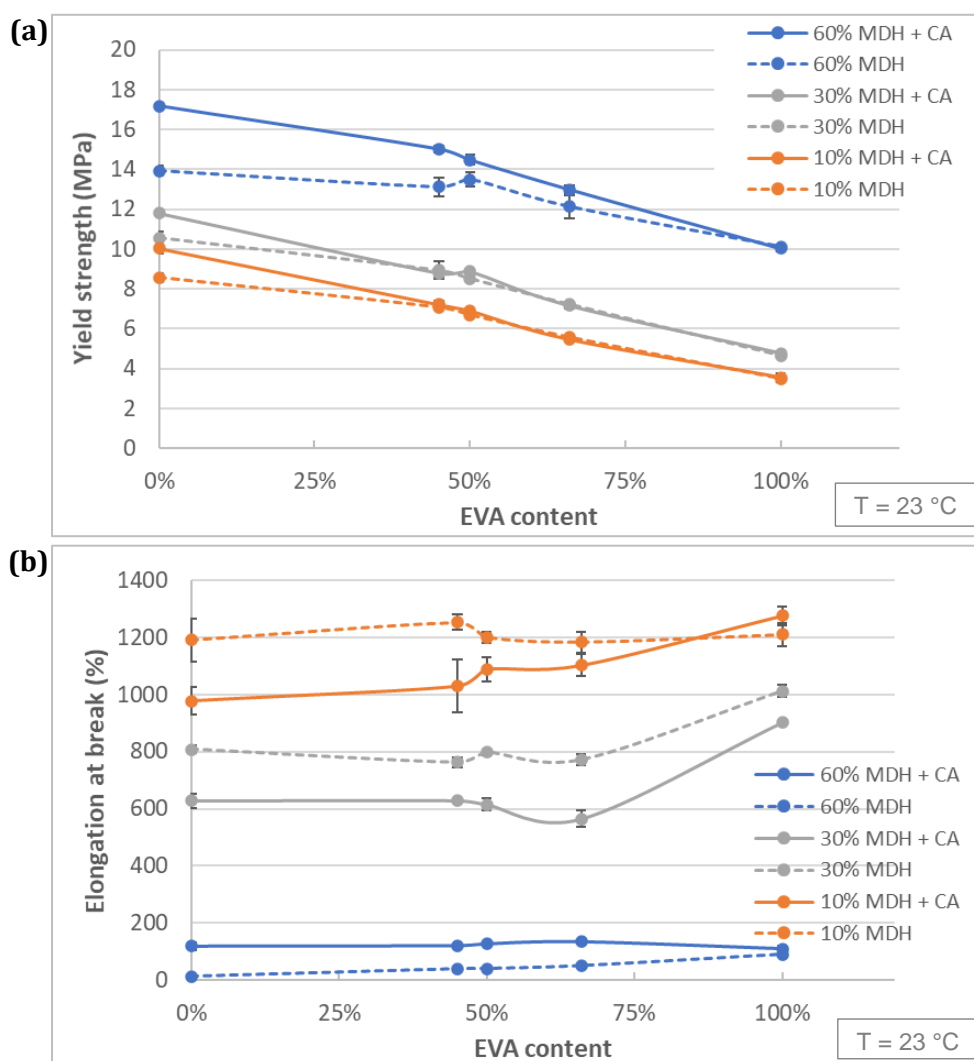
Figure 46   Tensile tests of filled EVA/LLDPE blends with different dosages of Magnesium-di-hydroxide (MDH) with and without MAA-grafted coupling agent (CA)

The addition of filler also influences the compound flexibility significantly. This can be seen in the hysteresis measurements of filled 50/50 % - EVA/LLDPE blends (Figure 47). As already seen in the tensile tests, the tensile stress levels increase with increasing filler content. The same can be seen for the tensile set which roughly doubles from 16 % of the unfilled sample to 32.8 % of the sample containing 60 % MDH. This results in a reduced elastic elongation. In the later cable application, this leads to an increase of the minimum allowed bend radius of the cable before the jacket material deforms permanently or cracks. The influence of a coupling agent will be shown in combination with filler coating variations in section 6.3.2.
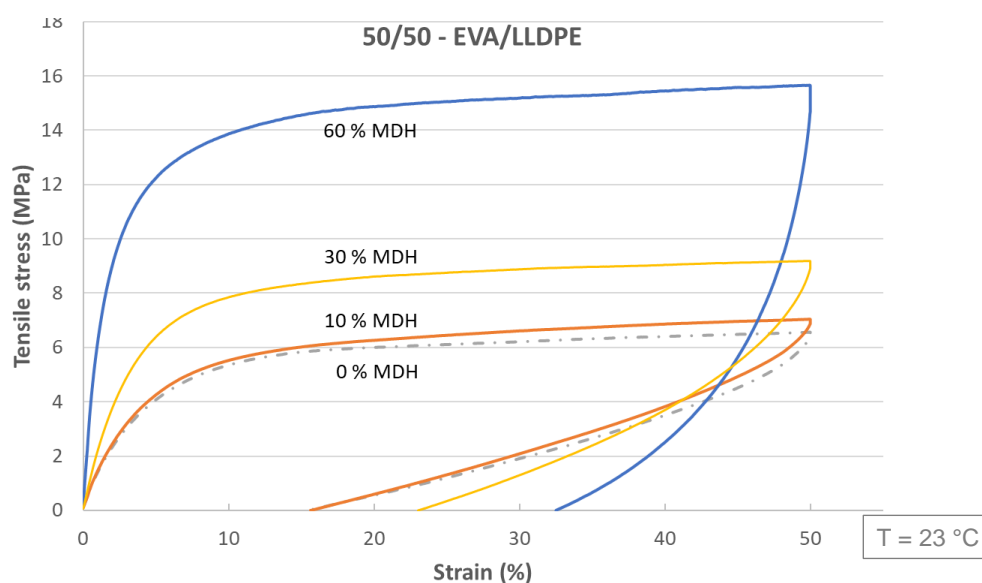
Figure 47   Hysteresis measurements of filled 50/50 % - EVA/LLDPE blends with different dosages of uncoated Magnesium-di-hydroxide (MDH)

To further investigate the thermo-mechanical stability, DMA tests were carried out comparable to the tests of the unfilled blends in section 6.1.3. Samples made of pure EVA (a), pure LLDPE (b) and the 50/50 blend (c) are shown in Figure 48. As expected from the rheological measurements and the tensile tests at room temperature, the storage modulus of all tested samples is increasing with increasing filler content. The EVA sample (a) shows a distinct drop in the modulus around the glass transition temperature (-28 °C), followed by a collapse of the samples close to the melting temperature (80 °C). It is visible that higher filler content increases the thermal resistance of the samples slightly. Comparing the 10 % and 60 % sample, a shift of 5 – 10 °C in the thermo-mechanical performance (modulus drop at T_g and T_m) is observed. For all pure EVA samples (a), no influence by the added MAA-g-EVA as coupling agent is visible. As already seen for the unfilled samples, pure LLDPE (b) shows a certain thermal stability with slow softening throughout the temperature range without remarkable drops. At temperatures below 0 °C, no significant influence of the coupling agent is visible. At higher temperatures (e.g. above 50 °C), all samples containing coupling agent show slightly increased modulus, strongest improvement for the highly filled blends (60 %). Looking at the filled 50/50 blends (c), the modulus dependency is comparable to the unfilled blends shown in Figure 37 with a drop in modulus around the T_g of EVA (-28 °C). The storage modulus curves of the samples with and without coupling agent start to differ from this temperature. The compounds with coupling agent show improved thermo-mechanical performance, the strongest effect seen for the 60 % filled sample at higher temperatures. Even the melting effect of EVA above 70 °C is compensated. This surprises as the used coupling agent is based on LLDPE and was not expected to interact with EVA.

(a)

(b)

(c)
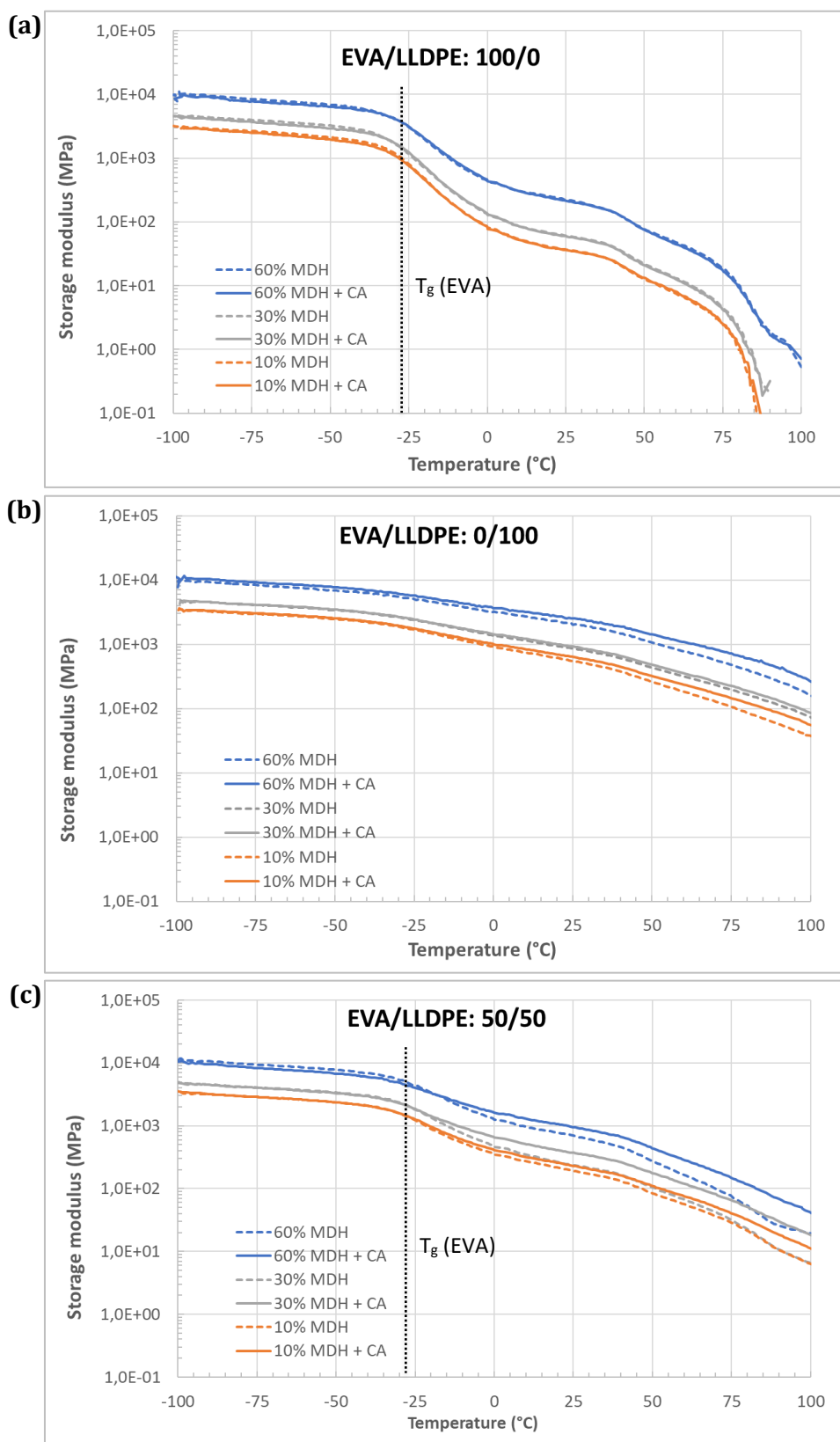
Figure 48   Storage modulus in DMA testing of EVA (a), LLDPE (b) and 50/50 % - EVA/LLDPE (c)
with different dosages of magnesium-di-hydroxide (MDH), with and without MAA-grafted
coupling agent (CA)

The intensity of improvement by adding the MAA-g-LLDPE coupling agent in the 50/50 blend system was not expected. It is not clear why the LLDPE-based coupling agent is able to improve the weaker performance of the EVA in the 50/50 blend. The coupling agent has shown only minor improvements in pure LLDPE and section 6.1.4 has clearly indicated two separate polymer phases of EVA and LLDPE+MAA-g-LLDPE. Further investigations of this effect are described in the following section.

For future cable applications, CTE and contraction stress measurements were performed (see Figure 49). Comparable to the results shown in section 6.1.3, the CTE (a) increases with increasing EVA content. The step caused by phase inversion is still visible but becomes smaller with reduced polymer content due to filler addition. As expected, the overall CTE is reduced by the mineral filler addition. No significant influence by the coupling agent is visible, differences are caused by a relative high deviation of the measurements themselves. The contraction stress (b) is reduced with increasing EVA content, comparable to the results of the unfilled systems shown in section 6.1.3. The addition of filler increases the modulus (as seen in Figure 48) which results also in higher contraction stress. An influence of the coupling agent can be identified above a certain filler amount, seen at the 60 % filled sample. Filler coupling causes a higher contraction stress resulting from a higher degree of force transmission through the sample.
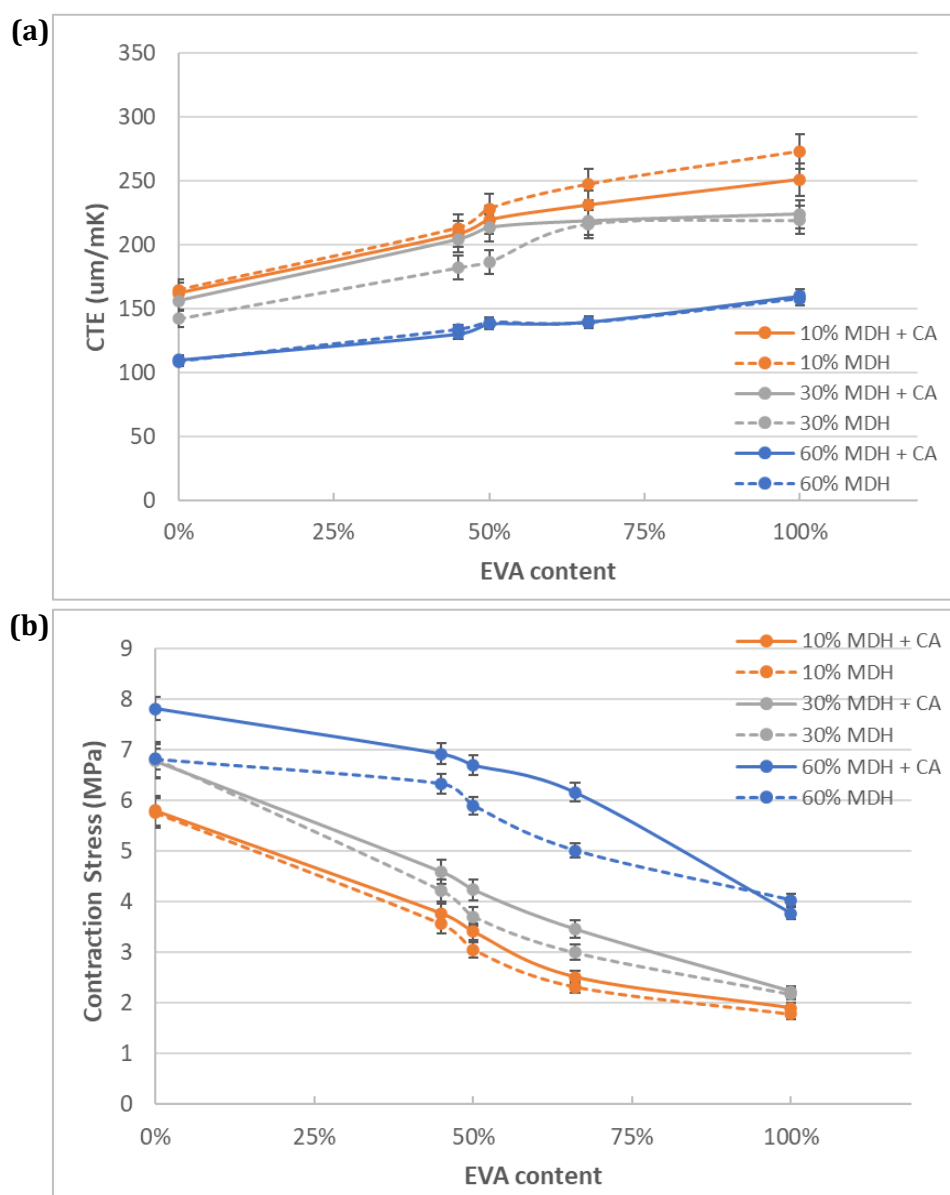
Figure 49   Coefficient of thermal expansion (a) and contraction stress (b) of filled EVA/LLDPE
             blends with different dosages of Magnesium-di-hydroxide (MDH) with and without MAA-
             grafted coupling agent (CA)

6.2.4 Morphological characterization

The compound morphology was investigated using cryo-fractured samples and SEM microscopy on 50/50 % - EVA/LLDPE blends with and without 5 % MAA-g-LLDPE coupling agent. To highlight the influence of the filler, only 30 % and 60 % samples are shown, as no influence of 10 % MDH was identified in the recent sections. To distinguish the polymer phases and to enhance the contrast, staining was used for sample preparation. The resulting SEM images are shown in Figure 50. For comparison reasons, the magnification was kept stable at 1,000x. As the observed

structures become smaller with increasing filler level, additional pictures with 10,000x are shown for both 60 % MDH samples. The unfilled polymer blends investigated in section 6.1.4 are shown for comparison.

The polymeric phases of the blends can still be recognized in the 30 % MDH sample. In addition, it is observable that the filler is mainly located in one phase in absence of coupling agent. Looking at the same recipe with coupling agent (30 % MDH + CA), the blend morphology can be hardly identified. The filler seems to be more evenly distributed throughout the sample. Due to the increasing amount of filler, the blend morphology is not visible in the 60 % filled samples, neither with nor without coupling agent. In general, the sample with coupling agent shows a finer structured fracture surface. This is a sign for improved coupling and reduced polymer phase sizes. This can be seen at the images taken with higher magnification. The filler particles are surrounded by a finer structured morphology. Contrary to the expectations, signs of polymer-filler interaction can also be observed for the sample without coupling agent.

Figure 50   SEM images of cryo-fractured and RuO4 stained surfaces of filled 50/50 % - EVA/LLDPE
             blends with different dosages of Magnesium-di-hydroxide (MDH) with and without MAA-
             grafted coupling agent (CA)

To investigate the morphology more in detail, the investigated cryo-fractured samples were etched to remove the EVA portion. The residual structures can be seen in Figure 51 with a magnification of 1,000x to judge the morphology. The unfilled samples are shown for comparative reason. The phase size reduction of LLDPE caused by increased polarity is visible (see section 6.1.4). The addition of 30 % filler decreases the LLDPE phase size of both sample variants. The effect of the coupling agent reducing the LLDPE phase size is also maintained. Comparing the LLDPE residue, the sample without coupling agent shows a smooth surface and no inclusions of flame-retardant filler in the LLDPE. In comparison to this, the residue of the sample with coupling agent shows very rough structures which seem to consist of flame-retardant. The morphology is getting even finer when looking at the 60 % filled samples. The effect of smaller phases due to the coupling agent can be clearly seen for all samples, with and without filler, which supports the theory of increased polarity. Co-continuity of the LLDPE fraction is maintained throughout all samples. Deeper investigations about the filler location using a higher magnification are following in the next paragraph.
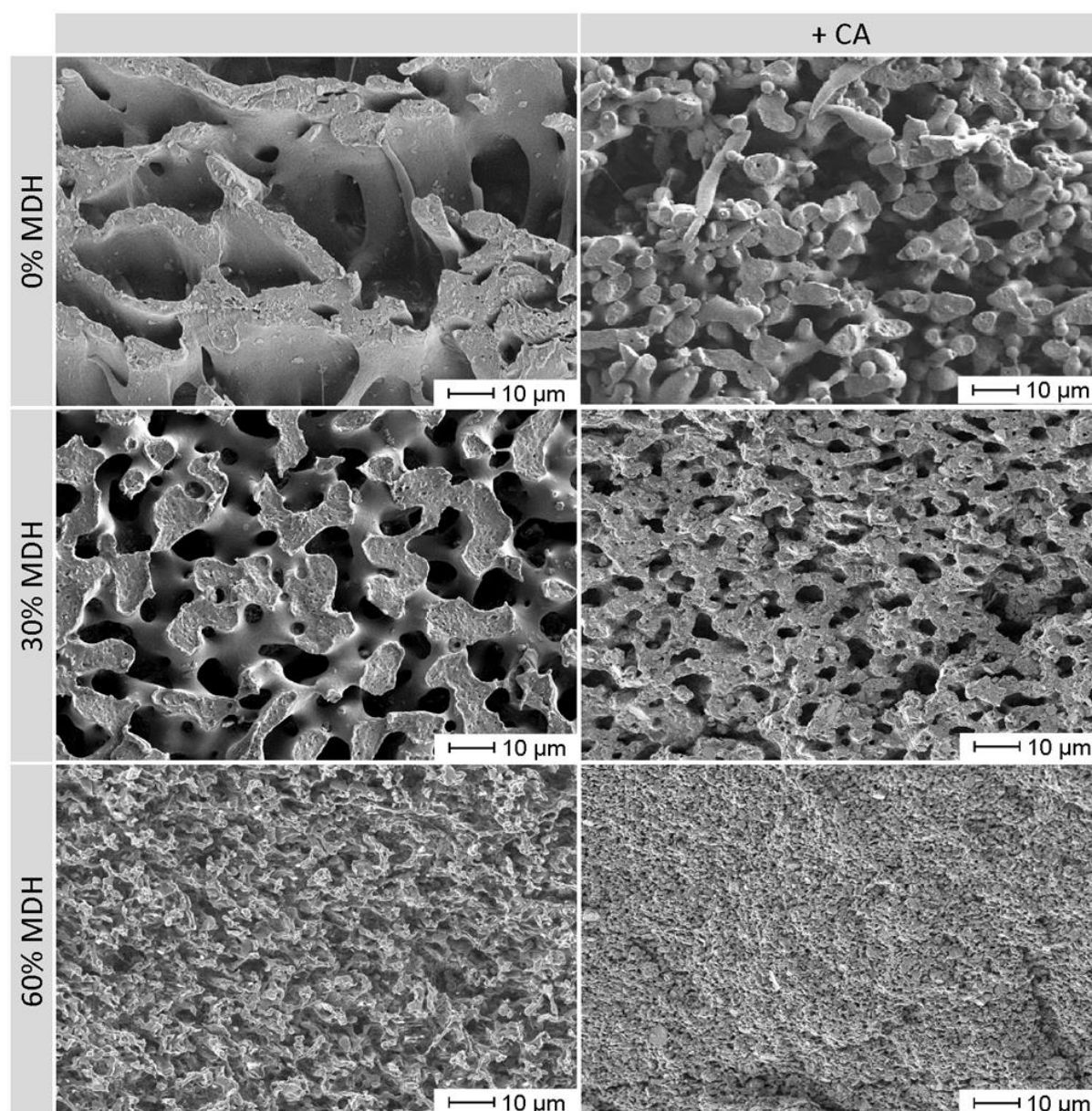
Figure 51   SEM images of cryo-fractured and xylene etched surfaces of filled 50/50 % - EVA/LLDPE
             blends with different dosages of Magnesium-di-hydroxide (MDH) with and without MAA-
             grafted coupling agent (CA) – magnification 1,000x

For easier determination of the filler location, the etched samples were investigated with higher magnification, see Figure 52. Significant differences in between the samples with and without coupling agent can be observed. Looking at the samples without coupling agent (left), the filler was completely removed with the EVA phase. Only a few stray particles remained on the sample surface after etching. A check for inclusions was performed by optical investigation of the cryo-fracture plane and EDX analysis - no filler was detectable in the LLDPE phase.

Analyzing the samples containing coupling agent (right), it can be observed that the flame-retardant filler remains after etching. The filler is located at the LLDPE surface which represents the blend interphase between LLDPE and EVA. In some cases, filler was partially stuck in the LLDPE but a check for filler inclusions in the LLDPE using EDX on the larger fracture surfaces was negative. All particles seen at the surface show free space where the EVA was located. It can also be seen that the polymeric phases become smaller with increased filler content (60 % MDH) resulting in a phase diameter close to the filler particle size. Here a clear determination of the filler location and interaction with the polymer is not possible anymore.
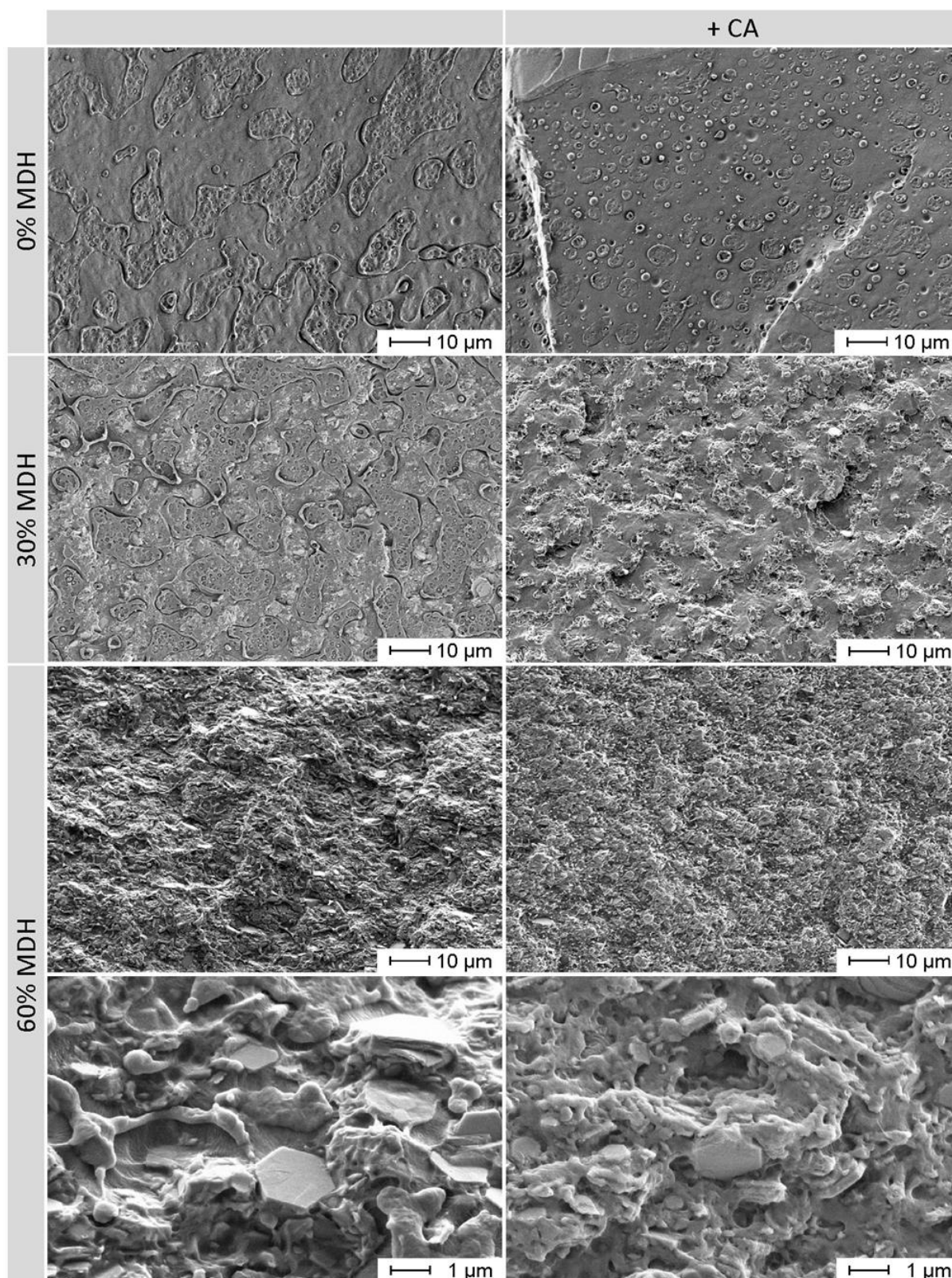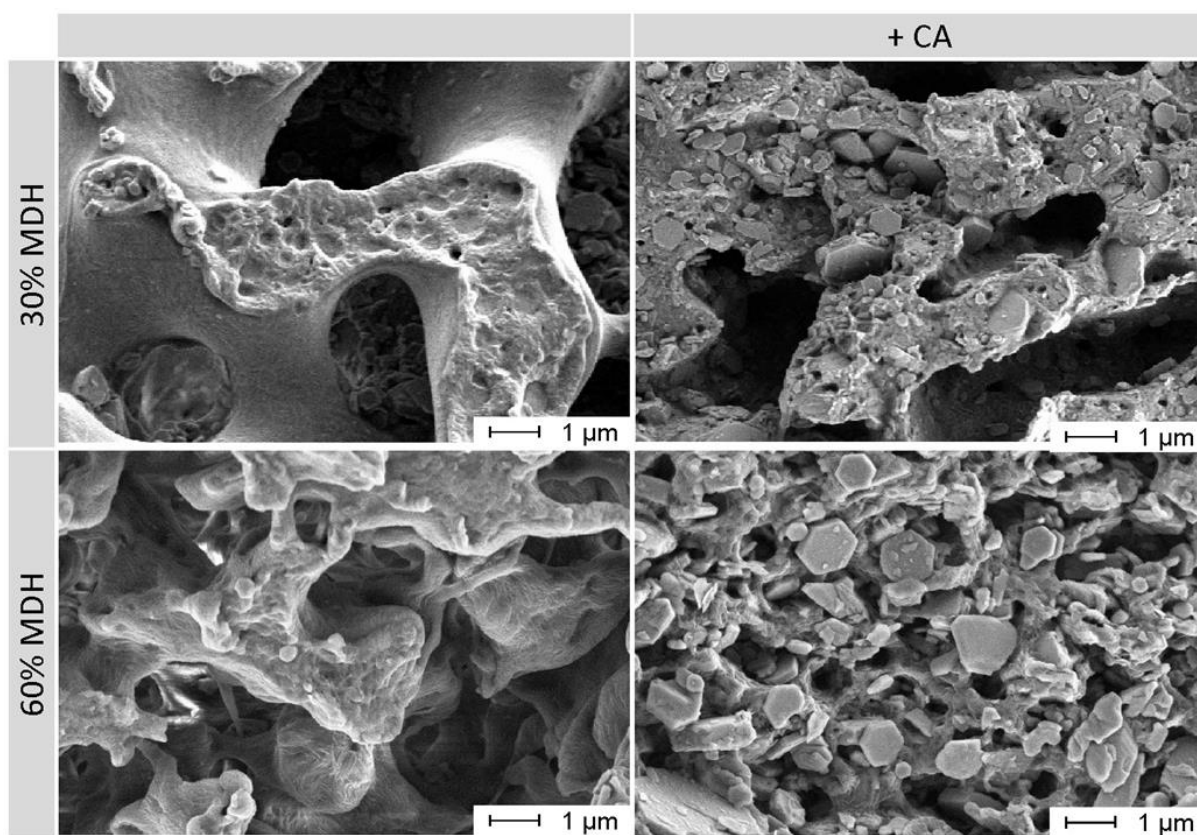

Figure 52   SEM images of cryo-fractured and xylene etched surfaces of filled 50/50 % - EVA/LLDPE blends with different dosages of Magnesium-di-hydroxide (MDH) with and without MAA-grafted coupling agent (CA) – magnification 10,000x

Further investigations to determine the filler location were tried using TEM microscopy, but the filler caused sample break during microtome cutting. A try to cut the samples with an ion-beam degraded the polymers. TEM microscopy of thicker samples was still performed but the contrast between both polymers was lost due to the high intensity of the filler.

6.2.5 Conclusion

The DSC measurements have shown that neither the usage of a coupling agent, nor the addition of filler caused a change in crystallinity of the investigated EVA/LLDPE based compounds. A change in the melting peak shape is very likely caused by the superposition of the coupling agent and the LLDPE. Nevertheless, a nucleation effect of the filler particles on crystallization of the PE backbone cannot be completely excluded.

Parallel plate rheology measurements of the EVA/LLDPE blends showed an influence of the filler content, but none for the coupling agent. In addition, viscosity measurements of the pure polymer components containing the same degree of filler with and without coupling agent were performed. Based on these rheological results, the expected phase inversion of the unfilled and filled immiscible blends was calculated. Depending on the filler distribution within the polymer phases, 3 scenarios were estimated:

    (1) equal filler distribution or
    (2) full incorporation in either the EVA or
    (3) the LLDPE phase

Not included in the calculation is scenario (4) with the filler in the interphase. While the first scenario of the calculation did not predict significant changes in the morphology, scenarios (2) and (3) did. Based on the filler location in the compounds, the scenario in samples without coupling agent can be identified as "(2) filler only in EVA". The previously described yield stress effect in melt viscosity at low shear rates was only observed in the pure LLDPE. In presence of EVA (e.g. the 50:50 blend without coupling agent), this effect is absent due to interactions of the filler with the EVA phase. As soon as coupling agent is present in the formulation, the filler is located in the interphase which fits to scenario (4). Both, the presence of EVA or MAA-g-LLDPE therefore increase the rheological filler percolation threshold by a more sufficient filler coverage.

The blend morphology and the phase sizes were determined analyzing cryo-fractured surfaces. It was observed that the morphology of all samples was affected by the coupling agent. In addition, the flame-retardant filler showed a preferential incorporation in the EVA phase. Both effects where further investigated.

By etching the EVA portion in the compound, a clear view on the morphology of LLDPE was possible. The LLDPE phase becomes finer with increasing filler content. This is not only caused by the flame-retardant filler as a third volumetric fraction, but also by preferential filler incorporation. The size reduction of the residual LLDPE structures by addition of the coupling

agent could be identified for all filler loadings. It needs to be considered that this leads to an increase of the blend interphase. This potentially supports the observed effect of filler relocation into the interphase, described in the following paragraph.

By analyzing the images at a higher magnification, it was possible to determine the detailed filler location in the blend systems. The samples without coupling agent show no presence of filler in the LLDPE phase. This observation is described by Tham et.al. [71] in 2016 where interactions of EVA and the OH-groups of uncoated silica by hydrogen bonds were reported. The observed morphology fits good to the former calculated results from the rheological measurements with the scenario "(2) filler only in EVA" and a significant shift of the phase inversion point towards the LLDPE. By closer investigation of the etched samples containing coupling agent, it was observed that the LLDPE phase is covered with flame-retardant filler. Based on EDX investigations it was identified that the flame-retardant is located in the interphase between the LLDPE and EVA.

The observed filler locations fit to the effects seen in mechanical analysis at room temperature (tensile tests), where throughout all samples, no improvement by adding MAA-g-EVA was observed. The modulus of the blends was increased by adding the flame-retardant filler independently from coupling agent usage. Above a certain threshold, the influence of the coupling agent became visible, mainly on the LLDPE rich blend ratios. This was seen also in DMA, where the usage of coupling agent, especially in the 50/50 blends caused a significant improvement of the mechanical properties at elevated temperature. The earlier melting and softening of the EVA phase are compensated by the more stable LLDPE phase in presence of MAA-g-LLDPE and filler although both polymer phases stay immiscible.

This leads to the theory that the filler in combination with the coupling agent creates a connection between the polymer blend components. For further clarification, a graphical model is shown in Figure 53. EVA interacts with the flame-retardant filler through hydrogen bonds. In systems without coupling agent, the LLDPE has no chance to interact with the filler. By adding the LLDPE based coupling agent, the LLDPE phase interacts with the filler chemically through covalent and physically through hydrogen bonds. This moves the filler into the interphase which creates a strong interaction with the polymers and consequently results in a finer morphology.
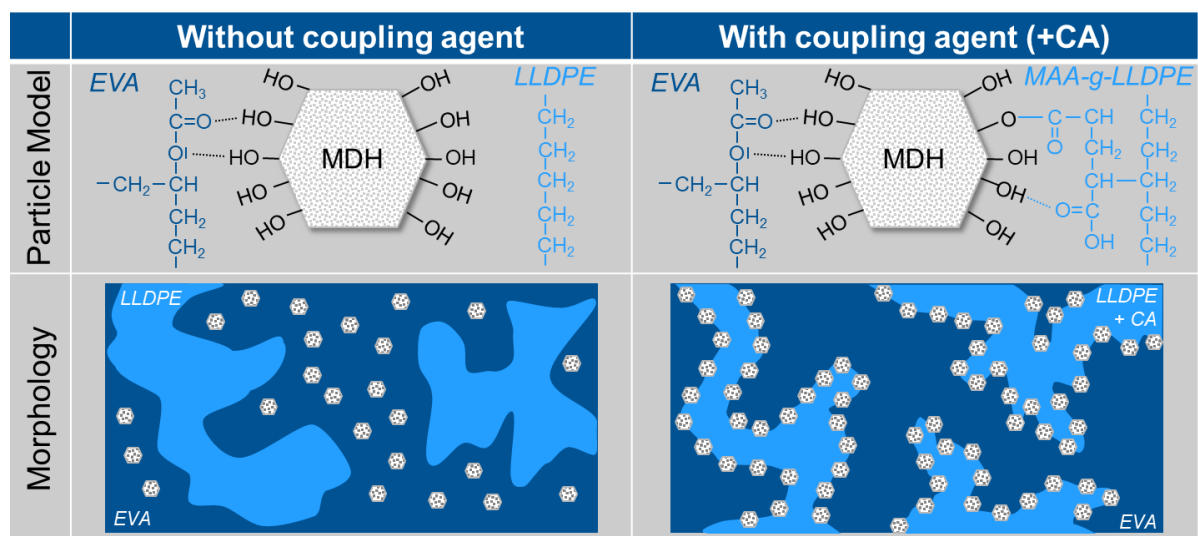
Figure 53   Graphical model of the polymer-filler interactions with and without coupling agent

6.3 Surface modified fillers and compatibilized EVA/LLDPE blends

This chapter aims to describe the impact from the addition of surface modified mineral based flame-retardant additives into the investigated systems from section 6.2. The interaction of these modifications with the polymers, the maleic-acid-anhydrite based coupling agents and the resulting blend properties and morphology shall be understood.

Comparable to section 6.2, EVA/LLDPE blends consisting of 0 %, 45 %, 50 %, 67 % and 100 % EVA were compounded to cover the pure polymers, the regions before and after phase inversion and a typical cable recipe. The formulations are filled with different ratios (30 %, 60 %) of Magnesium-di-hydroxide (MDH) with two different silane coatings. The used fillers are commercially available, and pre-coated with vinylsilane (recommended for reactive extrusion) or aminosilane (recommended for EVA based systems). The two coatings are chosen to represent different types of filler-polymer interaction: the ability to form covalent bonds in the presence of radicals (vinylsilane) and the ability to form hydrogen bridges (aminosilane) as shown in section 4.4.2. A question to be answered is, if the vinylsilane can still form a covalent bond in the presence of an activated maleic-acid-anhydrite coupling agent. Comparable to the recent sections, all samples were compounded with and without MAA-g-LLDPE coupling agent (CA), except for the 100 % EVA sample which was mixed with MAA-g-EVA. The coupling agent dosage remained stable at a ratio of 2 phr coupling agent per 10 wt% of mineral filler.

In the following paragraphs, the investigated properties are described. The thermal analysis by differential scanning calorimetry did not show any effects caused by the filler coatings and therefore will not be shown. The number of highly filled samples (60 % MDH) with this work package allowed comparative investigation of the burning behavior and flame-retardancy of these formulations.

6.3.1 Rheological characterization

To further understand the blend mixing dynamic in the presence of filler and to calculate potential new phase inversion points, the pure blend components and the blends were characterized in parallel plate rheometry. It is expected that the viscosity and the filler location in the melt are affected by the filler coating.

A comparative overview of the rheological analysis in a frequency sweep for EVA (a), LLDPE (b) and 50/50 % – EVA/LLDPE (c) with different amount of filler is shown in Figure 54. The unfilled version of each polymer composition is shown as a reference in yellow. The samples without

coupling agent are drawn in dotted lines, the samples containing coupling agent in solid lines. In pure EVA (a), the general behavior does not show any difference caused by the filler coating. Comparable to the results shown in section 6.2.1, the coupling agent does not show any effect in EVA for the silane coated filler versions. The samples containing uncoated and aminosilane (AS) coated filler show similar results. The sample using vinylsilane (VS) shows comparable behavior with a shift to lower viscosity values which can be a sign for reduced filler-polymer interaction. The viscosity curves of the pure LLDPE compounds (b) also show the lowest viscosity for the vinylsilane coated filler version. In absence of coupling agent, the already described "yield stress effect" of the uncoated filler caused by percolation effects can also be observed for the aminosilane and the vinylsilane coated filler. The three dotted curves proceed parallel throughout the whole measurement with the uncoated sample showing the highest viscosity. This is a sign that both filler coatings show particle-particle interaction at low frequencies. By using the MAA-g-LLDPE coupling agent, these effects are significantly reduced with the uncoated filler showing the strongest difference, followed by the aminosilane sample. The 50/50 % – EVA/LLDPE blend (c) also shows a reduced viscosity of the vinylsilane sample without coupling agent. All other samples are in a very comparable range, uncoated and aminosilane filler show no differences whether coupling agent is present or not.
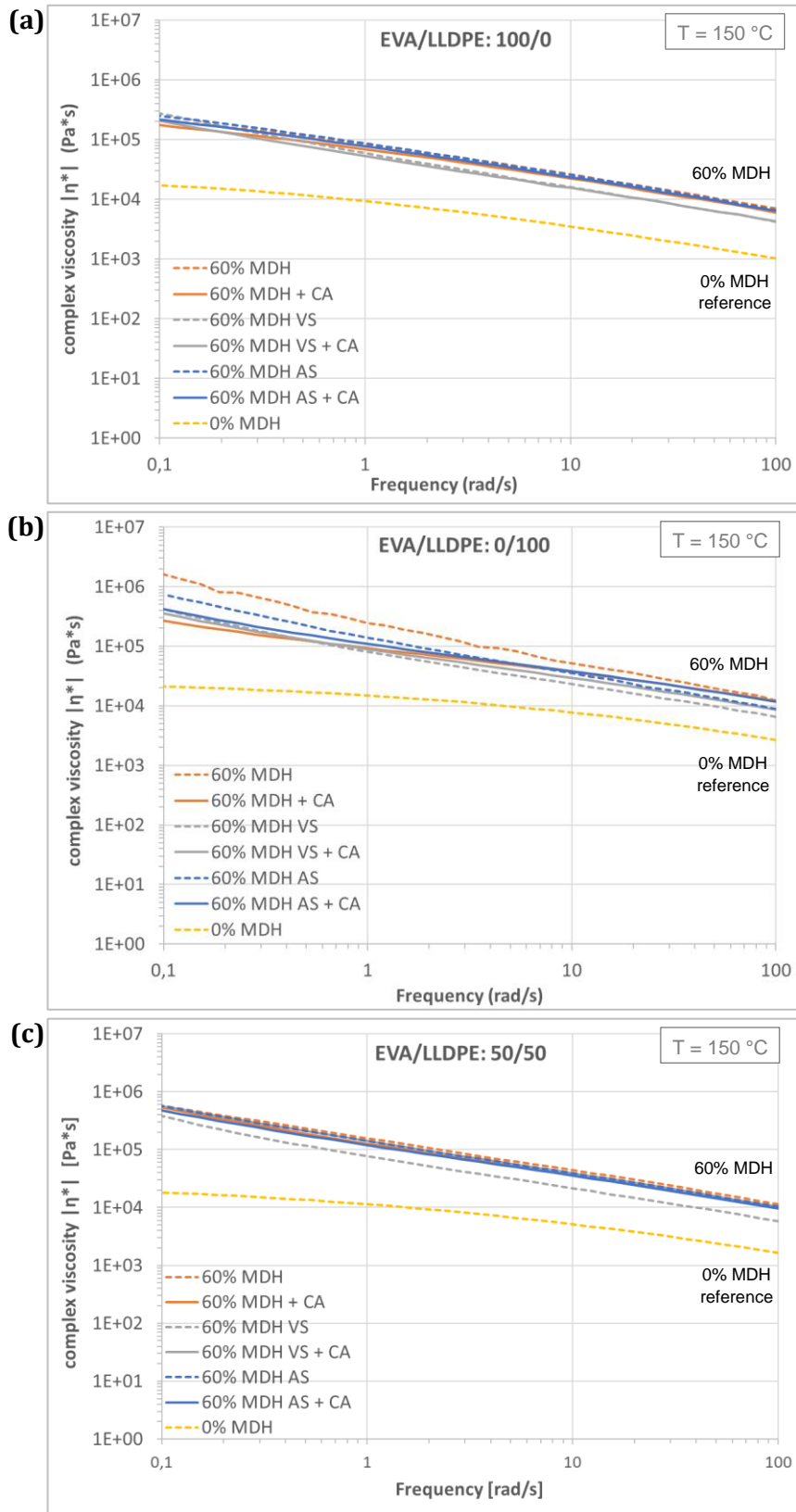
Figure 54   Frequency sweep of EVA (a), LLDPE (b) and 50/50 % - EVA/LLDPE (c) with uncoated, vinylsilane (VS) and aminosilane (AS) coating of magnesium-di-hydroxide (MDH), with and without MAA-grafted coupling agent (CA)

In the previously shown results, it can be observed, that the incorporation of filler affects the viscosity especially for pure LLDPE. Therefore, the theoretical phase inversion point will be calculated after the filler location is exactly determined by morphological studies in the following paragraphs.

The difference between the vinylsilane coated particles and the other two filler versions becomes more visible in melt flow rate testing (see Figure 55). The uncoated and the aminosilane coated filler show no significant influence of the coupling agent which points towards a comparable filler-polymer interaction. The vinylsilane coated particles show signs of interaction with the coupling agent in the LLDPE rich regions which is lost towards increasing EVA content. In absence of the coupling agent, no interaction is seen, and the melt flow rate is significantly higher.

Figure 55   Melt volume rate of EVA/LLDPE blends filled with 60 % of uncoated, vinylsilane (VS) and aminosilane (AS) coated magnesium-di-hydroxide (MDH), with and without MAA-grafted coupling agent (CA)

6.3.2   Thermo-mechanical characterization

The compounds using different filler coatings were extruded as strands and then tested in a tensile test. As the 60 % filled versions are of highest interest for the cable application, these results in EVA, LLDPE and 50/50 % - EVA/LLDPE are shown in Figure 56. Comparable results were also observed for the 30 % filled samples. The pure EVA matrix (a) shows the strongest interaction with the aminosilane coated filler resulting in the highest tensile strength, followed by the uncoated filler. Vinylsilane does not show any signs of polymer-filler interaction resulting a

high elongation at break values with strong necking of the samples, but low tensile strength. Only minor improvement by the applied coupling agent is visible for all filler types.

The higher stiffness of the neat LLDPE systems (b) can be seen in the higher yiel stress and lower elongation values. The vinylsilane coated filler shows the same signs of missing intraction as observed in neat EVA. This changes by the addition of coupling agent resulting in a slight increased yield strength and significant reduction in elongation at break. Also, both other coatings show improvement in polymer-filler interaction by combination with the coupling agent. The combination of the MAA-g-LLDPE coupling agent with uncoated MDH leads to highest improvements in tensile strength and elongation at break.

Beneficial effects of the coupling agent can also be seen in the 50/50 % - EVA/LLDPE blend (c). The addition results in increased strength of all samples. Very comparable properties of the aminosilane coated and uncoated MDH can be seen. The samples using vinylsilane coated filler show signs of coupling by increased tensile strength, but still weaker than the other two filler types. This leads to the assumption that either the vinylsilane filler coating shows low coupling reactivity or the MAA-g-LLDPE coupling agent reacts with sections on the filler surface that are not fully covered with coating.

Figure 56   Stress/strain curves of EVA (a), LLDPE (b) and 50/50 EVA/LLDPE (c) filled with 60 % of
             uncoated, vinylsilane (VS) and aminosilane (AS) coated magnesium-di-hydroxide (MDH),
             with and without MAA-grafted coupling agent (CA)

For the overall picture, yield strength and elongation values for the whole investigated range of EVA/LLDPE blends are shown in Figure 57. The trend of decreasing yield stress (a) with increasing EVA content is still visible for all coatings. In general, the samples using uncoated and aminosilane coated filler behave very comparable, with and without coupling agent. Improvement by usage of the coupling agent can be seen for all fillers, strongest effects on the LLDPE rich blends. The vinylsilane filler shows the weakest performance and the performance with coupling agent is still lower compared to the other two filler types without. This indicates that the filler coating reduces the filler-polymer interaction with both EVA and LLDPE. This can also be seen in the elongation at break values (b) where the results follow the behavior observed in the melt flow test from Figure 55. This further proves the reduced interaction of the vinylsilane filler, especially in the EVA rich regions. Differences in between the uncoated and aminosilane coated samples were identified in the neat polymer. There the sample MDH+CA performs better in LLDPE (left) and the samples MDH AS and MDH AS + CA show improved performance in EVA (right). This is a sign, that the aminosilane coating further improves the interaction to EVA, as it was expected and described in section 4.4.2.
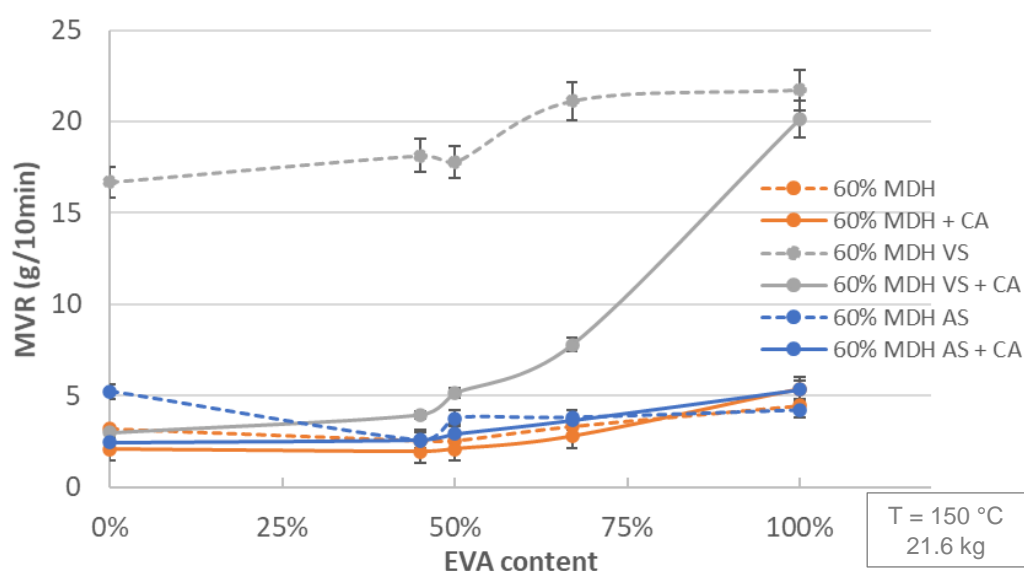
(a)

(b)

Figure 57   Yield strength (a) and elongation at break (b) of EVA/LLDPE blends filled with 60 % of uncoated, vinylsilane (VS) and aminosilane (AS) coated magnesium-di-hydroxide (MDH), with and without MAA-grafted coupling agent (CA)

The influence of the filler coating and coupling agent on the tensile stress can be also identified in the hysteresis measurements (Figure 58), as these tests are performed in the same way until 50 % elongation is reached. While the tensile stress level of the samples is clearly dominated by the strength of polymer-filler coupling, the tensile set is very comparable for all samples. The only significant exception is the sample with uncoated filler without coupling agent (MDH) that did not reach 50 % elongation.

Figure 58   Hysteresis measurement of EVA/LLDPE blends filled with 60 % of uncoated, vinylsilane (VS) and aminosilane (AS) coated magnesium-di-hydroxide (MDH), with and without MAA-grafted coupling agent (CA)

To further investigate the thermo-mechanical stability, DMA tests were carried out. Filled samples made of pure EVA (a), pure LLDPE (b) and exemplary the 50/50 blend (c) are shown in Figure 59. The modulus of the pure EVA (a) sample is not significantly affected by the coating of the filler. Only the vinylsilane samples show a decrease in modulus above 20 °C which underlines the theory of reduced interaction. As seen in the previous results, no influence of the MAA-g-EVA coupling agent can be observed. The LLDPE (b) samples show a clear improvement by the usage of a coupling agent for all filler surface variants. The thermo-mechanical stability of the sample using uncoated filler is the highest, followed by the aminosilane sample and vinylsilane as the weakest. This order of performance is valid for the samples with and without coupling agent. This means that the aminosilane coating still interacts more with LLDPE than vinylsilane. Nevertheless, the interaction is reduced in comparison to uncoated MDH. Looking at the 50/50 blend (c), the same order of performance can be observed. The usage of coupling agent improves the modulus at higher temperatures where the EVA performance shows weakness. This works for both filler coatings, as it was already seen for the uncoated MDH in section 6.2.3. It is observable, that the mechanic stability at higher temperatures is defined by the filler-LLDPE interaction.
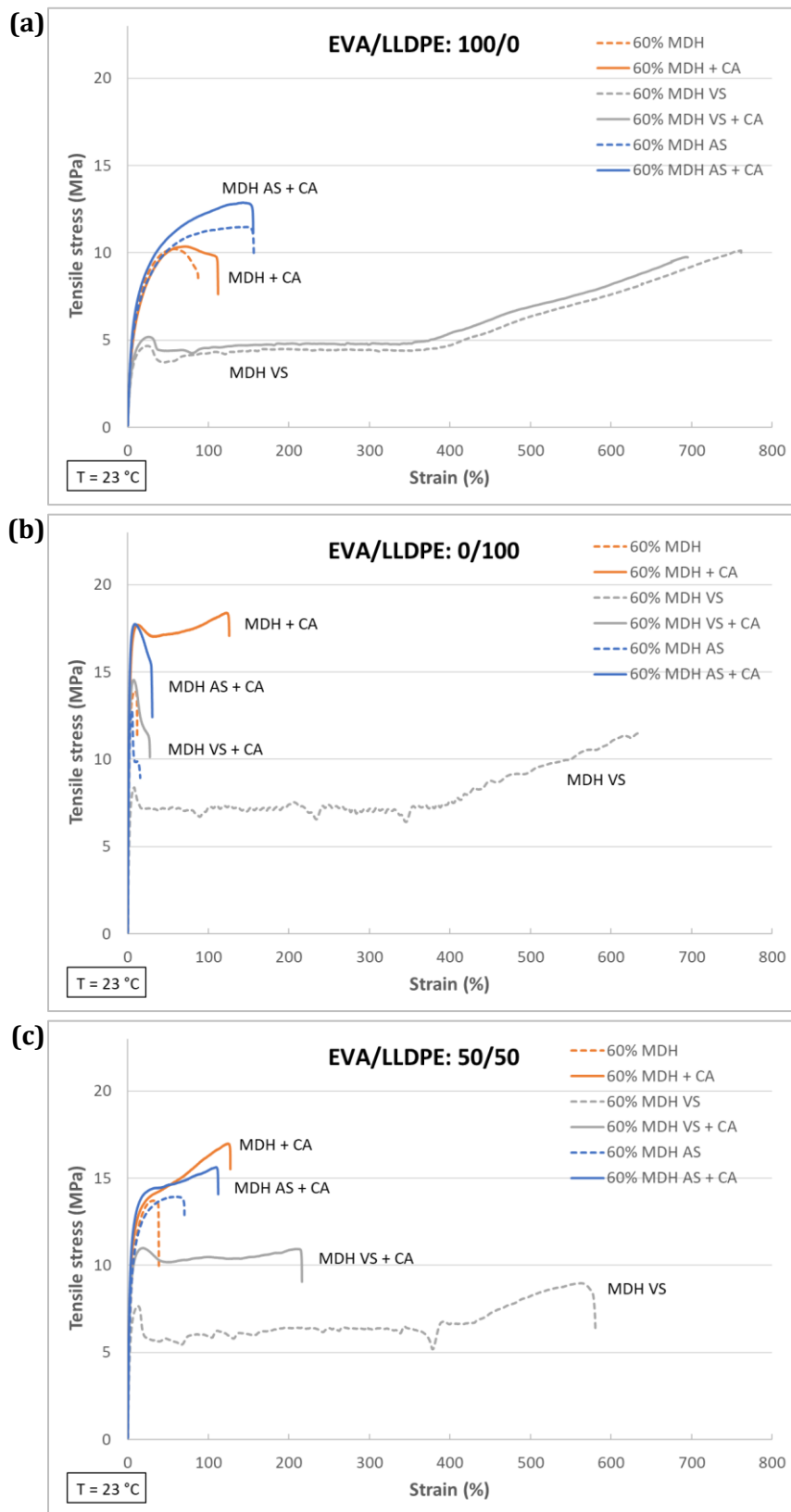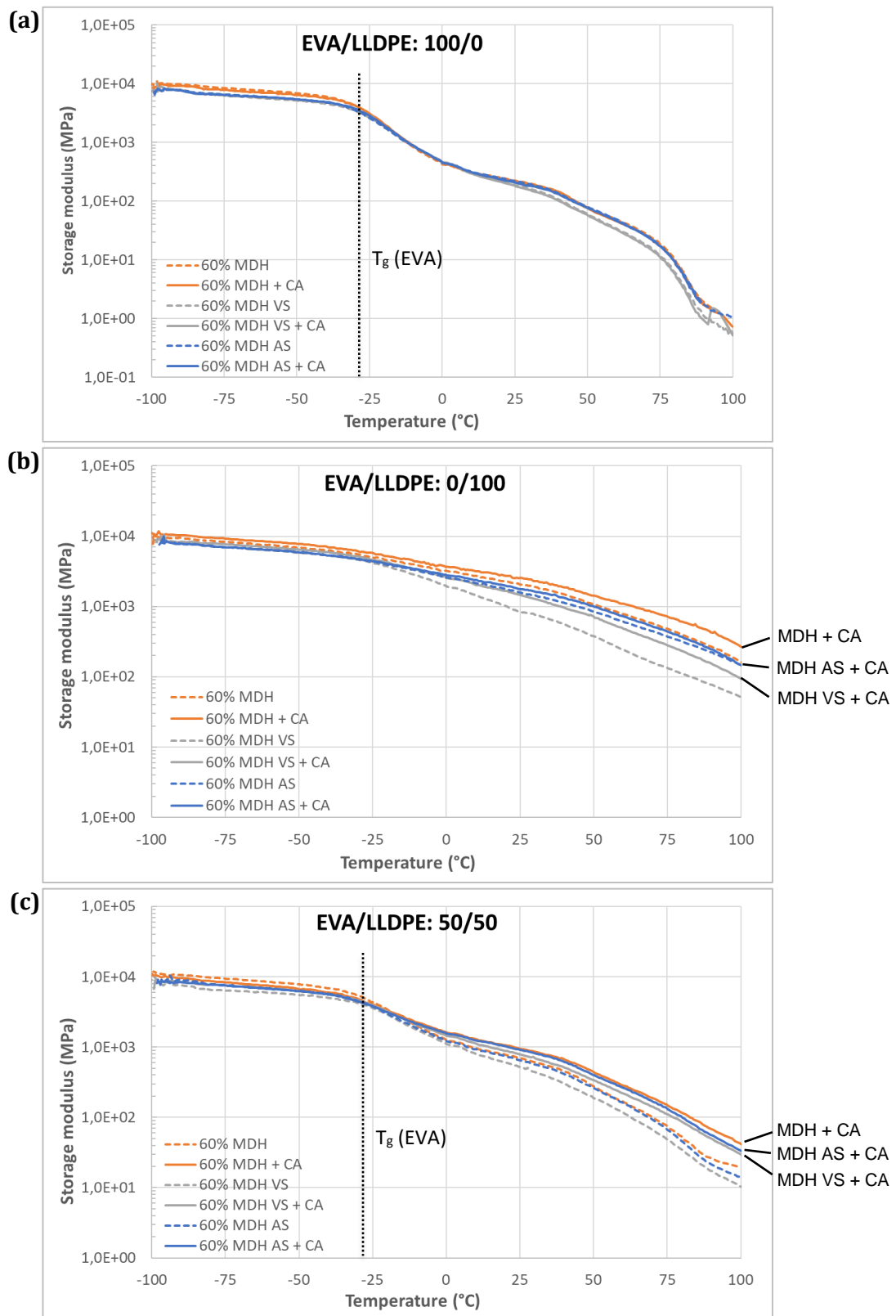
Figure 59   DMA testing of EVA (a), LLDPE (b) and 50/50 - EVA/LLDPE (c) filled with 60 % of uncoated, vinylsilane (VS) and aminosilane (AS) coated magnesium-di-hydroxide (MDH), with and without MAA-grafted coupling agent (CA)

For further information about the shrinkage performance of these compounds, CTE and contraction stress tests were performed (see Figure 60). The CTE values (a) are reduced in the presence of the coupling agent which is a clear sign that filler-polymer interaction occurs. Vinylsilane shows again the weakest results, especially without coupling agent. This filler coupling effects can also be observed in the contraction stress (b) where the usage of coupling agent increases the values. For both measurements, uncoated and aminosilane coating perform comparable.
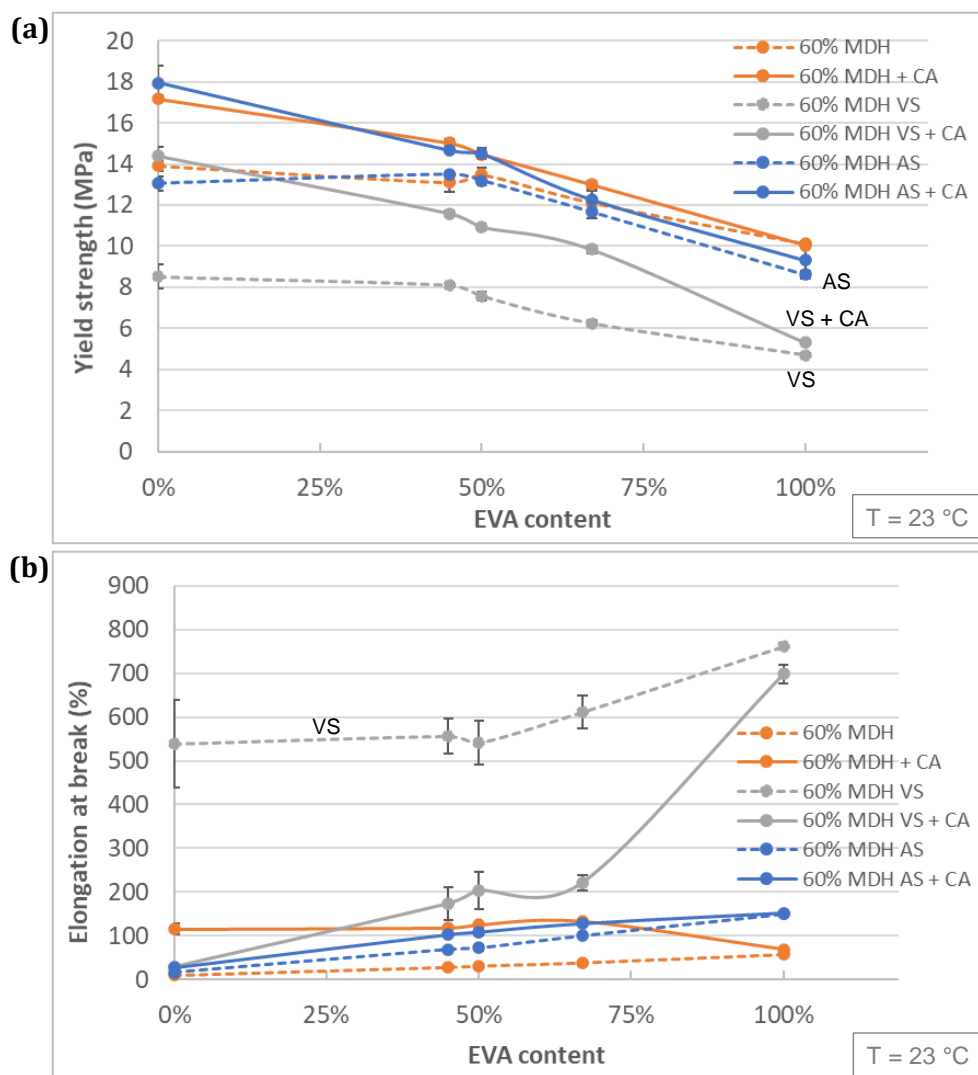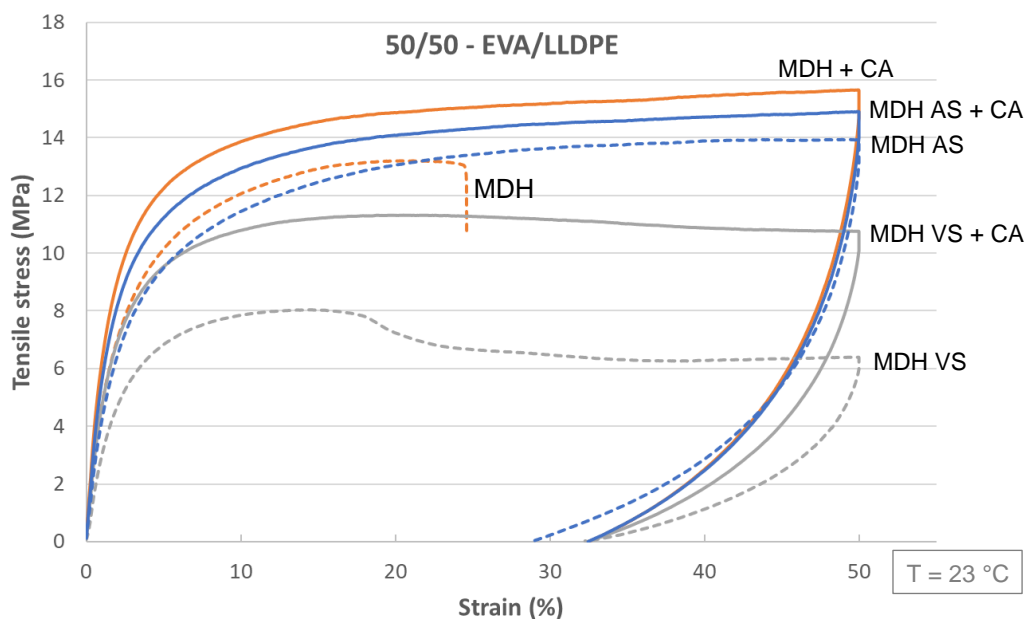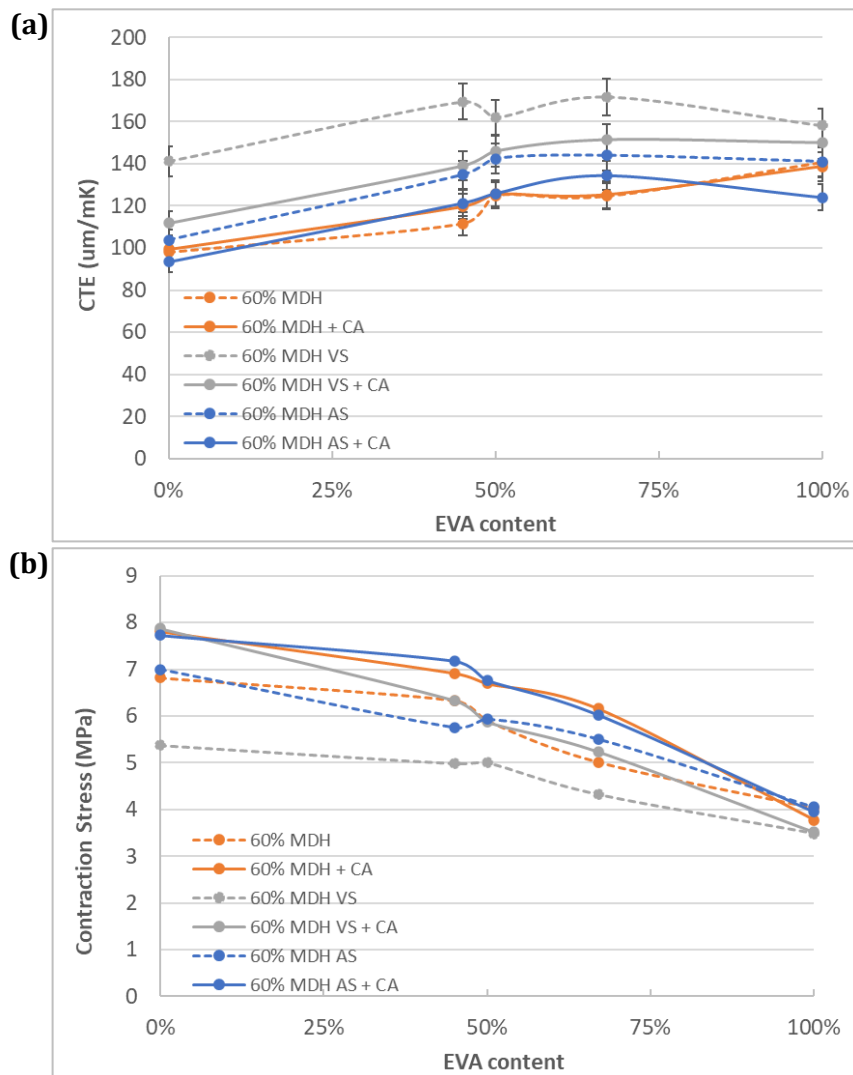

Figure 60   Coefficient of thermal expansion (a) and contraction stress (b) of EVA/LLDPE blends filled with 60 % of uncoated, vinylsilane (VS) and aminosilane (AS) coated magnesium-di-hydroxide (MDH), with and without coupling agent (CA)

6.3.3 Morphological characterization

Before investigating the morphology of the blends, the interaction of the filler using different surface modifications with each polymer needs to be understood. Therefore, samples of pure EVA and LLDPE filled with 60 % of the three flame-retardant filler types were analyzed using SEM microscopy on cryo-fractured specimen (Figure 61).

A closer look at the filler-polymer interactions in presence of the coupling agent is also shown in Figure 62 and the mentioned effects further highlighted. The uncoated filler shows adhesion to the EVA polymer matrix, as it was already observed in section 6.2.4. The same is visible for the sample using aminosilane coating, the fillers are surrounded by polymer and seem to be even more incorporated. This adhesion can be seen especially on the corners of the large filler particle in Figure 61. The free uncovered area on the filler particle is the result of exfoliation effects where adhered layers of MDH were separated during cryo fracture. This is a sign, that the polymer-filler interaction is strong. Looking at the vinylsilane sample, no interaction of the filler with the EVA can be identified. The sample shows filler particles with gaps in the polymer around and holes where filler particles were pulled out without signs of resistance or adhesion. The uncoated and the aminosilane coated fillers show good adhesion while the vinylsilane coated filler still shows no signs of interaction with the EVA. For all samples, no difference between the presence and absence of coupling agent is visible.

Figure 61   Scanning electron microscopy of cryo fractured EVA filled with 60 % MDH with different surface modifications, with and without MAA-g-EVA coupling agent (CA) – magnification 10,000x

Figure 62   Scanning electron microscopy of cryo fractured EVA filled with 60 % MDH with different
             surface modifications, with MAA-g-EVA coupling agent (CA)

Fractured surfaces of the samples of pure LLDPE with 60 % magnesium-di-hydroxide with uncoated, vinylsilane coated and aminosilane coated surface, with and without coupling agent are shown in Figure 63. In the absence of coupling agent, no filler variant (uncoated, vinylsilane, aminosilane) shows signs of interaction with the LLDPE. This can be identified by the polymer-pullout effects between the filler particles. This deformation effect during cryo fracture can be seen for LLDPE due to the lower glass transition temperature of LLDPE (T_g - 110 °C), but not for the EVA samples (T_g -28 °C). Furthermore, no adhesive effects at the filler corners were observed. This changes with the addition of MAA-g-LLDPE coupling agent. The sample using uncoated MDH

shows incorporation of the filler into the polymer. An improvement can also be seen for the silane coating surface modified fillers as the pullout effects are reduced. While the vinylsilane sample shows only minor improvement and still barely polymer coverage at the filler surface, the aminosilane coated filler is incorporated into the polymer much better and shows stronger wetting by the polymer. The described filler-polymer interactions will be shown closer in the next paragraph.
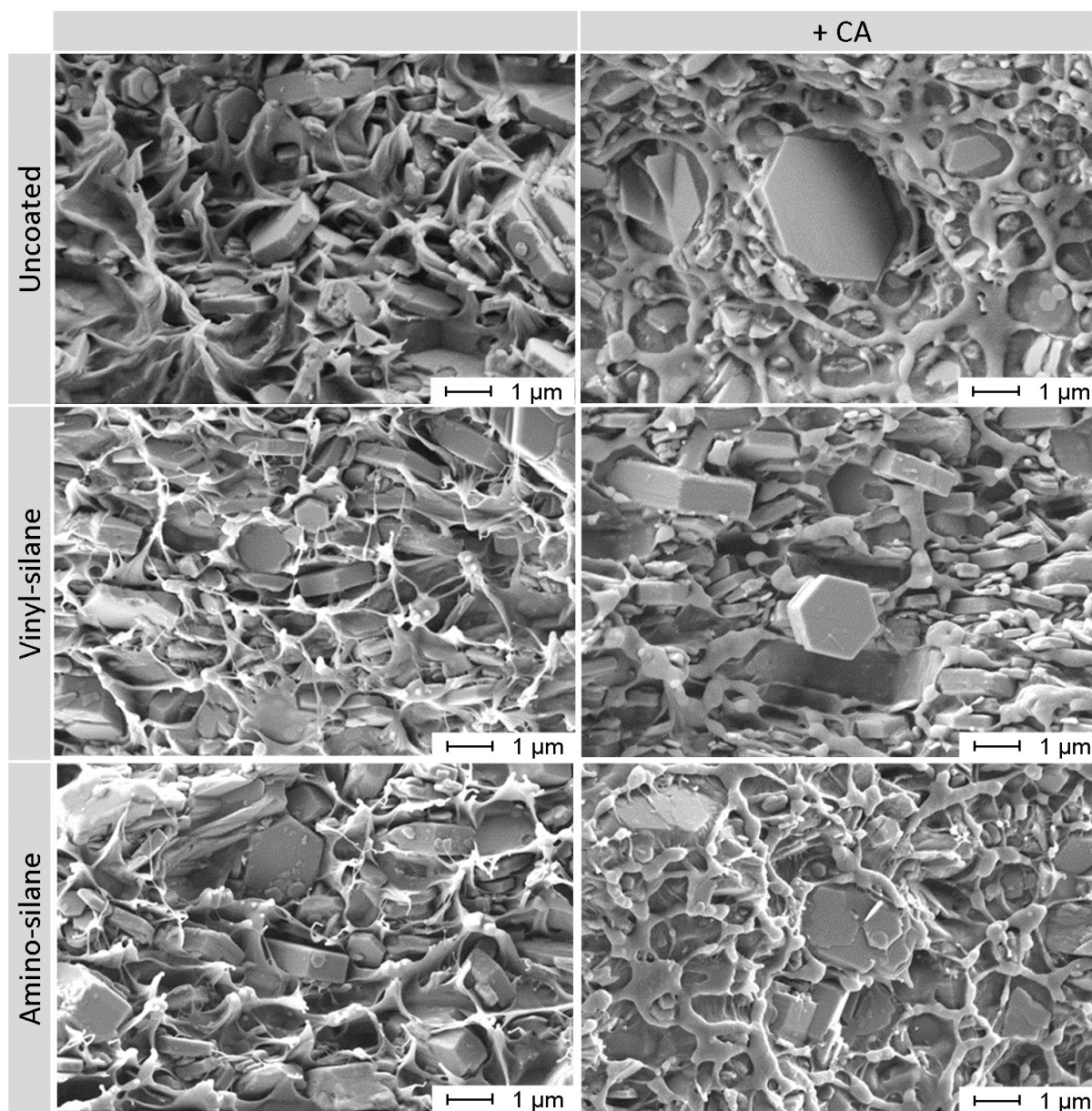
Figure 63   Scanning electron microscopy of cryo fractured LLDPE filled with 60 % MDH with different surface modifications, with and without MAA-g-LLDPE coupling agent (CA) – magnification 10,000x

To further describe the observed filler-polymer interaction in the presence of coupling agent, the areas of interest are enlarged and shown in Figure 64. The uncoated MDH is incorporated into the LLDPE polymer matrix and shows coupling interaction at the sides of the filler particles. This can be also seen at the aminosilane sample. The vinylsilane coated fillers seem not to interact with the coupling agent as smooth residual surfaces after particle pullout can be seen. Only very minor polymer residue on the sides of the particles is observed which might be signs of slight coupling.
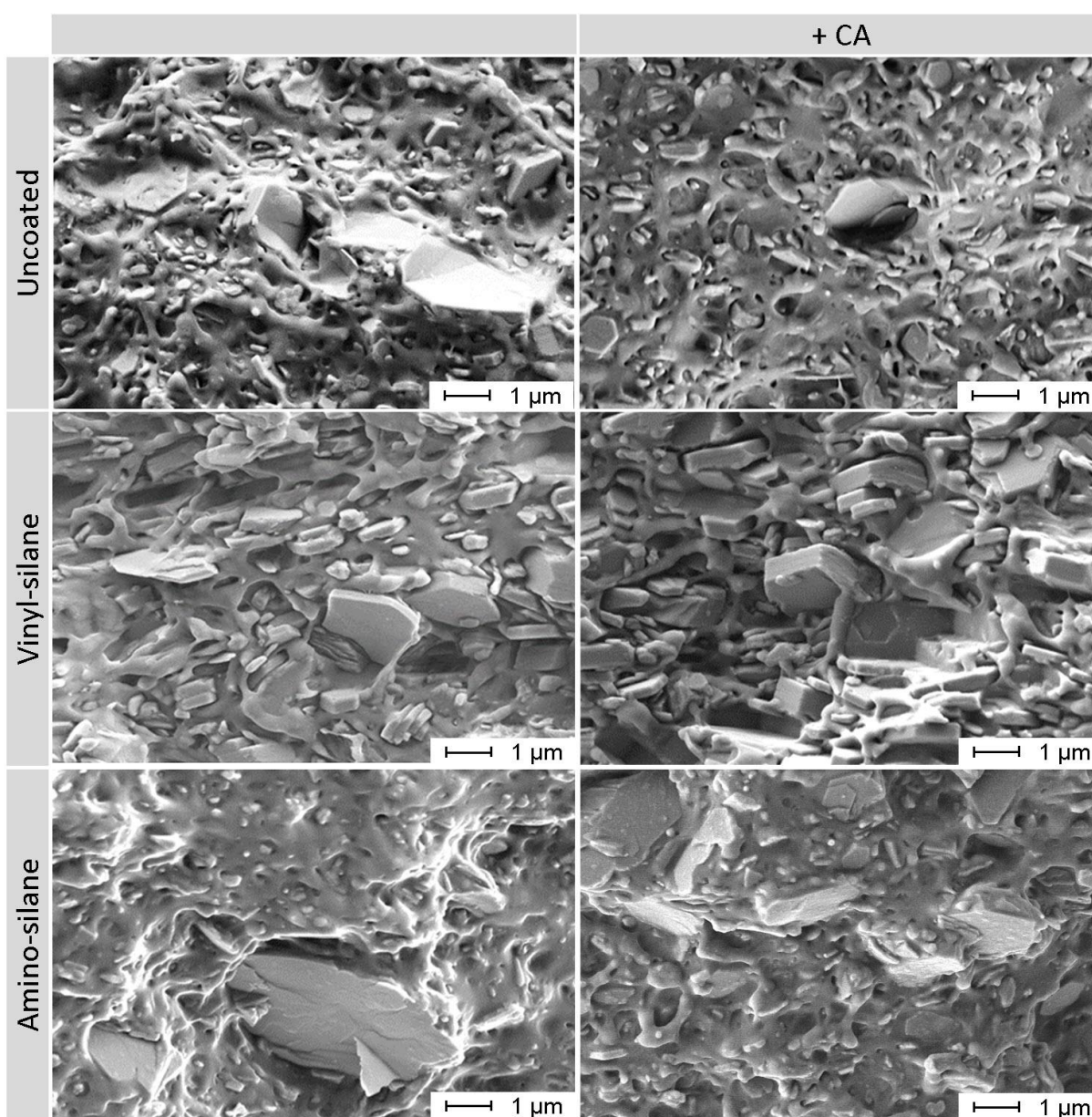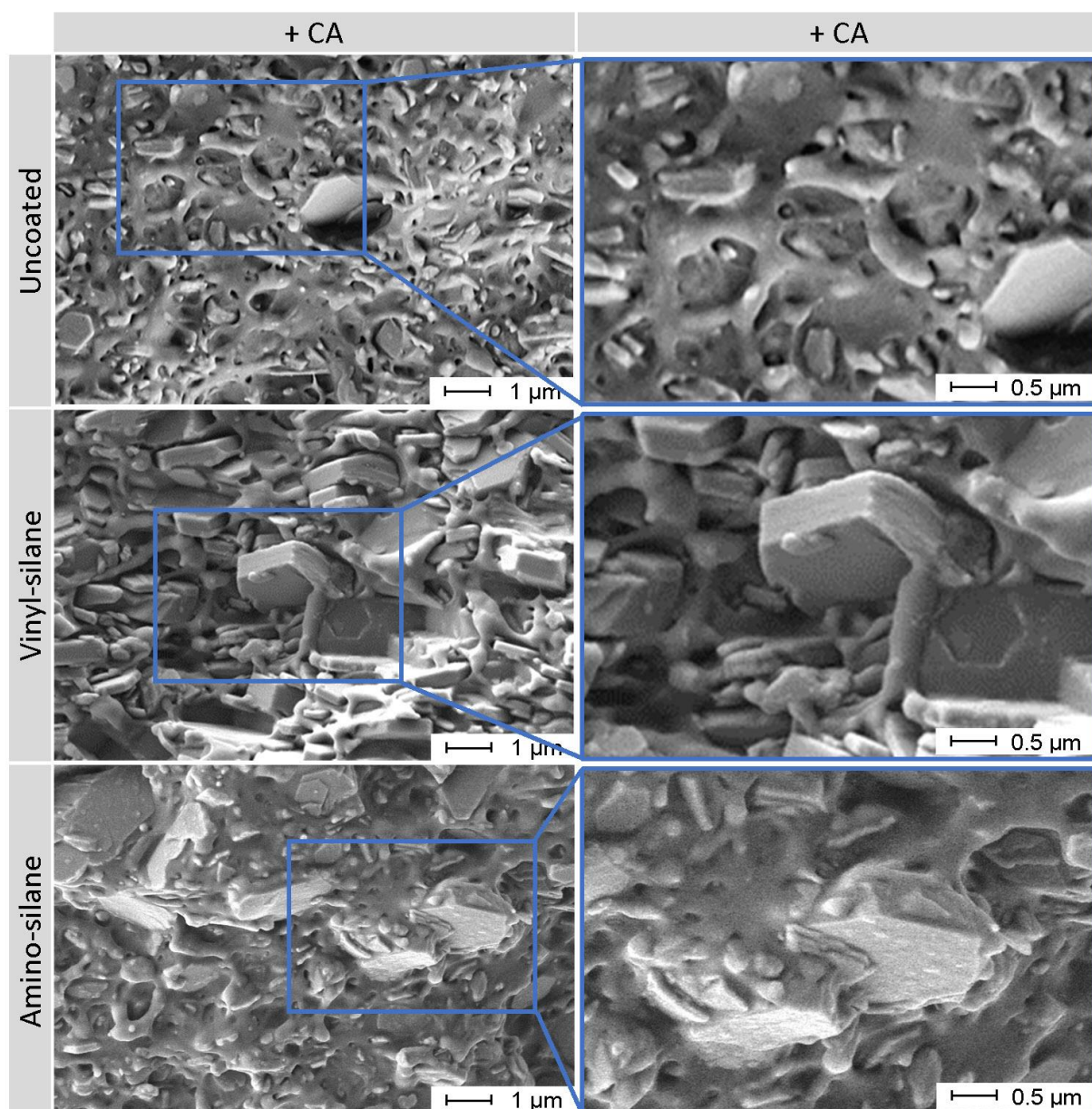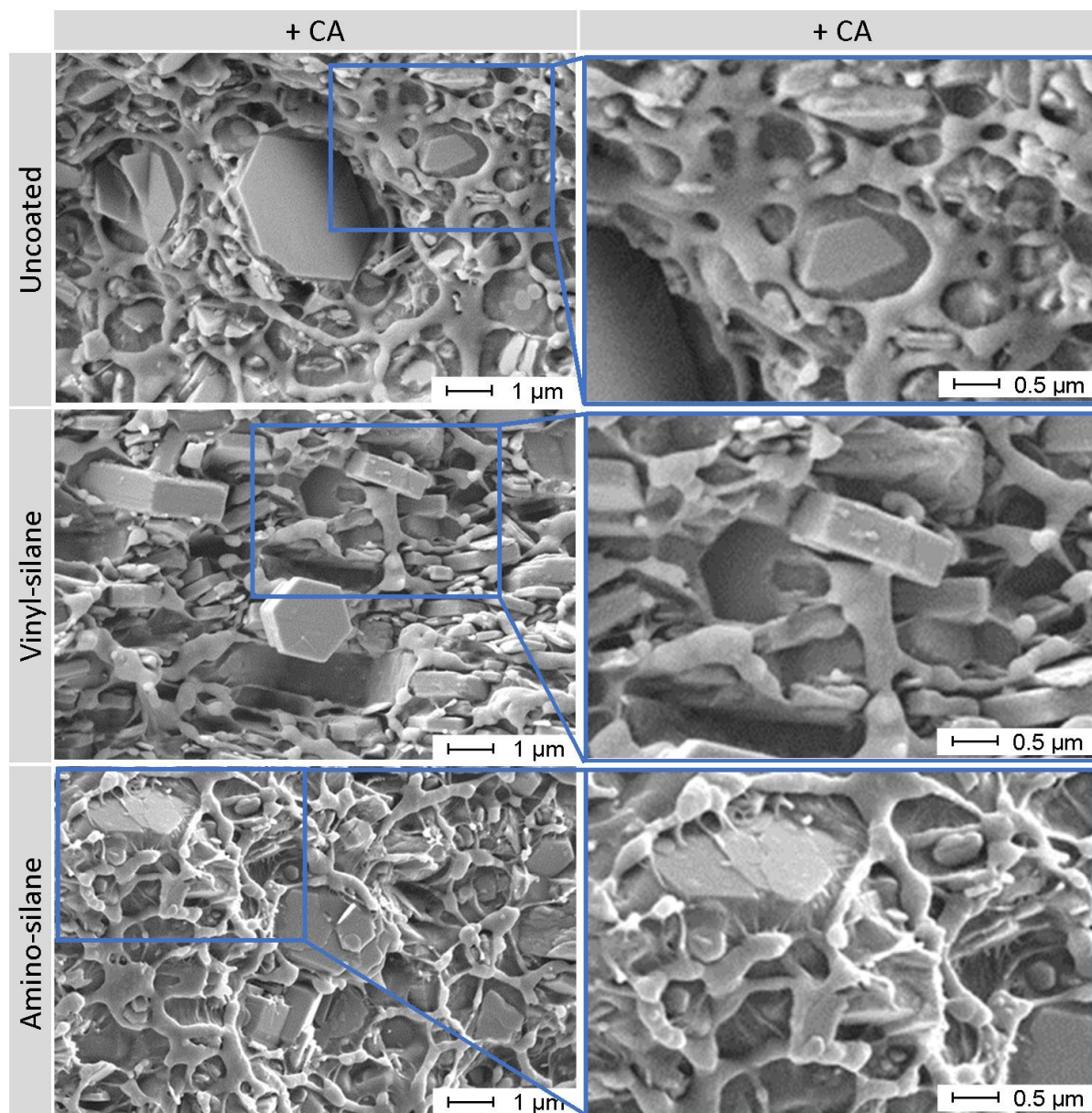

Figure 64   Scanning electron microscopy of cryo fractured LLDPE filled with 60 % MDH with different surface modifications, with MAA-g-LLDPE coupling agent (CA)

Based on a visual judgement of the SEM images, the filler-polymer interaction in pure EVA and LLDPE in presence of the coupling agent can be rated as the strongest for the uncoated and the aminosilane coated filler. Vinylsilane shows the weakest interaction in both polymer and coupling agent scenarios.

These observations give a good overview about the polymer-filler interactions to be expected in the blend systems. To understand these, cryo-fractured blends filled with 30 % and 60 % of both silane coated MDH types were etched and the EVA fraction was removed.

To investigate the resulting blend morphology and phase behavior, the scanning electron microscopy results of 30 % MDH filled 50/50 - EVA/LLDPE blend system with and without MAA-g-LLDPE coupling agent are shown in Figure 65. (More detailed polymer-filler interactions will be shown in the next paragraph.) The already described effects for uncoated filler from section 6.2 can be observed: The LLDPE residue of the sample without coupling agent shows a smooth surface and no signs of flame-retardant filler. The addition of coupling agent reduces the LLDPE phase size and moves the filler from the EVA phase into the interphase where it can be seen covering the LLDPE phase. The LLDPE residue of the sample using vinylsilane coated filler without coupling agent (middle left) shows a more irregular surface in comparison to the residue of the uncoated filled sampe (top left). This can be caused by the irregular shape of incorporated filler but will be further discussed in the next paragraph. Looking at the aminosilane samples without coupling agent, the morphology looks very similar to the uncoated filler. The LLDPE residue shows a smooth surface. Due to incomplete etching, parts of the EVA fraction containing all MDH filler is still visible between the LLDPE structures. This observation further proves the theory of complete MDH incorporation in the EVA.

Figure 65   Scanning electron microscopy of cryo fractured and EVA etched 50/50 % – EVA/LLDPE
                blends filled with 30 % MDH with different surface modifications, with and without MAA-g-
                LLDPE coupling agent (CA) – magnification 2,500x

To identify the filler locations in the 30 % MDH filled 50/50 % - EVA/LLDPE blend systems, more detailed SEM images are shown in Figure 67. The already described effects of the samples containing uncoated filler (first row) can be clearly identified. The sample without coupling agent (top left) shows only small amount of MDH residue from etching on the surface but no filler in the LLDPE phase. In presence of coupling agent (top right), the filler was found covering the LLDPE surface and not being extracted.

The samples using vinyl silane filler (middle left) shows no signs of filler incorporation, although the phase shape looks more irregular than the uncoated sample. Also TGA and EDX analysis have shown that the LLDPE structures without coupling agent do not contain MDH. This result leads to the hypothesis that this structure is still caused by irregular filler shape, but from the interphase side, where the MDH is located. Contrary to the uncoated filler with coupling agent, the vinylsilane filler does not interact with any of the polymers and therefore moves into the interphase. This also results in a smaller LLDPE phase size because the filler does not contribute to any of the polymer volumes. After addition of coupling agent, parts of the filler were identified in the LLDPE showing surface coupling - marked in the SEM image (middle right). This fits to the observation of slightly improved filler-LLDPE interaction seen in Figure 63. In comparison to the uncoated sample (top right), it is visible that only parts were moved from the interphase to the LLDPE. Further analysis to quantify this effect was performed using TGA, the results will be described in the next section.

The aminosilane sample (bottom left) shows residual EVA containing all MDH filler in the background and the LLDPE phase in the front being free of filler. By adding coupling agent (bottom right), the LLDPE phase becomes finer and shows few filler particles coupled in the LLDPE (highlighted in image). To further understand this effect, TGA analysis was also performed (see Table 14).

Figure 66   Scanning electron microscopy of cryo fractured and EVA etched 50/50 % – EVA/LLDPE
             blends filled with 30 % MDH with different surface modifications, with and without MAA-g-
             LLDPE coupling agent (CA) – magnification 10,000x

The just shown etched samples were cut in thin slices and analyzed using TGA to measure the amount of filler content. The amount of MDH in the sample was calculated based on the inorganic residue after thermal decomposition and the molar decomposition reaction shown in section 2.1.1. For etched samples, the values were referenced to the whole compound formulation to also include the EVA and represent the whole compound.

The TGA results of the etched samples are shown in Table 14. In comparison, the blends without etching were also tested in TGA. The analysis of these "original samples" show that the MDH

content is very stable around 30 %. The samples without coupling agent show a very low amount of filler which proves the observations in Figure 65. The values higher than 0 % are caused by contamination which was already seen in the etched aminosilane SEM picture. A significant difference is introduced by the coupling agent. While most of the uncoated filler sticks to the LLDPE, the vinylsilane and aminosilane samples show a lower MDH content. The values fit very well to the observations from SEM analysis of the 50/50 blends but also of the pure LLDPE samples. This is a sign for partial interaction of the coated fillers with the MAA-g-LLDPE coupling agent. The improved interaction of the aminosilane coating with the coupling agent in comparison to the vinylsilane can be quantified by an increase of the filler content from 4.5 % to 9.5 %.

Table 14   Content of magnesium-di-hydroxide filler calculated based on TGA analysis

Filler	Original sample	Sample after EVA etching	
			+ CA
Uncoated	29.8 %	0.7 %	25.7 %
Vinylsilane	30.1 %	0.6 %	4.5 %
Aminosilane	30.2 %	1.9 %	9.5 %

To further investigate the situation in a more realistic cable formulation, the higher filled samples containing 60 % MDH were also etched and analyzed using SEM (see Figure 67). The blend morphology and the phase size decrease significantly to the size of the filler particles. Therefore, the analysis of the SEM images has shown limitations in in identifying interactions. Judgement of the filler adhesion was not possible as the residual LLDPE phase acts as a filter holding the larger filler particles back during etching. Nevertheless, the same trends can be observed. The LLDPE residue of the uncoated (top left) and aminosilane coated (bottom left) samples without coupling agent shows no signs of filler. The aminosilane sample shows a filler particle that is entangled in LLDPE and restricts the extraction during etching (highlighted). Remaining EVA fractions that are blocked by entangled filler were identified at the vinylsilane sample (middle left). As former identified, the filler of this sample is located in the interphase (opposite to the other fillers located in EVA). With a high concentration of filler in the interphase, the chance of particles being stuck on the LLDPE surface and creating residuals after etching is high. The usage of coupling agent enables interaction between the LLDPE and the MDH for all samples. The strongest effect is seen for the uncoated filler (top right) which covers the whole LLDPE structure. Both silanes show reduced amount of MDH, which is mainly entangled for the vinylsilane (middle right) and incorporated for the aminosilane samples (bottom right).
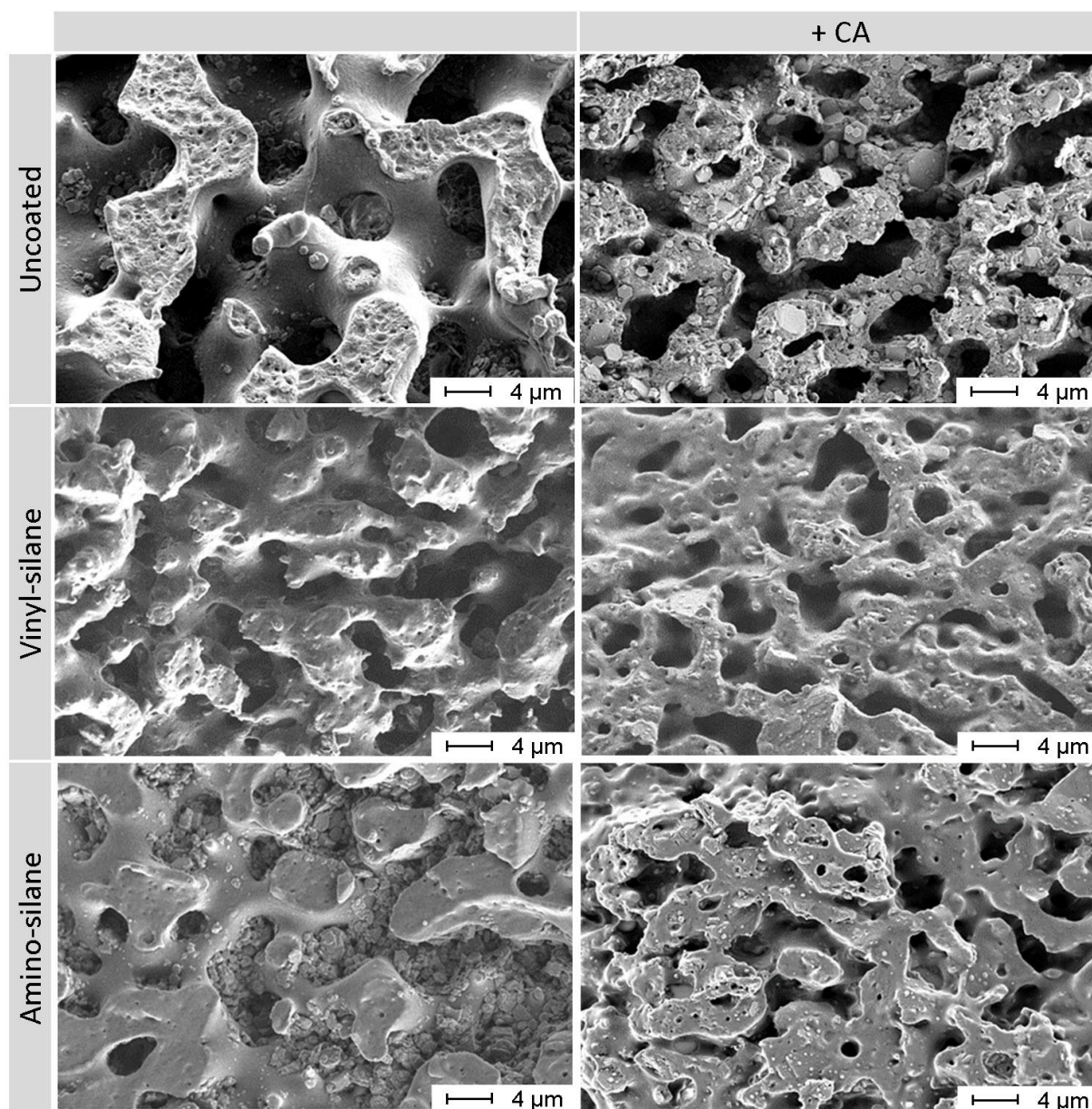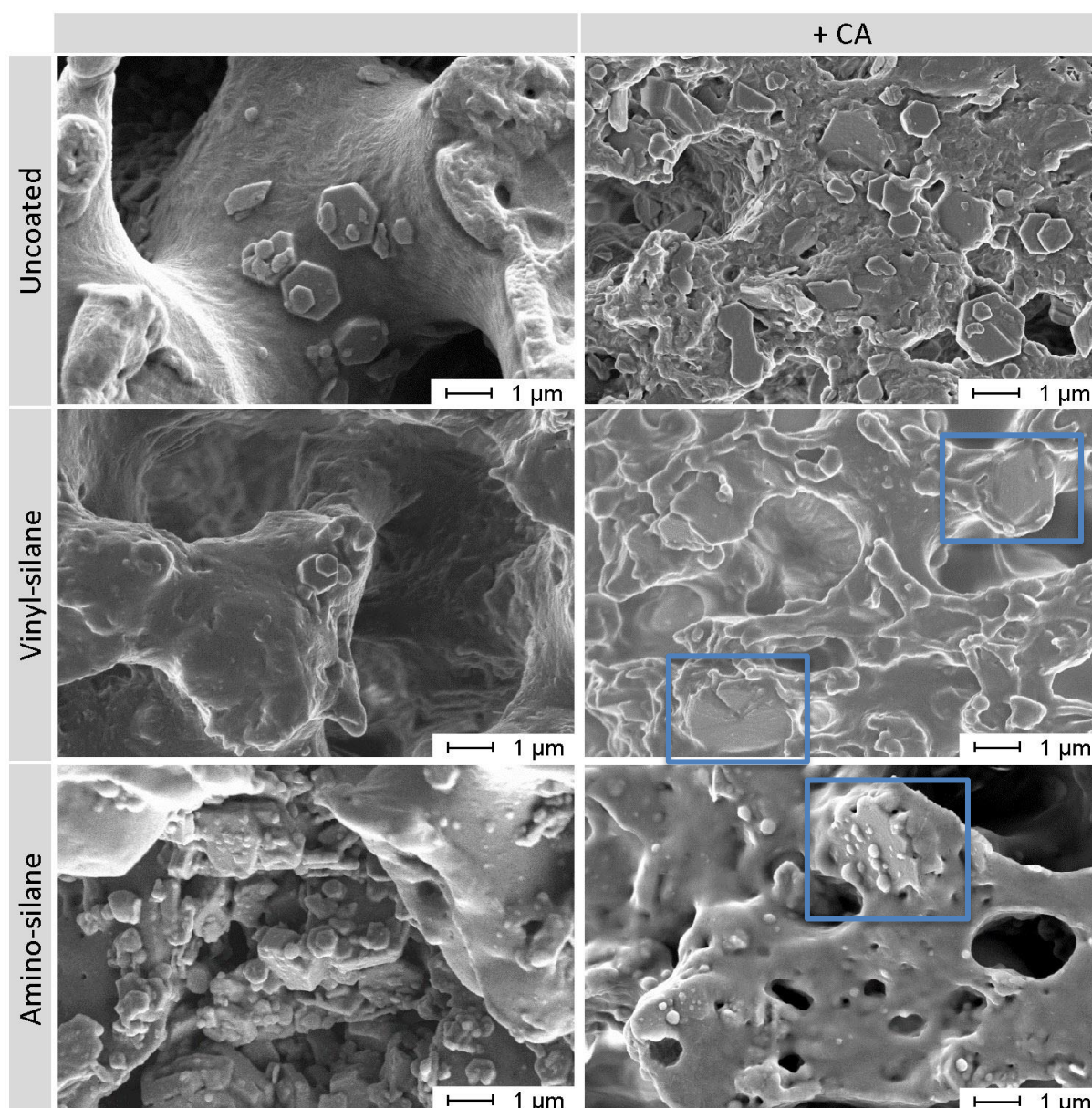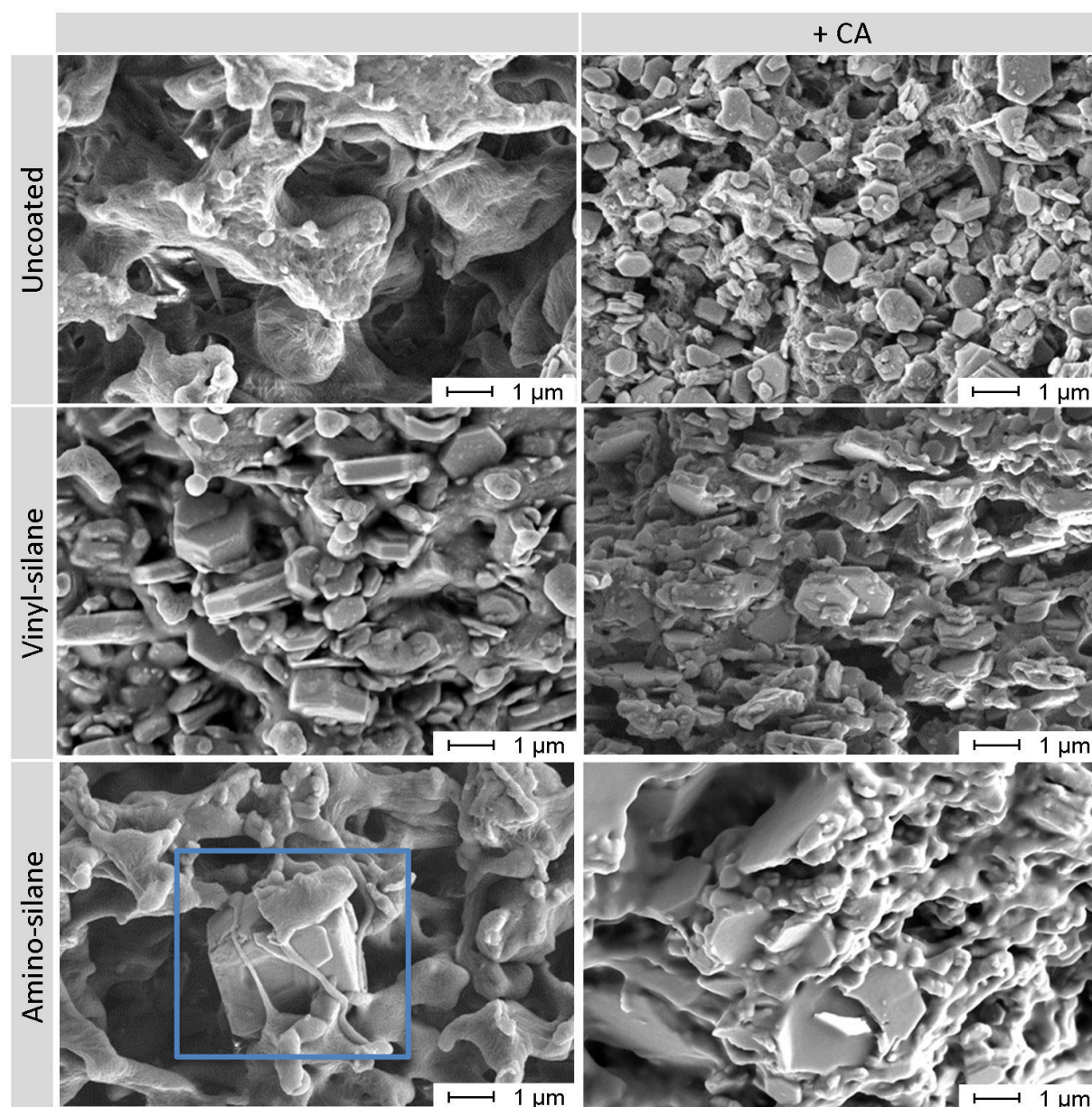
Figure 67   Scanning electron microscopy of cryo fractured and EVA etched 50/50 % – EVA/LLDPE blends filled with 60 % MDH with different surface modifications, with and without MAA-g-LLDPE coupling agent – magnification 10,000x

6.3.4   Burning behavior

As flame-retardancy is the main reason to incorporate the magnesium-di-hydroxide filler, the burning behavior of the investigated compounds was tested in cone calorimetry. Samples with 0 %, 10 %, 30 % and 60 % filler were tested, but strong fluctuations with low amount of flame-retardants were observed. Especially parameters like peak heat release rate show strong scattering for low dosages of flame-retardants. Cable compounds usually contain 60 % and more MDH. The results for the peak heat release rate and total heat release are shown in Figure 68. The

peak heat release rate (a) is increasing with increased EVA content. The curves are very close, especially in the samples up to 50 % EVA. The values above increase and show a stronger difference in between the coatings. The values show strong scatter and no clear picture. For pure EVA, uncoated MDH shows the lowest and vinylsilane the highest values in presence of coupling agent. This order is different for the 67/33 blend where aminosilane shows the best performance. The total heat release rate (b) is clearly decreasing with increasing EVA ratio. The y-axis is not starting from 0 to increase the resolution and display the curves that normally would not be distinguishable. The values are lying all within other's standard deviation and show very comparable values.
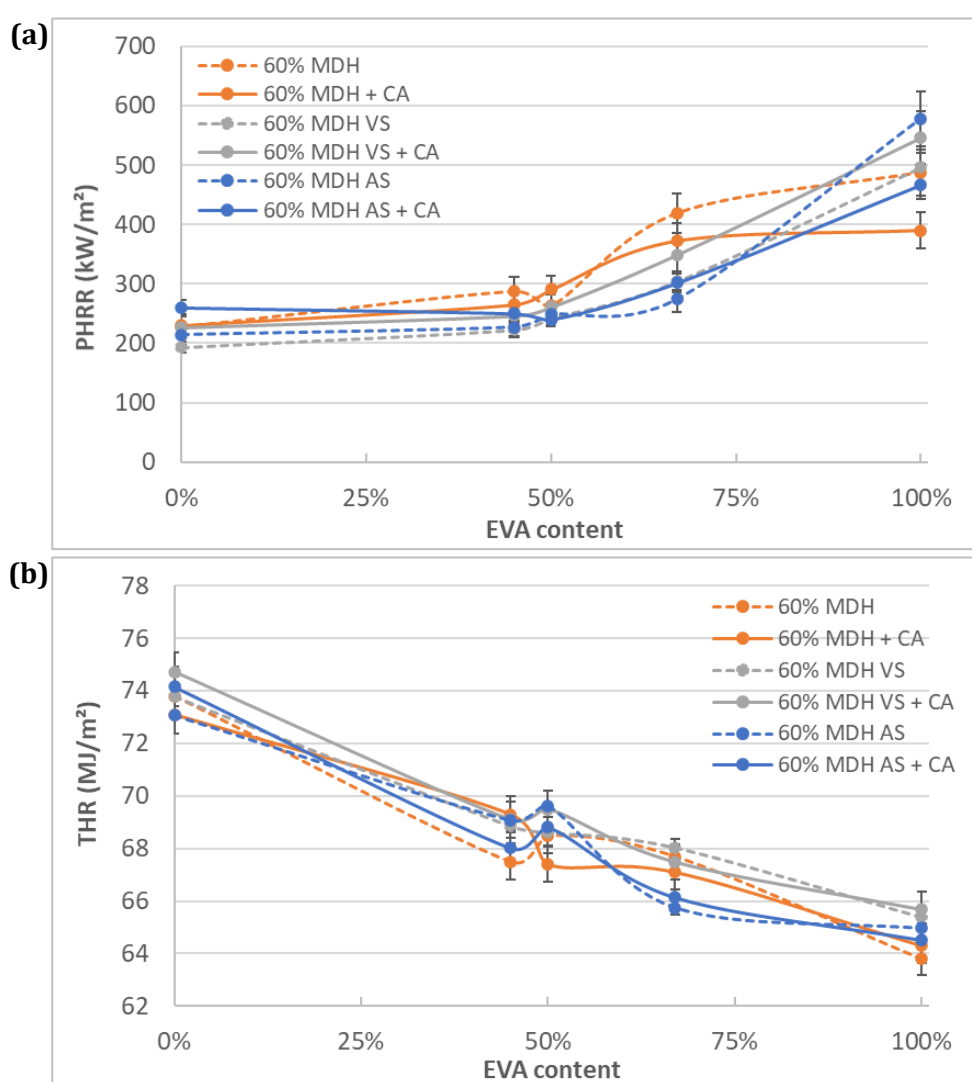
Figure 68   Peak heat release rate (a) and total heat release (b) of EVA/LLDPE blends filled with 60 % of uncoated, vinylsilane (VS) and aminosilane (AS) coated magnesium-di-hydroxide (MDH), with and without coupling agent (CA)

It was seen that no significant influence of the filler surface modification on the burning behavior was identified. This is different for the polymer composition as the peak heat release rate increases and the total heat release rate decreases with increasing EVA content. This is a sign for an EVA related decomposition effect which was already reported by El Hage et. al. [80]. Around 370 °C deacetylation of the EVA occurs, in addition to the thermal decomposition of the polyethylene backbone around 485 °C. This effect can also be observed on the residue after burning, as it is shown in Figure 69. The deacetylation creates a black incombustible residue that does not contribute to the total heat release rate.

0/100 – EVA/LLLDPE	50/50 – EVA/LLDPE	100/0 – EVA/LLDPE
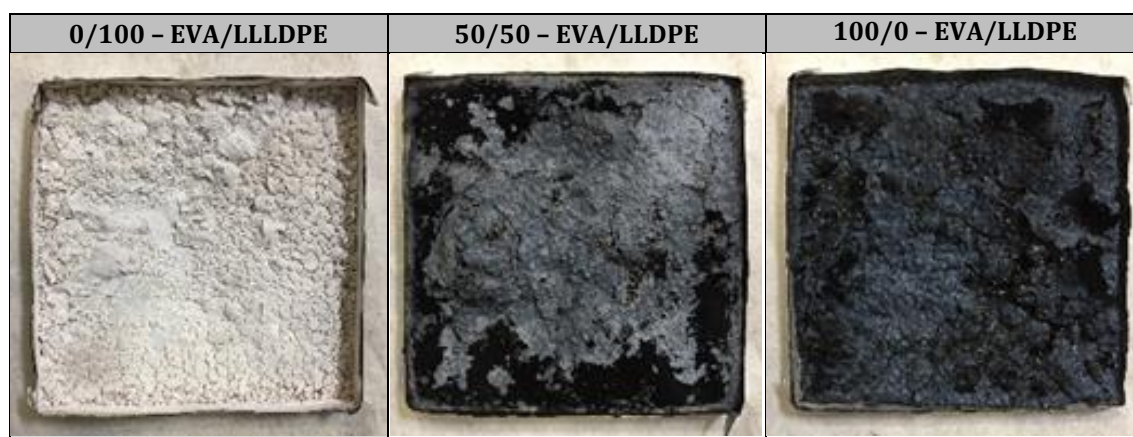
Figure 69   Residues of EVA/LLDPE blends filled with 60 % MDH from cone calorimeter testing

6.3.5   Conclusion

Objective of this section is to understand the influence of surface modified silane coated filler on the investigated blend systems. Vinylsilane and aminosilane were chosen based on the different interaction mechanisms in cable compounds. It is of interest if the vinylsilane coating can react with the maleic-acid-anhydrite group and form covalent bonds. Furthermore, the strength of the aminosilane interaction with EVA and maleic-acid coupling agent in comparison to uncoated MDH was investigated. To characterize the interaction with different EVA/LLDPE polymer blend systems, rheological, thermo-mechanical and morphological analysis was performed.

In the rheological measurements, the different surface modifications were compared with uncoated filler in EVA, LLDPE and a 50/50 % - EVA/LLDPE blend system. The pure LLDPE systems show the already described "yield stress effect" for all samples without coupling agent in parallel plate rheology. This indicates particle-particle interaction and insufficient filler-polymer coupling. The addition of coupling agent obsoletes this effect for the uncoated and the aminosilane sample. Vinylsilane shows the lowest viscosity and only very small improvement by a coupling agent

addition which is a sign for overall insufficient interaction with the polymer matrix. Pure EVA does neither show the yield stress effect, nor significant differences in between the coatings or the coupling agent. This further translates into the 50/50 % – EVA/LLDPE blend where the uncoated and aminosilane coated filler perform comparable, with and without coupling agent. Such effects were already observed for the uncoated samples in section 6.2, where EVA interacted with the filler even without any coupling agent. The melt volume index shows stronger differences, especially for the EVA rich blends where clear signs of incompatibility between polymer and vinylsilane coating is observed.

In mechanical testing, a trend of decreasing yield stress and increasing elongation at break with increasing EVA content is visible for all filler types. Vinylsilane shows clear signs of incompatibility (reduced strength and increased elongation) throughout all EVA/LLDPE ratios which are improved but cannot be overcome by the addition of a coupling agent. The samples using uncoated and aminosilane coated filler perform very comparable, except for the pure polymers where uncoated filler shows benefits in pure LLPDE and aminosilane coated filler in pure EVA. The elasticity of the compounds was rated in hysteresis measurements. While the tensile stress is significantly affected by the filler coupling mechanism, the tensile set is identified as a major function of the polymer matrix.

In DMA, especially at elevated temperature, the addition of a coupling agent improved the thermo-mechanical stability in the presence of LLDPE. The coupling agent enables an interaction between the more stable LLDPE and the filler. The strongest effects are observed for uncoated MDH, followed by aminosilane coated MDH. This order of filler-polymer interaction was also observed in CTE and contraction stress measurements, where the uncoated filler-polymer interaction was identified as the strongest, followed by aminosilane and vinylsilane coated as the weakest.

These observations can be clearly correlated with the morphological behavior of the pure polymers and the blends identified in SEM analysis. The aminosilane coating interacts with EVA by hydrogen bridges, as it was expected. In the same way, the uncoated filler does, although it has no special surface modification. Vinylsilane does not show any signs of interaction, regardless of the presence of a MAA-g-EVA coupling agent. In pure LLDPE, no coupling without MAA-g-LLDPE coupling agent is observed for any filler type. The addition of the coupling agent leads to an observable interaction of the uncoated and the aminosilane coated filler. This answers the question, if the expected aminosilane coating interaction with MAA-g-LLDPE will occur. Based on the thermo-mechanical analysis, this interaction is slightly weaker than the coupling with the uncoated filler. This can be related to a higher amount of OH- attachment points or reduced steric

hindering for the covalent bonding of the uncoated filler in comparison to the organic part of the aminosilane coating (see section 4.4.2). The vinylsilane coated filler still struggles to interact with the polymer matrix but shows signs of interaction which might be caused by an incomplete coverage of the filler.

The morphological analysis of etched highly filled 50/50 % – EVA/LLDPE blends has shown phase sizes close to the size of the MDH filler. In absence of coupling agent, all residual LLDPE phases are free of flame-retardant filler. For uncoated and aminosilane coated filler, the flame-retardant is fully incorporated in the EVA phase. The vinylsilane coated filler is mainly located in the interphase between EVA and LLDPE due to incompatibility with both polymers. This leads to a further reduced LLDPE phase size. The effect of interconnection of both polymer phases in by the filler in the presence of coupling agent as already described in section 6.2 was further underlined. This effect is not observed for the silane coated fillers. The partial coupling of aminosilane with MAA-g-LLDPE moves parts of the filler from the EVA phase into the LLDPE. TGA analysis has proven that around one third of the MDH is in the LLDPE phase, whereas the residual filler seems to remain in the EVA. The DMA results also point to partial location in the interphase, where the filler improves the overall compound performance, comparable to the uncoated filler. This was not observed in the SEM analysis. The vinylsilane coated filler is also moved from the interphase into the LLDPE in very small parts (around 15 % of the filler). It is expected to be related to an incomplete coverage of the coating and therefore some OH- interaction points with the coupling agent. A covalent bonding of the vinylsilane initiated by the maleic-acid-anhydrite coupling reactivity (ring opening according to Figure 18) was not observed.

The just described filler location in the blend systems allows a calculation of the theoretical phase inversion points according to the calculation performed in section 6.2.1. The viscosity ratios of unfilled samples were used for interfacial location and 30 % filled samples for partial location. The results are shown in Table 15. The observed reduction in LLDPE phase size of the samples using vinylsilane coated filler is caused by the change in the viscosity ratio. The usage of a coupling agent moves the phase inversion point towards the LLDPE side which leads to increased thermo-mechanical performance. The strongest effect is seen for the uncoated MDH sample which describes the highest improvements in the mechanical analysis for this filler.

Table 15   Theoretical phase inversion points of 50/50 % – EVA/LLDPE blends with different filler coatings and coupling agent

Filler coating	Coupling agent	Filler location	Phase inversion point (% EVA)
Uncoated	-	EVA	58 %
	+ CA	Interphase	49 %
Vinylsilane	-	Interphase	49 %
	+ CA	LLDPE + Interphase	46 %
Aminosilane	-	EVA	56 %
	+ CA	EVA + LLDPE	50 %

The flame-retardant performance was investigated using cone calorimetry. Interactions of the filler with EVA were identified which led to an increased peak heat release rate and a reduced total heat release rate. Within the whole range of EVA/LLDPE mixing ratio, no significant difference was observed for all filler coatings or the usage of coupling agents.

6.4 Optimization of the compound formulation based on the derived structure-property-relationships

The objective of this section is to extract the major key learnings and transfer these into an optimized formulation that fulfills the stringent requirements for applications as a cable compound as described in section 2.1.1. The list of properties shows that a balance between mechanical performance, processability and flame retardancy will be the key. These are represented by the thermo-mechanical analysis, rheological and morphological investigations, and cone calorimetry. For industrial application, a fourth field of interest is important: cost.

The state-of-the-art formulations shown in section 2.1.3 were simplified for a deeper investigation using only the main components. Therefore, the following outcome focusses on the targeted ratio of the polymers, the usage of filler coatings and coupling agents. Further ingredients like processing aids, thermal and UV-stabilizers and flame-retardant synergists need to be adjusted towards a more detailed application later.

The incompatibility of EVA and LLDPE is the major concern in regard of the thermo-mechanical properties. The addition of a coupling agent has shown to overcome the incompatibility by using the flame-retardant filler as connection between both polymers. This fact brought the mechanical properties (yield strength, elongation at break) in a range that allows the application as a cable compound. LLDPE rich blends show improved mechanical performance (e.g. higher yield strength) and thermal stability in DMA. But hysteresis measurements have shown that a certain flexibility and processability needs to be maintained for the later cable application, especially when the mineral filler is added. The addition of EVA reduces the flexural modulus and the viscosity which helps in extrusion processing. The elongation at break values throughout the EVA/LLDPE blends do not differ significantly, but values below 150 % in some of the 60 % filled systems are too low. Unfortunately, exactly these systems show the best yield strength because of the polymer-filler coupling. The same competing behavior is seen for the shrink back performance. While the coefficient of thermal expansion is reduced with high LLDPE content and good filler coupling, contraction stress increases.

It becomes clear that the end application will have a major impact on the defined compound formulation. It needs to be clarified whether a high yield strength (cable stiffness) or elongation at break (cable flexibility) is of interest. This is often defined by the cable design or more specific the wall thickness of the jacket layer. A thinner layer requires higher stiffness to maintain a certain abrasion resistance.

In general, the outcome of the work packages can be translated into several action items for compound formulation. The usage of uncoated filler and aminosilane coated filler in combination with the maleic-acid-anhydrite grafted LLDPE coupling agent has shown the best mechanical performance. The ratio of EVA/LLDPE should be chosen rather on the EVA rich side to enable filler uptake even above the investigated 60 wt%. This will be needed as the achieved flame-retardant properties of the investigated basic recipes are not in the range of the commercial products used by the cable industry. If no pure EVA polymer base is used, no benefit in using a silane coated filler was identified as the usage of uncoated filler has shown comparable results. The observed interaction between pure EVA and uncoated filler also obsoletes the usage of MAA-g-EVA coupling agent. These factors can result in cost advantage. Most of the properties were significantly improved by using the right coupling agent and filler combination. But as already described, the competing performance brings tradeoffs and leads to some properties out of specification, especially when even more filler is added. This leads to the thought that not perfect coupling, but rather controlled coupling is the key to an optimized compound. It was observed that the flame-retardant performance is not significantly affected by the filler-polymer coupling if a high quality of dispersion is achieved. This would allow to control the compound properties within the shown range by adjusting the type and ratio of filler and coupling agent. An example would be the partial replacement of uncoated filler with vinylsilane coated filler to increase elongation at break and MFI and decrease contraction stress. In fine steps, this can be done without affecting yield strength and CTE too much.

To prove this approach, an exemplary compound was made based on the best result of EVA/LLDPE ratio (67/33), MAA-g-LLDPE coupling agent and uncoated filler. Parts of the uncoated filler were then replaced by vinylsilane coated filler. The formulations, resulting properties and a commercial reference compound is shown in Table 16. The compound properties can be adjusted by the ratio of uncoated filler that interacts with the coupling agent and vinylsilane coated filler that shows reduced interaction. The elongation at break is increased above the critical threshold of 150 % while maintaining a reasonable strength. Significant improvement can be seen in MVR and contraction stress. As expected, the CTE is slightly increased and fire behavior shows no significant difference. The values are very close to the reference material, except for the fire behavior. This is caused by additional usage of flame-retardant synergists in the reference material.

Table 16   Formulations and results of compounds using filler combinations and a reference material from application

Recipe	WP4-1	WP4-2	WP4-3	WP4-4	Reference
EVA	26.8 %	26.8 %	26.8 %	26.8 %	
LLDPE	8.4 %	8.4 %	8.4 %	8.4 %	
MAA-g-LLDPE	4.8 %	4.8 %	4.8 %	4.8 %	proprietary
MDH	60.0 %	50.0 %	40.0 %	30.0 %	
MDH VS (vinylsilane)		10.0 %	20.0 %	30.0 %	
Properties					
Yield strength (MPa)	12.9	11.8	10.6	10.2	9.8
Elongation at break (%)	133.1	151.7	168.2	177.2	151.1
MVR (cm^3/10min)	2.8	3.1	3.8	5.3	5.1
CTE (um/K)	125.0	130.1	132.4	138.1	135.6
Contraction stress (MPa)	6.0	5.9	5.5	5.3	5.8
PHRR (MJ/m^2)	372.4	368.3	358.4	361.1	225.3
THR (kW/m^2)	67.4	67.3	66.9	67.1	65.7

7 Summary

The objective of this work was to generate a fundamental scientific understanding of the influence of various coupling mechanisms on the structure-properties-relationships of highly filled, flame-retardant EVA/LLDPE based cable compounds. Due to the complexity of the investigated compound systems, it was observed, that several ingredients are interacting with each other in various ways. Splitting these investigations into four independent working packages allowed a clear identification and differentiation of effects.

The incompatible blend components EVA and LLDPE were investigated and the influence of the blend ratio on mechanical, thermal and rheological properties were correlated with the resulting morphology. The theoretical phase inversion point around 48 % EVA was calculated based on rheological measurements and proven using TEM and SEM analysis. Furthermore, the influence of maleic acid anhydrite grafted co-polymers as potential coupling agents in the absence of mineral filler was investigated. This was performed to clearly differentiate the observed effects. No signs of incompatibility of MAA-g-EVA and MAA-g-LLDPE in their base polymers were observed up to a dosage of 50 %. While the measured blend properties through all EVA/LLDPE ranges were not significantly affected by the coupling agent, a small reduction in phase size by MAA-g-LLDPE addition was still observed. This was caused by a change in polarity of the LLDPE phase increasing the compatibility to EVA slightly, but not enough to overcome the immiscibility. An effect on crystallization and crystallinity could be ruled out. These observations lead to the assumption that all following described effects are caused purely by polymer-filler interactions.

Mineral flame-retardant filler (MDH) was added to the system in different dosages to understand the response of the system and the effect of the coupling agent. Measurements were carried out with pure polymers and different EVA/LLDPE blends with 10 %, 30 % and 60 % filler. Rheological measurements have shown a yield stress effect at low frequencies in 60 % filled pure LLDPE which is a sign for particle-particle interaction caused by internal friction and percolation. This effect disappeared after adding the MAA-g-LLDPE coupling agent. Furthermore, this effect could not be seen in pure EVA and all blends containing EVA which is a sign of interaction, even in the absence of coupling agent. This was also seen in the mechanical tests, where the influence of coupling agent was mainly visible for the high filled sample in the LLDPE rich regions. The upcoming theory of EVA interaction with the uncoated filler was further underlined by DMA measurements. All EVA/LLDPE blends have shown significant improvements in the thermo-mechanical properties above the glass transition temperature of EVA when uncoated filler and LLDPE based coupling agent was present. This led to the conclusion that EVA interacts with the

filler via hydrogen bonds. In presence of the MAA-g-LLDPE, this filler couples also with the more stable LLDPE phase which leads to a mechanical improvement of the whole compound. This was proven in morphological analysis. It was also observed that the addition of mineral filler reduced the phase size of LLDPE caused by filler incorporation into the EVA phase and resulting viscosity changes. This could be proven by recalculations of the theoretical phase inversion points. By addition of LLDPE based coupling agent, the uncoated filler moved into the interphase where it created the mentioned connection between both phases. This filler could be still seen after etching the EVA phase as a residue covering the LLDPE phase. A graphical model of these effects is shown in Figure 53 on page 78.

After the interaction between both polymers and the uncoated filler has shown such influence, fillers with different surface modifications were investigated. Vinylsilane and aminosilane coated MDH with the same particle size and particle size distribution were used. They represent different methods of bonding ability and have shown interactions with EVA and LLDPE in the past. The same EVA/LLDPE blends and pure polymers were filled with 30 % and 60 % of coated flame-retardant fillers and then investigated in the established analysis methods. Throughout all tests, differences in compatibility were observable. While uncoated MDH and aminosilane coated MDH performed very comparable, the vinylsilane coated filler showed reduced interaction with the polymer matrix. The addition of MAA-g-LLDPE coupling agent improved the performance of all filler types, but for vinylsilane coated not so much to overcome the signs of incompatibility. This was also visible in SEM analysis of the cryo-fractured samples, where vinylsilane coated filler did not show interaction with or without coupling agent. Uncoated and aminosilane coated MDH have shown good interaction in the presence of coupling agent and even with pure EVA. The ability to form hydrogen bonds to EVA was the reason why both fillers performed very comparable throughout all investigations. While uncoated MDH in presence of coupling agent moved from the EVA phase into the interphase, aminosilane coated filler has shown stronger interaction with EVA. This led to a majority of MDH (around 2/3) staying in the EVA and the interphase and the rest (1/3) moving into the LLDPE phase where it fully coupled with the MAA-g-LLDPE. Vinylsilane coated filler was located in the interphase due to incompatibility and was partially (1/6) incorporated into LLDPE in presence of MAA-g-LLDPE. This might be caused by uncovered areas in the filler coating. The filler location could be clearly identified in SEM, EDX and TGA analysis. This location was then transferred to the rheological measurements and it was possible to correlate the observed morphology with the calculated theoretical phase inversion points.

All these described effects and observations where then used to create a guiding for compound formulation and a possibility to finetune compound properties without affecting the fire behavior.

It was observed that some compound properties are competing. The basic compound performance is defined by choosing primarily the EVA/LLDPE ratio. A good performance throughout the whole temperature range can be achieved by a sufficient coupling. This later needs to be controlled and potentially reduced to adjust and finetune the product performance for the later application.

8 Zusammenfassung

Ziel der vorliegenden Arbeit war es, den Einfluss verschiedener Kopplungsmechanismen auf die Struktur-Eigenschafts-Beziehungen von hochgefüllten flammgeschützten EVA/LLDPE Compounds zu untersuchen. Die Komplexität der untersuchten Systeme führte zu verschiedenen Interaktionen der Einzelkomponenten untereinander. Die Untersuchungen in dieser Arbeit wurden deshalb in vier unabhängige Arbeitspakete unterteilt, um mögliche Effekte klar zu identifizieren und zu differenzieren.

Nicht mischbare Polymerblends aus EVA und LLDPE wurden untersucht, um den Einfluss des Mischungsverhältnisses auf die mechanischen, thermischen und rheologischen Eigenschaften zu ermitteln und mit der resultierenden Morphologie zu korrelieren. Die theoretische Phaseninversion bei 48 % EVA konnte auf Basis rheologischer Messungen berechnet und durch TEM- und REM-Aufnahmen belegt werden. Des Weiteren wurde der Einfluss von Maleinsäureanhydrid (MAA) gepfropften Co-Polymeren als potenzielle Polymer-Füllstoff-Kopplungsadditive auf die Blendeigenschaften untersucht. Dies wurde zunächst ohne mineralischen Füllstoff durchgeführt, um die beobachteten Effekte klar zu differenzieren. Zugegebenes MAA-g-EVA oder MAA-g-LLDPE zeigte in dem jeweiligen Basispolymer bis zu einer Dosierung von 50 % durchweg gute Kompatibilität. Die gemessenen Blendeigenschaften zeigten im Rahmen aller untersuchten EVA/LLDPE-Mischungsverhältnisse keine signifikante Beeinflussung durch die Kopplungsadditive. Dennoch wurde eine Reduktion der Phasengröße durch Zugabe von MAA-g-LLDPE beobachtet. Grund hierfür war eine Zunahme der Polarität der LLDPE-Phase und damit eine leicht verbesserte Kompatibilität, die jedoch nicht zur Mischbarkeit führte. Ein Einfluss des Kopplungsadditivs auf das Kristallisationsverhalten und die Kristallinität konnte ausgeschlossen werden. Diese genannten Beobachtungen führten zu der Annahme, dass alle im Weiteren beschriebenen Effekte rein auf die Polymer-Füllstoff-Interaktion zurückzuführen sind.

Mineralisches Flammschutzmittel (MDH) wurde in verschiedenen Dosierungen in die untersuchten Blendsysteme zugegeben, um die Reaktion des Gesamtsystems und den Einfluss des Kopplungsadditivs zu verstehen. Die Untersuchungen betrafen die reinen Polymere und verschiedene EVA/LLDPE Blends mit 10 %, 30 % und 60 % Füllstoff. In rheologischen Messungen an 60 % gefülltem LLDPE wurde bei niedrigen Anregungsfrequenzen ein „Yield stress" Effekt beobachtet. Dieser Effekt ist ein Anzeichen für Partikel-Partikel-Wechselwirkungen wie z.B. innere Reibung oder Perkolation und verschwand durch Zugabe von MAA-g-LLDPE-Kopplungsadditiv. Ein solcher Effekt war in reinem EVA (mit oder ohne MAA-g-EVA-Kopplungsadditiv) nicht zu erkennen, was ein Zeichen für eine Polymer-Füllstoff-Interaktion war. Diese Beobachtung

belegten die Ergebnisse der mechanischen Tests, bei denen ein Einfluss des Kopplungsadditivs vor allem für LLDPE-reiche Mischungsverhältnisse sichtbar wurde. Die Theorie einer EVA-Füllstoff-Interaktion konnte durch DMA-Messungen gestützt werden. Alle EVA/LLDPE-Blendsysteme zeigten signifikante Verbesserungen der thermo-mechanischen Eigenschaften durch die Zugabe von MAA-g-LLDPE oberhalb der Glasübergangstemperatur von EVA. Dies führte zur Schlussfolgerung, dass EVA mit dem Füllstoff durch Wasserstoffbrückenbindungen interagiert. Bei Zugabe von MAA-g-LLDPE koppelt der Füllstoff zudem an die thermisch stabilere LLDPE-Phase, was zu einer mechanischen Verbesserung des Compounds führt. Die Zugabe von mineralischem Füllstoff führte zu einer Reduktion der Phasengröße des LLDPE, hervorgerufen durch Füllstoffeinlagerung in die EVA-Phase und daraus resultierende Viskositätsänderungen. Dies konnte durch Morphologiestudien und Neuberechnung der theoretischen Phaseninversion belegt werden. Durch Zugabe des LLDPE-basierten Kopplungsadditivs bewegte sich der Füllstoff in die Grenzschicht, wo die bereits beschriebene Kopplung zwischen EVA und LLDPE hergestellt wurde. Es war möglich, diesen Füllstoff nach Kryobruch und Lösen der EVA-Phase auf der Oberfläche des LLDPE-Rückstands zu identifizieren. Ein graphisches Modell der beschriebenen Effekte ist in Figure 53 auf Seite 78 dargestellt.

Im nächsten Schritt wurden Füllstoffe mit verschiedenen Oberflächenmodifizierungen untersucht. Hierfür wurde mit Vinylsilan oder Aminosilan beschichtetes Magnesiumhydroxid (MDH) mit gleicher Partikelgröße und Partikelgrößenverteilung eingesetzt. Die Beschichtungen wurden wegen verschiedener Varianten der Kopplung ausgewählt und hatten in Vorversuchen Wechselwirkungen mit EVA und LLDPE gezeigt. Den bereits untersuchten EVA/LLDPE-Blends und reinen Polymeren wurden 30 % und 60 % der beschichteten Flammschutzmittel zugegeben. Die Proben wurden anschließend mit den etablierten Analysemethoden untersucht. In allen Tests konnten Unterschiede in der Kompatibilität festgestellt werden. Während unbeschichtetes MDH und Aminosilan-beschichtetes MDH relativ vergleichbare Werte zeigten, interagierte Vinylsilan deutlich weniger mit der Polymermatrix. Die Zugabe von MAA-g-LLDPE-Kopplungsadditiv verbesserte die Eigenschaften aller Füllstofftypen, bei Vinylsilan jedoch nur marginal. Diese mangelnde Interaktion mit und ohne Kopplungsadditiv war auch in REM-Aufnahmen zu erkennen. Unbeschichtetes und Aminosilan-beschichtetes MDH zeigten hingegen gute Interaktion bei Zugabe von Kopplungsadditiv und auch in reinem EVA. Vergleichbare Ergebnisse unter Verwendung beider Füllstoffe sind in der Fähigkeit, Wasserstoffbrückenbindungen mit EVA zu bilden, begründet. Während sich unbeschichtetes MDH bei Zugabe von Kopplungsadditiv von der EVA-Phase in die Grenzschicht bewegte, zeigte das mit Aminosilan beschichtete MDH stärkere Wechselwirkung mit EVA. Dies führte dazu, dass bei Verwendung von Kopplungsadditiv ein

größerer Teil des Füllstoffs im EVA und der Grenzschicht verblieb (etwa 2/3). Der Rest interagierte mit dem MAA-g-LLDPE durch kovalente Bindungen und lagerte sich vollständig in der LLDPE-Phase ein. Der Vinylsilan-beschichtete Füllstoff lagerte sich wegen mangelnder Kompatibilität zu beiden Polymerphasen in der Grenzschicht an. Bei Verwendung von MAA-g-LLDPE war ein kleiner Teil in der LLDPE-Phase nachweisbar (etwa 1/6), was auf eine nicht vollständig geschlossene Füllstoffbeschichtung hinweist. Die jeweilige Lage des Füllstoffs konnte durch REM-, EDX- und TGA-Analysen ermittelt werden. Der Transfer dieser Ergebnisse auf entsprechende rheologische Messungen ermöglichte die Berechnung und Korrelation der theoretischen Phaseninversionspunkte.

Abschließend wurden alle beschriebenen Effekte und Beobachtungen betrachtet, um daraus Hinweise und Richtlinien zur Compound-Rezepturentwicklung abzuleiten. Eine Möglichkeit zur Feinabstimmung der Compoundeigenschaften ohne merkliche Beeinflussung der Brandeigenschaften wurde exemplarisch vorgestellt. Im Rahmen der Untersuchungen wurde beobachtet, dass einige der Compoundeigenschaften miteinander konkurrieren. Die grundsätzlichen Compoundeigenschaften können primär durch das EVA/LLDPE-Verhältnis eingestellt werden. Um im gesamten Temperaturbereich gute Eigenschaften zu erzielen, ist eine starke Polymer-Füllstoff-Kopplung nötig. Diese muss im nächsten Schritt gesteuert und möglicherweise gezielt reduziert werden, um die Eigenschaften genauer auf die Anwendung abzustimmen.

9 Outlook

The shown investigations have led to a fundamental understanding of the interactions related to filler coupling, the role of EVA and LLDPE in the blend systems and the influence of coupling agents and surface modifications. The established understanding can be further broadened by further filler coating types and combinations of these. A look towards the systems response to filler coupling using reactive peroxide extrusion would be also worthwhile. In this process, in-situ grafting and coating of the filler in one single compounding step is used. A different direction of investigation would be the polymeric compatibilization of EVA and LLDPE to enable a fully even distribution of the flame-retardant filler in the compound.

The observed correlations and effects will be used in future compound development workstreams to develop halogen free flame-retardant cable compounds with improved properties regarding mechanical performance, thermal stability, processability and flame-retardancy.

Bibliography

[1]   G. ALLERMANN, C. DE SANTOS, „Cables Conference" in *Prospects and Developments for the Wire & Cable Industry*, Cologne, 2018.

[2]   K. COUSINS, Polymers for Wire and Cable - Changes Within an Industry, iSmith Rapra Publishing, 2000.

[3]   C. DE SANTOS, „Cables Conference" in *The global wire and cable industry: Market trends and opportunities*, Duesseldorf, 2019.

[4]   C. DE SANTOS, „Cables Conference" in *Insights into the European cable market from a global perspective*, Duesseldorf, 2020.

[5]   G. PRITCHARD, Plastics Additives, Springer Science, 1998.

[6]   IEC 60794-1-2, *Optical fibre cables: Generic specification - Basic optical cable test procedures - General guidance,* 2017.

[7]   S. H. WASSERMAN, „Wire and Cable Applications of Polyethylene," in *Handbook of Industrial Polyethylene and Technology*, Scrivener Publishing LLC, 2018, pp. 1126 - 1146.

[8]   ZVEI e.V., „Whitepaper - Brandschutzkabel erhöhen die Sicherheit," in *Kabel als vorbeugender Brandschutz nach der europäischen Bauprodukteverordnung*, 2017.

[9]   CORNING OPTICAL COMMUNICATIONS, „Product overview: indoor fiber optic cables," 07 07 2020. [Online]. Available: http://corning.com/optical-communications/.

[10]   EU REGULATION NO. 305/2011, „Construction Products Regulation (CPR)," 2011.

[11]   FTT - FIRE TESTING TECHNOLOGIES, „Burning of bunched cables," https://www.fire-testing.com/burning-behaviour-of-bunched-cables/, 2018.

[12]   G. SKINNER, „Flame retardancy: the approaches available," in *Polymer Additives*, Springer Science, 1998, pp. 260 - 267.

[13]   A. SUT, „Fire residues design: the chemistry behind synergistic effects in multicomponent polymeric systems," Berlin, 2016.

[14]   S. C. BROWN, „Flame retardants: inorganic oxide and hydroxide systems," in *Plastics Additives*, Springer Science, 1998, pp. 287 - 296.

[15]   S. KIM, „Flame retardancy and smoke suppression of magnesium hydroxide filled polyethylene," *Polymer Physics 41(9),* pp. 936-44, 2003.

[16]   Y. Z. WANG, „Halogen free flame retardants," in *Advances in fire retardant materials*, Woodhead Publishing, 2008, pp. 67 - 94.

[17]   S. V. LEVCHIK, E. D. WEIL, „Developments in phosphorous flame retardants," in *Advances in fire retardant materials*, Woodhead Publishing, 2008, pp. 41 - 66.

[18]   R. SAUERWEIN, „Mineral Filler Flame Retardants," in *Non-Halogenated Flame Retardant Handbook*, Scrivener Publishing LLC, 2014, pp. 75 - 141.

[19]   HUBER, „Product brochure: Non-halogen fire retardant additives," 2019.

[20]   H. TANG, X.-B. ZHOU, X.-L. LIU, „Effect of Magnesium Hydroxide on the Flame Retardant Properties of Unsaturated Polyester Resin," *Procedia Engineering 52,* pp. 336 - 341, 2013.

[21]   NABALTEC, „Product brochure: Metal hydrates for cables," 2019.

[22]   HUBER, „Halogen-free flame retardants for the Cable Industry," 2017.

[23]   M. A. SPALDING, „Preface," in *Handbook of Industrial Polyethylene and Technology*, Scrivener Publishing LCC, 2017, p. xiii.

[24]   C. DOBBIN, „An Industrial Chronology of Polyethylene," in *Handbook of Industrial Polyethylene and Technology*, Scrivener Publishing LLC, 2018, pp. 4 - 23.

[25]   Y. V. KISSIN, „Catalysts for the Manufacture of Polyethylene," in *Handbook of Industrial Polyethylene and Technology*, Scrivener Publishing, pp. 26 - 55.

[26]   R. M. PATEL, „Types and Basics of Polyethylene," in *Handbook of Industrial Polyethylene and Technology*, Scrivener Publishing LCC, 2018, pp. 106 - 139.

[27]   K. MENARD, N. MENARD, „Thermal Analysis of Polyethylene," in *Handbook of Industrial Polyethylene and Technology*, Scrivener Publishing LLC, 2018, p. 231.

[28]   B. BORSOVA, J. KRESSLER, „Environmental stress-cracking resistance of LDPE/EVA blends," *Macromol Mater Eng,* pp. 288(6):509-15, 2003.

[29]   M. FAKER, M. K. RAZAVI ANGHJEH, M. GHAFFARI, S. A. SEYYEDI, „Rheology, morphology and mechanical properties of polyethylene/ethylene vinyl acetate copolymer (PE/EVA) blends," *European Polymer Journal 44,* pp. 1834-1854, 2008.

[30]   G. TAKIDIS, D. N. BIKIARIS, G. Z. PAPAGEORGIOU, D. S. ACHILIAS, I. SIDERIDOU, „Compatibility of low-density polyethylene/poly(ethylene-co-vinyl acetate) binary blends prepared by melt mixing," *J. Appl. Polym. Sci. 90(3),* pp. 841-52, 2003.

[31]   H. A. KHONAKDAR, U. WAGENKNECHT, S. H. JAFERI, R. HASSLER, H. ESLAMI, „Dynamic mechanical properties and morphology of polyethylene/ ethylene vinyl acetate copolymer blends," *J. Adv. Polym. Tech. 23(4),* pp. 307-15, 2004.

[32]   H. A. KHONAKDAR, S. H. JAFERI, A. YAVARI, A. ASADINEZHAD, U. WAGENKNECHT, „Rheology, morphology and estimation of interfacial tension of LDPE/EVA and HDPE/EVA blends," *Polym. Bull. 54,* pp. 75-84, 2005.

[33]   I. RAY, D. KHASTGIR, „Correlation between morphology with dynamic mechanical, thermal, physicomechanical properties and electrical conductivity for EVA-LDPE blends,“ *Polymer,* pp. 34(10):2030-7, 1993.

[34]   H. J. VAN OENE, „40:448,“ *J Colloid interface Sci.,* 1972.

[35]   J. F. PALIERNE, „Linear rheology of viscoleastic emulsions with interfacial tension,“ *Rheol Acta,* pp. 29(3):204-14, 1990.

[36]   L. A. ULTRACKI, „On the viscosity-concentration dependence of immicible polymer blends,“ *J Rheol,* pp. 35(8):1615-37, 1991.

[37]   S. STEINMANN, W. GRONSKI, C. FRIEDRICH, „Cocontinous polymer blends: influence of viscosity and elasticity ratios of the constituent polymers on phase inversion,“ *Polymer,* pp. 42(15):6619-29, 2001.

[38]   A. J. LOVINGER, M. L. WILLIAMS, „Tensile properties and morphology of blends of polyethylene and polypropylene,“ *J Appl Polym Sci,* pp. 25(8):1703-13, 1980.

[39]   M. M. RUEDA, M. AUSCHER, R. FULCHIRON, T. PÉRIÉ, G. MARTIN, P. SONNTAG, P. CASSAGNAU, „Rheology and applications of highly filled polymers: A review of current understanding,“ *Progress in Polymer Science,* pp. 22-53, 2017.

[40]   R. LARSON, The Structure and Rheology of Complex Fluids, OUP USA, 1999.

[41]   J. A. LEWIS, „Colloidal processing of ceramics,“ *Journal of the american ceramic society,* Bd. 83, pp. 2341-59, 2000.

[42]   A. UHS, H. Ke. PETER, W. Uerth, K. Ke. SPAETER, „Shear rheological properties of separated nutrient residue,“ *INT J HYG ENVIR HEAL,* 2017.

[43]   J. MÓCZÓ, B. PUKÁNSZKY, „Particulate Fillers in Thermoplastics,“ in *Fillers for Polymer Applications*, Springer, 2017, pp. 53-87.

[44]   D. M. BIGG, „Rheological behavior of highly filled polymer melts,“ *Polymer Engineering Science,* Bd. 23, pp. 206-10, 1983.

[45]   L. E. NIELSEN, Polymer Rheology, M. Dekker, 1977, p. 203

[46]   A. J. POSLINSKI, M. E. RYAN, R. K. GUPTA, S. G. SESHADRI, F. J. FRECHETTE, „Rheological behavior of filled polymeric systems II. The effect of a bimodal size distribution or particulates,“ *Journal of Rheology,* Bd. 32, pp. 751-71, 1988.

[47]   W. BRAUNHOFER, J. Z. KOVACS, „A review and analysis of electrical percolation in carbon nanotube polymer composites,“ *Composites Science and Technology,* Bd. 69, pp. 1486-98, 2009.

[48]   T. B. LEWIS, L. E. NIELSEN, „Viscosity of dispersed and aggregated suspensions of spheres,“ *Transactions of the Society of Rheology ,* Bd. 12, pp. 421-43, 1968.

[49]   Z. TADMOR, C. G. GOGOS, Principles of Polymer Processing, John Wiley & Sons, 2006.

[50]   D. M. KALYON, D. DALWADI, M. EROL, E. BIRINCI, C. TSENOGLU, „Rheological behavior of concentrated suspensions as affected by the dynamics of the mixing process," *Rheologica Acta,* Bd. 45, pp. 641-58, 2006.

[51]   O. SEYVET, P. NAVARD, „Collision-induced dispersion of agglomerate suspensions in a shear flow," *Journal of Applied Polymer Science,* Bd. 78, pp. 1130-3, 2000.

[52]   S. ZHOU, Y. LEI, H. ZOU, M. LIANG, „High thermally conducting composites obtained via in situ exfoliation process of expandable graphite filled polyamide 6," *Polymer Composites,* Bd. 34, pp. 1816-23, 2013.

[53]   D. M. KALYON, A. LAWAL, R. YAZIKI, P. YARAS, S. RAILKAR, „Mathematical modeling and experimental studies of twin-screw extrusion of filled polymers," *Polymer Engineering Science,* Bd. 39, pp. 1137-51, 1999.

[54]   C. KUMUDINIE, „Polymer–Ceramic Nanocomposites: Interfacial Bonding Agents," in *Encyclopedia of Materials: Science and Technology*, Pergamon, 2001, pp. 7574-77.

[55]   C. DEARMITT, R. ROTHON, „Surface Modifiers for Use with Particulate Fillers," in *Fillers for Polymer Applications*, Springer, 2017, pp. 30-53.

[56]   J. Z. LIANG, R. K. Y. Li, „Effect of filler content and surface treatment on the tensile properties of glass-bead-filled polypropylene composites," *Polymer International,* Bd. 49, pp. 170-74, 2000.

[57]   S. ZUERCHER, T. GRAULE, „Influence of dispersant structure on the rheological properties of highly concentrated zirconia dispersions," *J Eur Ceram Soc,* Bd. 25, pp. 863-73, 2005.

[58]   E. P. PLUEDDEMANN, „Adhesion through silane coupling agents," in *Fundamentals of Ahesion*, Springer, 1991, pp. 279-90.

[59]   B. BORUP, K. WEISSENBACH, „Silane Coupling Agents," in *Functional Fillers for Plastics*, Wiley-VCH, 2008, pp. 62 - 90.

[60]   T. CHEN, A. ISAROV, „Use of Surface - Modified Magnesium Hydroxide for Low - Smoke Flame Retardant Thermoplastics Applications," in *Functional Fillers for Plastics*, Toronto, 2005.

[61]   J. D. MILLER, H. ISHIDA, „Adhesive-Adherend Interface and Interphase," in *Fundamentals of Adhesion*, Springer, 1991, pp. 291-324.

[62]   A. I. MONCADA, W. HUANG, N. HORSTMAN, „Polyethylene Modification by Reactive Extrusion," in *Handbook of Industrial Polyethylene and Technology*, Scrivener Publishing, 2017, pp. 715-53.

[63]   C. A. CORREA, C. RAZZINO, E. HAGE, „Role of Maleated Coupling Agents on the Interface Adhesion of Polypropylene–Wood Composites,“ *Journal of Thermoplastic Composite Materials,* Bd. 20, pp. 323-39, 2007.

[64]   C. DEARMITT, R. ROTHON, „Particulate Fillers, Selection, and Use in Polymer Composites,“ in *Fillers for Polymer Applications*, Springer, 2017, pp. 4-27.

[65]   H. M. LAUN, „Rheological properties of aqueous polymer dispersions,“ *Angewandte Makromolekulare Chemie,* Bd. 123, pp. 335-59, 1984.

[66]   D. BONN, M. M. DENN, L. BERTHIER, T. DIVOUX, S. MANNEVILLE, „Yield stress materials in soft condensed matter,“ *Review of Modern Physics,* Bd. 89, pp. 2-34, 2017.

[67]   M. PISHVAEI, C. GRAILLAT, P. CASSAGNAU, „Rheological behaviour of polystyrene latex near the maximum packing fraction of particles,“ *Polymer,* Bd. 46, pp. 1235-44, 2005.

[68]   A. FALL, F. BERTRAND, G. OVARLEZ, D. BONN, „Shear thickening of cornstarch suspensions,“ *Journal of Rheology,* Bd. 56, pp. 575-91, 2012.

[69]   A. J. POSLINSKI, M. E. RYAN, R. K. GUPTA, S. G. SESHADRI, F. J. FRECHETTE, „Rheological behavior of filled polymeric systems I. Yield stress and shear-thinning effects,“ *J Rheol.,* Bd. 32, pp. 703-35, 1988.

[70]   S. JU, H. ZHANG, M. CHEN, C. ZHANG, X. CHEN, Z. ZHANG, „Improved electrical insulating properties of LDPE based nanocomposite: Effect of surface modification of magnesia nanoparticles,“ *Composites Part A: Applied Science and Manufacturing Volume 66,* pp. 183-192, Nov 2014.

[71]   D. THAM, N. TRANG, N. CHINH, N. GIANG, T. LAM, T. HOANG, „Sustainable composite materials based on ethylene-vinylacetate copolymer and organo-modified silica,“ *Green Process Synth,* 15 Mar 2016.

[72]   Y. HSU, R. W. TRUSS, B. LAYCOCK, M. P. WEIR, T. M. NICHOLSON, C. J. GARVEY, P. J. HALLEY, „The effect of comonomer concentration and distribution on the photo-oxidative degradation of linear low density polyethylene films,“ *Polymer,* Bd. 119, pp. 66-75, 2017.

[73]   DOW Chemicals, *Technical Datasheet: Dowlex 2045,* 2019.

[74]   SK functional polymer, *Technical datasheet: Evatane 24-03,* 2020.

[75]   Huber Martinswerk, *Technical datasheet: Magnifin grades H-5, H-5A, H-5IV,* 2020.

[76]   Silon SRO, *Technical datasheet: Tabond 3044,* 2018.

[77]   SK functional polymer, *Technical datasheet: Orevac 9304,* 2020.

[78]   A. IOANNIDIS, „Coupling agents based on organofunctional silanes,“ EVONIK Industries, 2018.

[79] M. J. FOLKES, P. S. HOPE, Polymer blends and alloys, Chapman and Hall, 1993.

[80] R. El Hage, A. Viretto, R. Sonnier, L. Ferry, J. Lopez-Cuesta, „Flame retardancy of ethylene vinyl acetate (EVA) using new aluminium-based fillers,“ *Polymer Degradation and Stability,* pp. 56-67, 2014.

[81] L. ULTRACKI, Commercial Polymer blends, Chapman and Hall, 1998, pp. 83-94.

[82] D. R. PAUL, C. B. BUCKNALL, Polymer blends, Vol. 2: Performance, John Wiley and Sons, 1999.

[83] O. OLABISI, L. M. ROBERTSON, M. T. SHAW, Polymer-polymer miscibility, Academic Press, 1979, pp. 1-17.

[84] L. A. ULTRACKI, Polymer alloys and blends: Thermodynamics and rheology, Hanser, 1989.

Curriculum Vitae

Personal Data	Michael Heinz	
	born on 03. February 1986 in Hof, Germany	
Marital Status	married	
Nationality	German	

Education	2006 – 2011	Universität Bayreuth
		Fakultät für Angewandte Naturwissenschaften
		Studies of Material Science
		Degree: Dipl.-Ing. (1,9)
	1996 – 2005	Johann-Christian-Reinhart Gymnasium Hof
		Matriculation standard

Occupation	since 2020	Process Development Supervisor
		Corning Optical Communications
	2014 – 2020	Materials Development Engineer
		Corning Optical Communications
	2011 – 2014	Development Engineer
		KBE Elektrotechnik
	2010 – 2011	Research Associate
		Hong Kong University of Science and Technology

Publications

Reviewed Publications

W. Stoecklein, M. Heinz, Z. Baneen
Measurement of the max. allowable push force for cables to be installed by blowing
International Wire, Cable and Connectivity Symposium, 15-3, 2020

M. Heinz
Cable friction - Influence of cable and duct materials in extended testing
International Wire, Cable and Connectivity Symposium, 6-5, 2021

M. Heinz, C. Callsen, W. Stoecklein, V. Altstädt, H. Ruckdäschel
Halogen free flame-retardant cable compounds: Influence of MDH filler and coupling agent on EVA/LLDPE blend system morphology
Polymer Engineering and Science, Volume 62, Issue 2, Feb 2022
DOI:10.1002/pen.25858

M. Heinz
HFFR cable compounds: Influence of flame-retardant filler and coupling agent on EVA/LLDPE blend systems
International Wire, Cable and Connectivity Symposium, 2022

Conference Contributions

M. Heinz
Fiber optic cables – the best choice for a future proof communication infrastructure
Cables Conference, Cologne, 06.-08.03.2018

M. Heinz
Responding to bandwidth demands utilizing ultra-high density fiber optic cable networks
Cables Conference, Duesseldorf, 03.-05.03.2020

M. Heinz
Measurement of the maximum push force for cables to be installed by blowing
Cables Conference, Cologne, 14.-16.09.2021

M. Heinz
Cable friction - Influence of cable and duct materials in extended testing
International Wire, Cable and Connectivity Symposium, 04.-08.10.2021

Patents

E. Gallo, M. Heinz, T. Kazmierczak, K. Langfeld
Optical fiber cable with improved fire protection performance
US11237347B2 (application 08.09.2020, published 25.02.2021, granted 01.02.2022)

M. Heinz, R. Kumar
Flame retardant fiber optic cable with halogen free sheath for blowing applications
US11256052B2 (application 09.06.2019, published 14.01.2021, granted 22.02.2022)

M. Heinz, R. Kumar
Talcum-free flame retardant fiber optical cable with micro-modules
US11256052B2 (application 09.06.2019, published 06.11.2020, granted 19.07.2022)